# SYNTHESIS OF NOVEL CYCLOBUTANE NUCLEOSIDE ANALOGS

**MUHAMMAD MURTAZA HASSAN**

**A THESIS SUBMITTED TO THE FACULTY OF GRADUATE STUDIES IN PARTIAL FULFILLMENT OF THE REQUIREMENTS FOR THE DEGREE OF MASTER OF SCIENCE**

**GRADUATE PROGRAM IN CHEMISTRY**

**YORK UNIVERSITY**

**TORONTO, ONTARIO**

**JUNE, 2017**

**Abstract**

A synthesis of cyclobutane nucleosides is described. The method involved the triflation of a β-hydroxymethyl-cyclobutanone and its subsequent displacement by a 6-chloropurinyl anion to generate *N*-7 and *N*-9 regioisomers. The stereoselective reduction of the *N*-alkylated ketones yielded the cis-alcohols quantitatively and the geometric configuration was confirmed by spectroscopic data and X-ray diffraction. Photolysis of *N*-7 and *N*-9 coupled ketones was carried out in methanol using quartz tubes to promote ring-expansion isonucleoside products. Photolysis did not yield any ring-expansion or cycloelimination products, rather, the products are suspected to be cyclopropanes from decarbonylation of the ketones, since these are less polar and show shielding of protons in their corresponding NMR spectra, consistent with substituted cyclopropanes.

**ACKNOWLEDGMENTS**

I want to first thank God for giving me the ability to succeed in all that I have accomplished. I would like to thank my family in particular my Mom and Dad, who raised me as a child with their support and blessed upbringing.

Above everyone else involved in my research, I am sincerely and immensely thankful to Dr. Edward Lee-Ruff for giving me the opportunity to work in his group and for guiding me throughout my roadblocks and for encouraging, and guiding me to become a critical thinker and chemist. He was always ready and available to help me more than anyone else with my MSc project. He was helpful in nurturing me as a chemist.

I am thankful to my supervisory committee, Dr. Arturo Orellana and Dr. Dasantila Golemi-Kotra for giving me feedback, support and their valuable time. Dr. Orellana taught me chemistry that I treasure as gems of knowledge and for that, I am very grateful. I want to thank Dr. Howard Hunter for always being ready to help with all aspects of NMR relevant to this project, whether it be analysis and interpretation or using his supplies and instruments. I would like to thank the York University Centre for Research in Mass Spectrometry for their willingness to help, in particular Isaac Lai, Aafreen Bagga, Justin Lau, and Brian Lam. I want to thank Dr. Yousaf for providing extra funding as well as Audette, Organ, and Orellana lab group members for assisting me with my work, for supporting me and for their friendship, in particular, Ayat Yaseen, Cristina Lento, Gregory Price, Christopher Lombardi, Andrei Nikolaev, Minhao Zhang, Faizaan Rasheed and Francesca Stillo (exchange student in our lab). I want to thank Zhibin Wu and Dirk Verdool for providing me with extra chemical supplies and glassware.

Finally, I would like to thank the department of chemistry at York University, in particular Mary Mamais and Magy Baket for their administrative support and guidance.

## TABLE OF CONTENTS

Abstract……ii

Acknowledgements……iii

Table of Contents……iv

List of Figures…….....vi

List of Abbreviations…….....viii

List of Equations…….....x

List of Schemes…….....xi

**Chapter 1**

1.0 Introduction……1

1.1 Biochemistry of Natural Nucleosides……1

1.2 Conception and classification of Nucleoside analogues……2

1.3 Nucleobase-modified nucleoside analogues…….....4

1.4 Carbocyclic Nucleosides…….....6

1.5 Synthesis of Nucleoside Analogues……...7

1.6 Charge distribution of purines……...9

1.7 Cyclobutanones as precursors for nucleoside analogues……..9

1.7.1 Photochemistry of Cyclobutanones.…….……10

1.8 Proposal…….....11

**Chapter 2**

2.0 Results and Discussion…….....14

2.1 Synthesis of substrate **49**……..14

2.2 Debenzoylation of cyclobutanone **49**……...14

2.3 Triflation of alcohol **50**…….....16

2.4 *N*-alkylation of triflate **57**…….....17

2.5 Reduction of cyclobutanones **60** and **61**…….…….33

2.6 Alkylation of purines…….……..39

**Chapter 3**

3.0 Photolysis of **60** and **61**……....44

**Chapter 4**

4.1 Conclusions and Comments……..……..48

4.2 Future Directions…….49

**Chapter 5**

5.0 Experimental……...….52

5.1 General Experimental……...…….……..53

5.2 Specific Experimental Procedures and Spectral Data……..…….…...59

5.3 References…….……...58

5.4 Appendix……..63

## List of Figures

Figure 1: Naturally occurring purine and pyrimidine nucleobases ……1

Figure 2: Hydrogen bond interactions between complimentary nitrogenous bases in DNA that stabilize the DNA double helix ……..……..2

Figure 3: Mechanism of action of nucleoside analogues …….…...3

Figure 4: Possible modifications for potential nucleoside analogues…….…….…….……...4

Figure 5: $^{1}$H NMR spectrum of alcohol **50**……15

Figure 6: $^{1}$H NMR spectrum of crude triflate **57**……...17

Figure 7: $^{1}$H NMR spectrum of *N*-9 coupled ketone **60**…..……..19

Figure 8: $^{13}$C-NMR spectrum of *N*-9 coupled ketone **60**……...……20

Figure 9: $^{1}$H-$^{13}$C HSQC spectrum of *N*-9 coupled ketone **60**……...…….21

Figure 10: Magnified $^{1}$H-$^{13}$C HSQC spectrum of *N*-9 coupled ketone **60**…….22

Figure 11: Magnified $^{1}$H-$^{13}$C HSQC spectrum of *N*-9 coupled ketone **60**……...…….....23

Figure 12: $^{1}$H-$^{13}$C HMBC spectrum of *N*-9 coupled ketone **60** ……...……24

Figure 13: Magnified $^{1}$H-$^{13}$C HMBC spectrum of *N*-9 coupled ketone **60**……...….25

Figure 14: Magnified $^{1}$H-$^{13}$C HMBC spectrum of *N*-9 coupled ketone **60**……...26

Figure 15: $^{1}$H-$^{15}$N HMBC spectrum of *N*-9 coupled ketone **60**…….……27

Figure 16: $^{1}$H NMR spectrum of *N*-7 coupled ketone **61**……..……...28

Figure 17: $^{13}$C NMR spectrum of *N*-7 coupled ketone **61**……..…….……...28

Figure 18: $^{1}$H-$^{1}$H COSY spectrum of *N*-7 coupled ketone **61**…….……...……29

Figure 19: Magnified$^{1}$H-$^{1}$H COSY spectrum of *N*-7 coupled ketone **61**……...……30

Figure 20: Magnified$^{1}$H-$^{13}$C HSQC spectrum *N*-7 coupled ketone **61**……...…..…..31

Figure 21: Crystal structure of *N*-7 coupled ketone **61** ……...……..32

Figure 22: $^{1}$H NMR spectrum of *N*-9 alcohol **62**……..35

Figure 23: Crystal structure of *N*-9 alcohol **62** ……36

Figure 24: $^{1}$H NMR spectrum of *N*-7 alcohol **63**……...37

Figure 25- Crystal structure of *N*-7 alcohol **64** ……..…38

## LIST OF ABBREVIATIONS & SYMBOLS

| | |
|---|---|
| 2-D | two-dimensional |
| 6-MP | 6-mercaptopurine |
| 6-TG | 6-thioguanine |
| ATCC 10145 | candida albicans |
| $Cy_2SI$ | 2,3-dicyclohexylsuccinimide |
| D- | dextrorotatory |
| DABCO | 1,4-diazobicyclo(2,2,2)-octane |
| DEAD | diethyl azodicarboxylate |
| DIAD | diisopropyl azodicarboxylate |
| DMF | dimethylformamide |
| DMSO | dimethylsulfoxide |
| DNA | deoxyribonucleic acid |
| $Et_2O$ | diethyl ether |
| EtOAC | ethyl acetate |
| FDA | Food and Drug Administration |
| FT-IR | Fourier Transform infrared |
| HCMV | human cytomegalovirus |
| HIV | human immunodeficiency virus |
| HMBC | heteronuclear multiple-bond correlation spectroscopy |
| HRMS | high resolution mass spectrometry |
| HSAB | hard-soft acid-base |
| HSQC | heteronuclear single quantum coherence |

| | |
|---|---|
| HSV-1 | herpes simplex virus type 1 |
| HSV-2 | herpes simplex virus type 2 |
| $h\nu$ | photon of light |
| $IC_{50}$ | half maximal inhibitory concentration |
| IR | infrared |
| L- | levorotatory |
| MeOH | methanol |
| mRNA | messenger ribonucleic acid |
| NMR | nuclear magnetic resonance spectroscopy |
| OXT-A | oxetanocin-A |
| Ⓟ | phosphate group |
| RNA | ribonucleic acid |
| SAH | *S*-adenosyl-*L*-homocysteine |
| TAS-102 | trifluridine/tipiracil |
| TBAB | tetrabutylammonium bromide |
| TBDPS | tert-butyldiphenylsilyl |
| TCAC | trichloroacetyl chloride |
| THF | tetrahydrofuran |
| TLC | thin-layer chromatography |
| tRNA | transfer ribonucleic acid |
| UV | ultraviolet |

## List of Equations

Equation 1: Synthesis of acyclic and isonucleoside analogs from photolysis of **28**.....10

Equation 2: Synthesis of carbocyclic nucleosides from reduction of **32**……...10

Equation 3: Synthesis of cyclobutanone **49** from allyl benzoate **55**……..14

Equation 4: Debenzoylation of **49** in mildly basic conditions……...14

Equation 5: Triflation of alcohol **50**……...16

Equation 6: Synthesis of ketones **60** and **61** via $S_N2$ protocol on triflate **57**……18

Equation 7: Stereoselective reduction of **60** to yield cis alcohol **62**……..35

Equation 8: Stereoselective reduction of **61** to yield cis alcohol **63**……..37

## List of Schemes

Scheme 1: *N*-alkylation of adenine to a haloalkane via $S_N2$ mechanism……7

Scheme 2: Nucleoside analog synthesis via an activation of an alcohol…….8

Scheme 3: Mitsunobu reaction of an alcohol to yield nucleoside analogs……..8

Scheme 4: Trost reaction with variety of nucleobases to yield nucleoside analogs……9

Scheme 5: Synthesis of cyclobutaonone by [2+2] cycloaddition of an alkene and dichloroketene……10

Scheme 6: Photochemistry of cyclobutanones……..11

Scheme 7: Proposed introduction of a nucleobase to cyclobutanone **49**……...…12

Scheme 8: Proposed synthesis of novel nucleoside analogs from cyclobutanone derivatives ….13

Scheme 9: Computational charge density of 6-chloropurinyl anion…….18

Scheme 10: Microwave assisted regioselective alkylation of purines and pyrimidines with α,β-unsaturated esters……40

Scheme 11: Microwave assisted regioselective alkylation of purines and pyrimidines with ally bromide……..……41

Scheme 12: Mechanism of Mitsunobu reaction…….42

Scheme 13: Photolysis of **60** and **61** under varying conditions to promote ring expansion……..44

Scheme 14: Cycloelimination alkene products from photolysis of **60** and **61**.....46

Scheme 15: Proposed cyclopropane derivatives **69** and **70** from decarbonylatinon of **60** and **61**……47

Scheme 16: Proposed synthesis of other *N*-alkylated cyclobutanones and their subsequent reduction and photolysis…….....50

Scheme 17: Proposed synthesis of other five-membered analogs…….51

# Chapter 1

### *1.0 Introduction*

### *1.1 Biochemistry of Natural Nucleosides*

"Nucleoside" is a term that was first introduced in 1909 by Levene and Jacob for subunits of nucleic acids which were isolated by the hydrolysis of nucleic acids.[1] Naturally occurring nucleosides consist of a purine (adenine and guanine) or pyrimidine base (uracil, cytosine and thymine), bonded to a furanose sugar moiety such as β-D-ribofuranose or β-D-deoxyribofuranose.

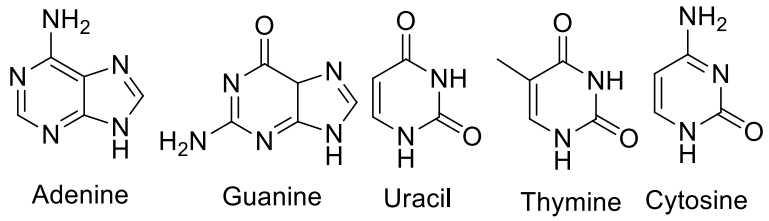


Figure 1- Naturally occurring purine and pyrimidine nucleobases

Natural nucleosides (Figure 1) play an essential role in regulatory and biosynthetic processes. Since nucleosides are the building blocks of nucleic acids, the information stored in deoxyribonucleic acid (DNA) depends solely on the sequence of nucleosides. Consequently, they are associated with conservation, replication and transcription of genetic information.

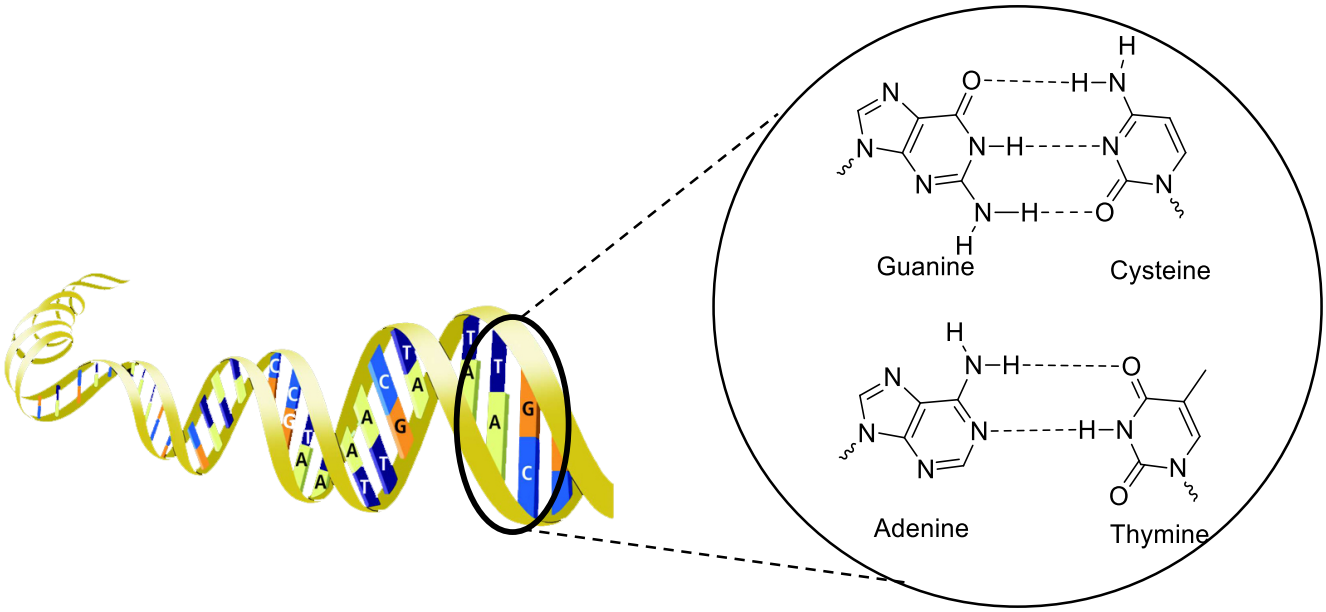


Figure 2- Hydrogen bond interactions between complimentary nitrogenous bases in DNA that stabilize the DNA double helix

DNA and RNA consist of strands that are held together by hydrogen bonds through complimentary base pairing of nucleosides (Figure 2). The mechanism of replication and transcription of DNA into RNA and DNA also occurs with the polymerization of nucleosides. The expression of proteins also proceeds via a biosynthetic process in which DNA is transcribed into messenger RNAs (mRNAs). mRNAs are then translated into protein amino-acid sequences with the involvement of transfer RNAs (tRNAs) that carry amino-acids and pair up with their complementary codon sequence (a set of three base-pair sequences) and act as adapters, between the mRNA and amino acids.

### *1.2 Conception and classification of Nucleoside analogues*

Upon intracellular phosphorylation by kinases, nucleosides can assume a biologically active role. Thus, the conception of analogues of phosphorylated nucleosides, commonly referred to as nucleotides, show significant chemotherapeutic potential in their ability to interfere

with biological processes involved in the rapid proliferation of tumour cells. However, nucleotides exist as dianonic species that are unable to pass easily through cellular membranes. Nucleosides and their analogues are neutral molecules that can enter the cell, which can then assume the therapeutic role upon intracellular phosphorylation by kinases via three main pathways: enzyme inhibition, incorporation into DNA & RNA, and DNA synthesis inhibition (Figure 3).

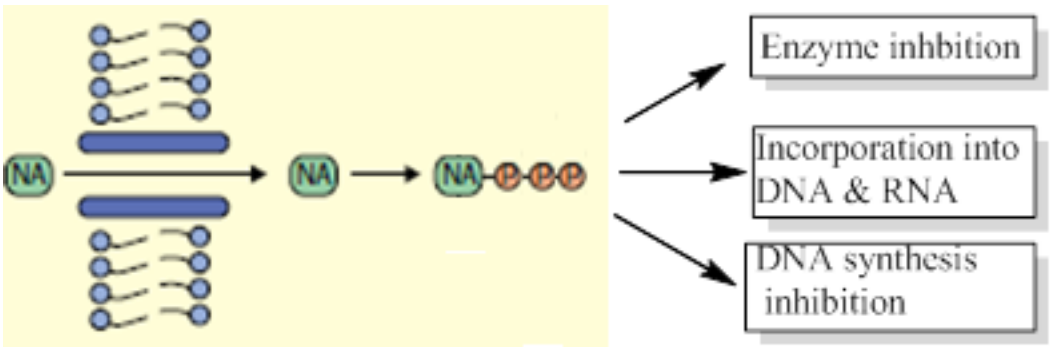


Figure 3- Mechanism of action of nucleoside analogues.[2]

Since natural nucleosides consist of two parts, a sugar moiety and a nucleobase, these two parts are susceptible to structural modifications for the design of nucleoside analogues. Several structural modifications can be made to the sugar moiety such as: the inversion of configuration from D to L, anomeric inversion of β to α, elimination or substitution of hydroxyl groups, modification to the ring size (ex. oxetanes, pyranose etc.), substitution of one or more atoms in the ring with heteroatoms, addition of various functional groups, changes to the nucleosidic linkage to the sugar (by a C-C or C-heteroatom linkage), and lastly changes to the heterocyclic base (nucleobase-modified nucleosides). Alteration of the nucleobase-furanose connectivity on C-2 to another position gives isonucleosides, and the absence of a methylene group on C-5 yields a nornucleoside (Figure 4).

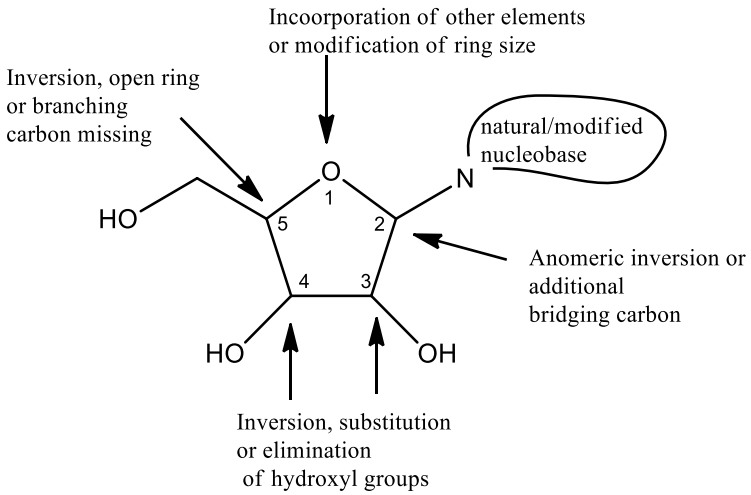


Figure 4- Possible modifications for potential nucleoside analogues

### *1.3 Nucleobase-modified nucleoside analogues*

Nucleoside analogues of thiopurines and fluorinated pyrimidines as modified nucleobases have demonstrated significant antiviral and anticancer activities. Elion's group discovered that substitution of guanine and hypoxanthine with sulfur at the 6 position resulted in inhibition of purine synthesis. 6-Mercaptopurine (6-MP) and 6-thioguanine (6-TG) nucleobases were shown to metabolize to the cytotoxic nucleoside 5'monophosphates that inhibit phosphoribosylpyrophosphate amidotransferase preventing the *de novo* purine biosynthesis. They also prevented the conversion of the inosine 5'monophosphate, the phosphorylated hypoxanthine nucleoside, to the guanine and adenine nucleotides.[1] They were shown to exhibit potent anticancer activities against various rodent tumours. 6-MP was FDA approved in 1953 for treatment of pediatric acute lymphocytic leukemia, a cancer of blood and bone marrow that leads to overproduction of immature lymphocytes. It still remains as a standard treatment for acute lymphocytic leukemia as well as autoimmune disorders such as psoriasis, ulcerative colitis and

rheumatoid arthritis. 6-TG is administered for treatment of acute myelogenous leukemia, a cancer of white blood cells that interferes with the production of normal white blood cells.

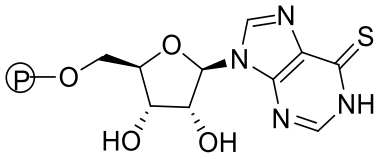

**6-TG**
**1**

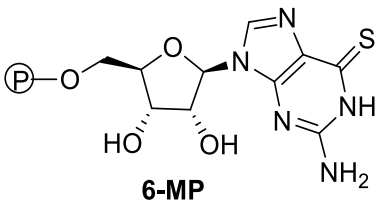

**6-MP**
**2**

Fluorinated drugs provide added stability without significantly altering the geometry of the non-fluorinated molecule, since hydrogen and fluorine are comparable in size and bond length, with a van der Waals radii of 1.20A˚vs1.47A˚ and average bond lengths of 1.08-1.10 1Å (C-H) vs. 1.26-1.411Å (C-F). The strength of C-F bonds (116 kcal/mol) also ensures greater metabolic stability compared to the C-H bonds (99 kcal/mol)[3] which leads to a greater bioavailability. Nucleosides of 5-fluorinated pyrimidines along with the nucleobases themselves are an essential class of antitumour agents that were first discovered by Rutman and co-workers in 1954. They observed the increased uptake of uracil and conversion of deoxyuridine-5'-monoophosphate 3, in rat liver tumour cells to thymidine-5'-monophosphate by thymidylate synthase. They speculated that 5-fluorouracil would prevent methylation at the 5-position, thus inhibiting thymidylate synthase and decreasing thymidine in cells, and that it would selectively target tumor cells since tumour cells displayed a higher uptake of uracil.[2] As they speculated, 5-fluorodeoxyuridine **3** (5-fluorouracil nucleoside) and 5-fluorouracil were found to be potent inhibitors of thymidylate synthetase and are currently used for the treatment of breast cancer, and solid tumours such as gastrinointestinal tumours.[1] The dosage treatment for 6-15 days for 0.5-1 mg/kg of **3**, is comparable to that of 15 mg/kg of 5-fluorouracil weekly.[1] Trifluorothymidine **4** has also been shown to exhibit promising anticancer activity, but it rapidly degrades within the body by the enzyme thymidine phosphorylase. Thus, it is coadministered with tipiracil

hydrochloride **5**, a thymidine phosphorylase inhibitor with a molar ratio of 2:1 by Taiho Pharmaceuticals as TAS-102, with an $IC_{50}$ of 35 nM. TAS-102 was FDA-approved for patients with colorectal cancer in Sept 2015.[2]

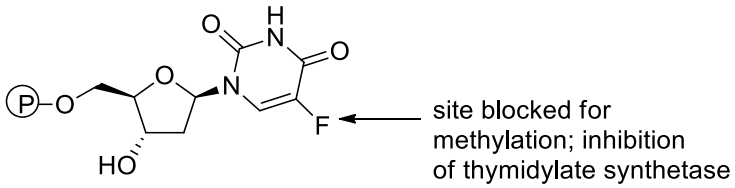


**5-fluorodeoxyuridine**
**3**

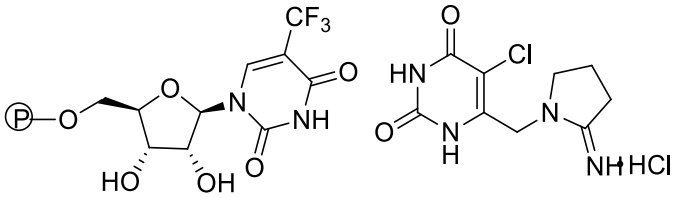

**Trifluorothymidine** **Tipiracil hydrochloride**
**4** **5**

### *1.4 Carbocyclic Nucleosides*

Carbocyclic nucleoside analogues contain a methylene in place of oxygen in the sugar moiety which increases metabolic stability towards hydrolases and phosphorylases of the C-N bond, which is otherwise labile and quite susceptible to cleavage.[1,2,4,5] Carbocyclic nucleoside analogues are generally non-natural in origin, however some natural-occuring ones include Aristeromycin **6** and Neplanocin A **7**. D-(-)-aristeromycin was isolated in 1968 from *Streptomyces citricolor*, whereas neplanocin A was discovered in 1981, both of which have been known to exhibit significant anti-tumour and anti-viral activity, and are speculated to inhibit the *S*-adenosyl-*L*-homocysteine (SAH) hydrolase.[5] Norcarbocyclic nucleosides are another class of carbocyclic nucleoside analogs that lack a methylene group at C-5'. These were first synthesized by Schneller and Trost in 1987.[4] These are more specifically referred to as 5'-norcarbocyclic

nucleosides and were first synthesized in an attempt at making analogues of neplanocin A and aristeromycin that exhibit a lower toxicity.[4] It was theorized that the absence of the methylene group would prevent phosphorylation and lower activity. Several research groups have shown that the cytotoxicity of these is much lower than Aristeromycin and Neplanocin A and their mode of action has been demonstrated to be the inhibition of *S*_Adenosylhomocysteine hydrolase (SAH hydrolase).[4]

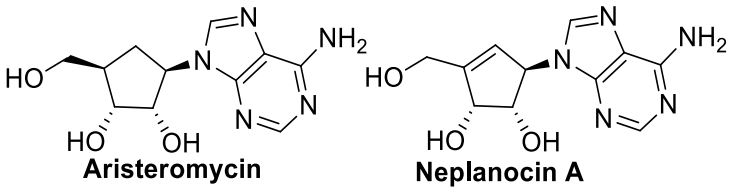


### *1.5 Synthesis of Nucleoside Analogues*

Various methods exist for the preparation of nucleoside analogues. One of the main routes is the introduction of nucleobases directly onto the sugar moiety. Heterocycles can be introduced by direct nucleophilic substitution via an $S_N2$ protocol. Examples of such are addition of a nucleobase to a haloalkane (Scheme 1).[6]

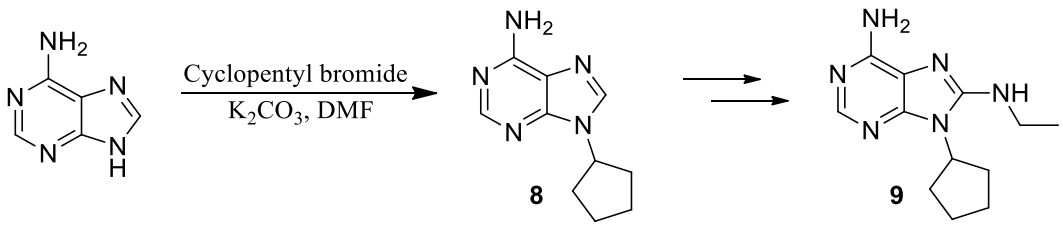


Scheme 1: *N*-alkylation of adenine to a haloalkane via $S_N2$ mechanism

Derivative **9** showed antifungal activity against Candida albicans (ATCC 10145), a fungi that grows as yeast and filamentous cells and is a cause of oral and vaginal infections.

Others have used activated alcohols in the form of tosylates[7–11] and triflates.[7,12,13] Tosylates have been employed as intermediates to synthesize biologically active cyclobutane

nucleoside analogues against a broad spectrum of herpes viruses (Scheme 2).[11]

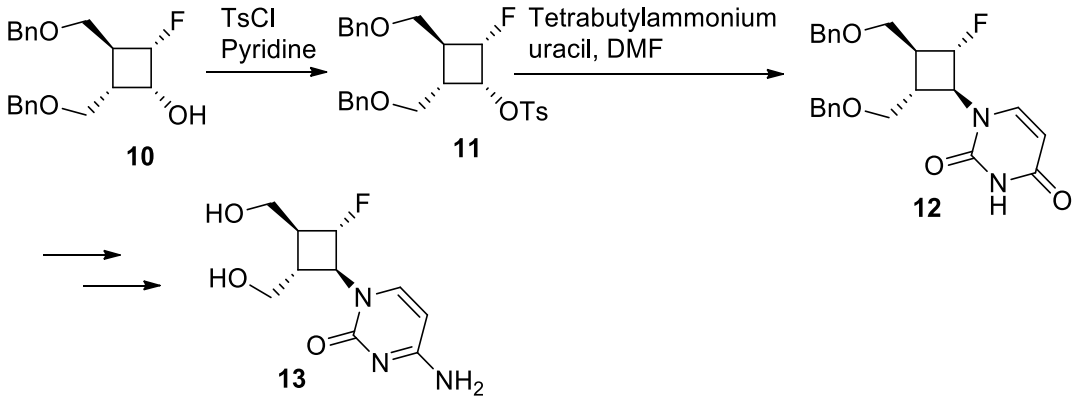


Scheme 2: Nucleoside analog synthesis via an activation of an alcohol

The Mitsunobu reaction has also been employed to synthesize various acylic,[14–16] carbocylic[15,17–20] and other nucleoside analogues[16] under mild conditions in moderate yields. Hubert and coworkers have employed the Mitsunobu reaction to prepare a cyclobutene carbovir analog (Scheme 3).[17] Advantages of the Mitsunobu reaction include mild conditions, one-pot reaction, applicability for a variety of purine and pyrimidine bases, and stereospecificity. The reaction proceeds with inversion of stereochemistry. Disadvantages include the production of stoichiometric amounts of triphenyl phosphene oxide and a mixture of *O*- and *N*-alkylations with pyrimidine bases.[20]

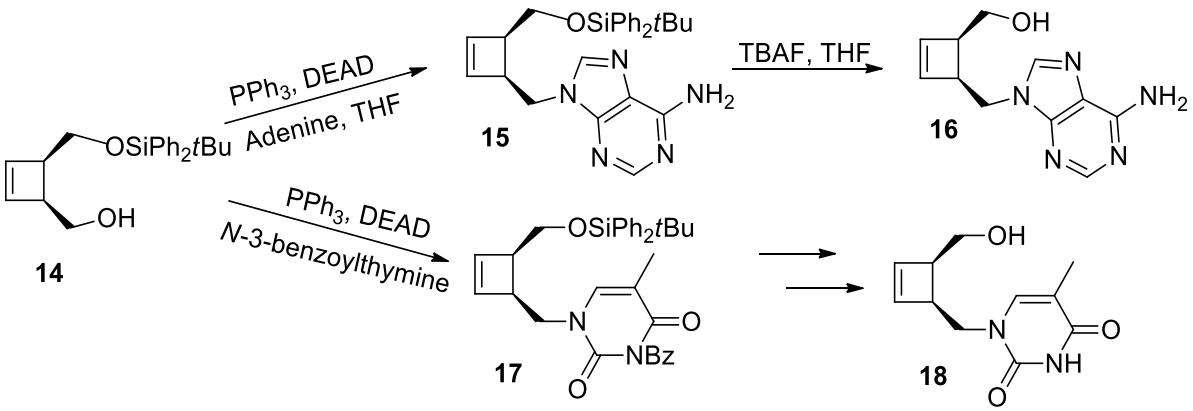


Scheme 3: Mitsunobu reaction of an alcohol to yield nucleoside analogs

Other methods of alkylation with a nucleobase include Michael additions and Trost reactions. These methods are restricted to activated alkene moieties. Trost proposed a highly regio- and stereoselective synthesis of nucleoside analogues from epoxycycloalkenes **19** with nucleobases (Scheme 4).[4]

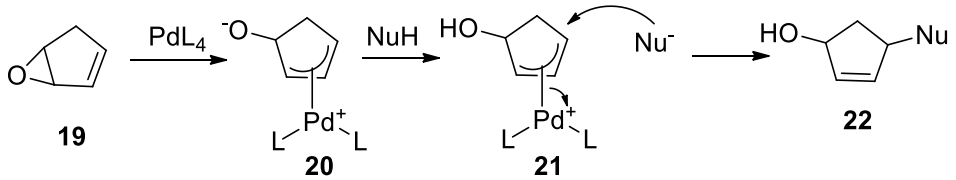


Scheme 4: Trost reaction with variety of nucleobases to yield nucleoside analogs

### *1.6 Charge distribution of purines*

The *N*-alkylation of purines often gives a mixture of *N*-7- and *N*-9-alkylated regioisomers. On deprotonation at *N*-9, the negative charge can be delocalized over three centres, *N*-7, *C*-8 and *N*-9. The negative charge mainly resides at *N*-9 with a smaller charge distribution at the N-7. Theoretical calculations show a charge distribution of (-0.59) for *N*-9 and (-0.37) on *N*-7 for 6-chloropurinyl anion and (-0.56) at *N*-9 centre and (-0.45) for *N*-7 for the parent purine anion.[21]

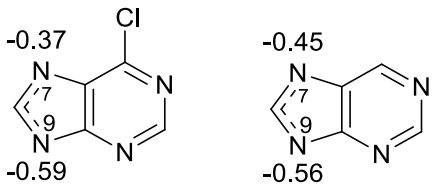


### *1.7 Cyclobutanones as precursors to nucleoside analogues*

Cyclobutanones can be readily synthesized by a [2+2] thermal cyloaddition of an alkene with dichloroketene, prepared *in situ* by dechlorination of trichloroacetyl chloride, followed by dechlorination of the resulting dichlorocyclobutanone (Scheme 5).[21–25] *N*-Alkylation of a

nucleobase to the cyclobutanone, followed by either reduction or photochemistry can be used to make acylic as well as, four and five-membered ring nucleoside analogues (Eq.1 & 2).[21]

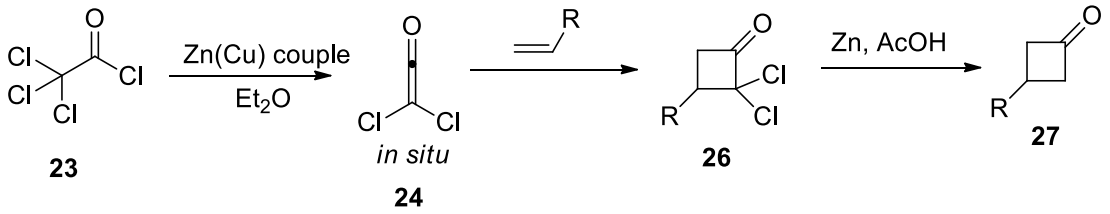


Scheme 5: Synthesis of Cyclobutanone by [2+2] cycloaddition of an alkene and dichloroketene

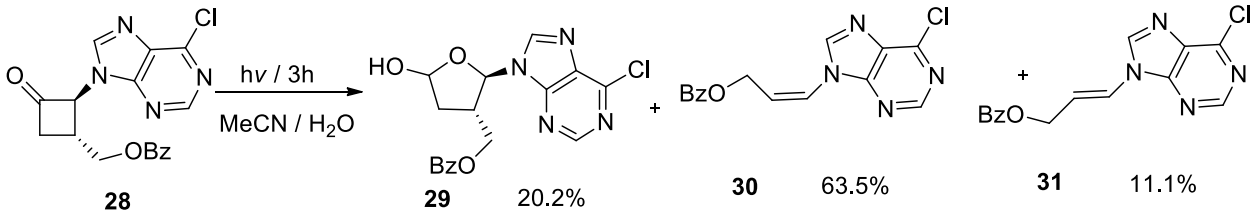


(1)

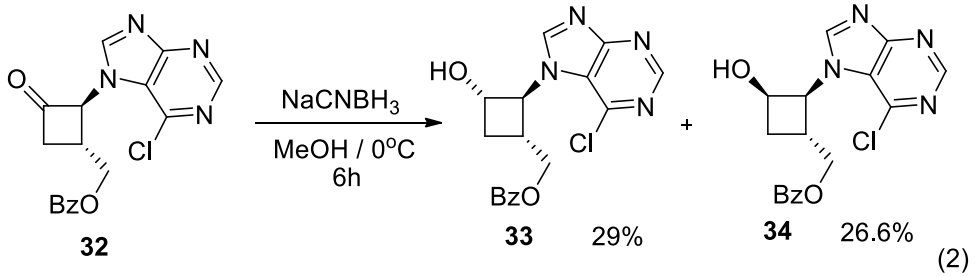


(2)

### *1.7.1 Photochemistry of Cyclobutanone*

Cyclobutanones can undergo three different photochemical pathways including: cycloelimination, ring-expansion and decarbonylation (Scheme 6).[26,27] On exposure to light, ketone **35** undergoes excitation to a singlet excited species ($S_1$) **36,** by n $\rightarrow \pi^*$ transition at a wavelength of 300 nm.[28,29] In its excited state, it can proceed by α-cleavage to a 1,4-acyl-alkyl biradical. The cleavage generally occurs at the more substituted position as a result of radical stabilization. This biradical **37** can lead to a ring-expansion isomerization to an oxa-carbene, with retention of stereochemistry [26] of the ring substituents, or cycloelimination to an alkene also

with stereochemical retention. The oxa-carbene can insert into acidic X-H groups such as alcohols or water to produce acetals, or acidic N-H to produce amino-acetals. In the absence of acidic carbene scavengers, cycloelimination occurs. The distribution of cycloelimination and ring-expansion products is also dependent on the polarity of the medium. [26] Dimerization is also possible in concentrated solutions.[26] One proposed mechanism for cycloelimination is the formation of the 1, 4 acyl-alkyl biradical followed by a β-cleavage. This yields a ketene and an alkene. Decarbonylation can occur through the triplet state ($T_1$). However, this state is rarely involved in direct irradiation since the release of strain in ring-expansion and cycloelimination from the singlet state makes this pathway very efficient. Decarbonylations of cyclobutanones from the triplet state is only accessible by triplet photosensitization in solvents such as acetone or in the gaseous phase.[30,31]

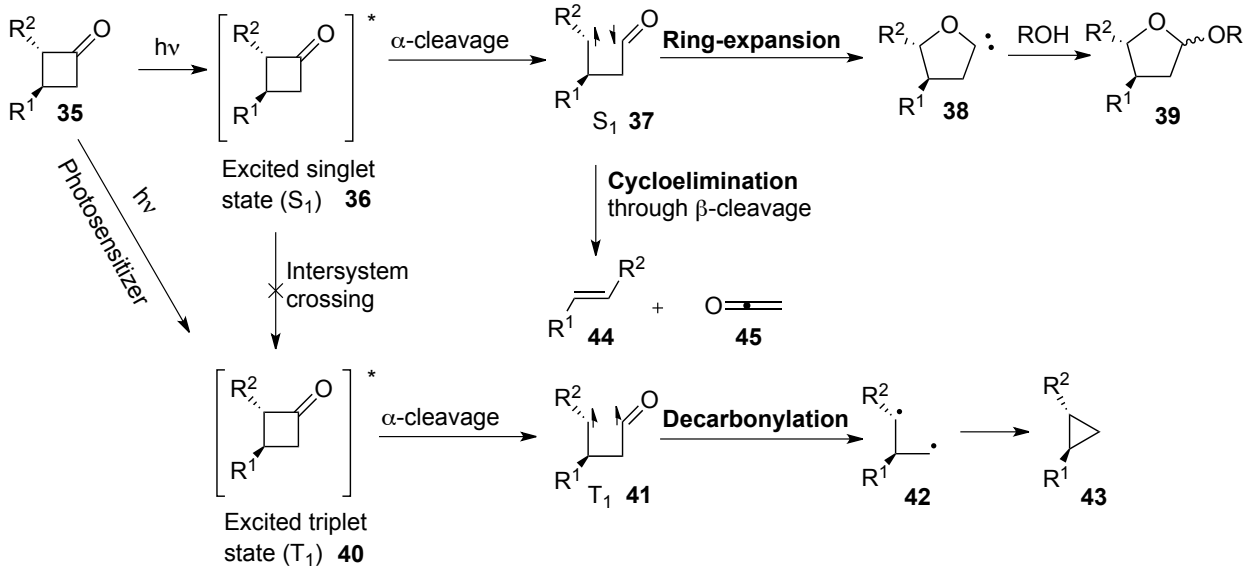


Scheme 6: Photochemistry of cyclobutanones

### *1.8 Proposal*

The objective of this research project was to make four-membered carbocyclic and furanose-analogs using cyclobutanones since the biological activities of three, four, five and six membered nucleoside analogues have been a target of interest due to the potential antiviral and

anticancer activities. This has led to the synthesis of cyclopropyl,[32,33] cyclobutyl[11,34,35] and cyclopentyl[36,37] nucleoside analogs. Oxetanocin-A (OXT-A) **46** is a naturally occurring four-membered adenine nucleoside that exhibits antiviral activity and is used as an antibiotic.[35] It's activity has motivated others to make carbocyclic analogues such as Cyclobut-A **47** and Cyclobut-G **48** which possess selective anti-HIV activity.[1,35,38]

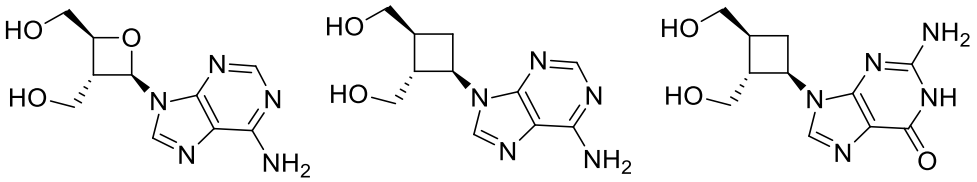


Due to the interesting photochemical transformation that cyclobutanones can undergo, they can potentially be used as precursors to analogues with varying ring sizes for the sugar moiety. The reduction of cyclobutanones could give four membered nucleoside analogues that could be used as oxetanocin carbocylic analogues. Cylcobutanones can also be used for synthesis to create three and five-membered ring nucleoside analogues.

Debenzoylation of **49** can be used to create a cyclobutanone with a hydroxyl methyl at the β- position, which can be coupled to purine and pyimidine nucleobases for the preparation of homonucleoside analogs of OXT-A (scheme 7).

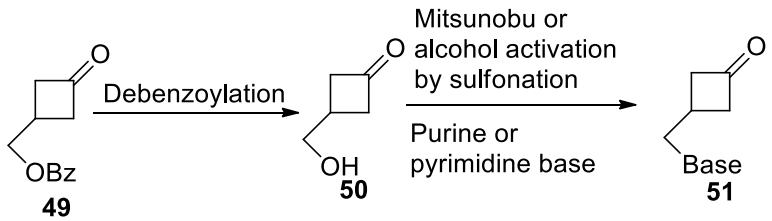


Scheme 7: Proposed introduction of a nucleobase to cyclobutanone **49**

The objective of this research project was to synthesize **52** and **54**, a four-membered carbocylic and a five-membered ring isonucleoside analog, from reduction or photolysis of **51,** respectively (Scheme 8).

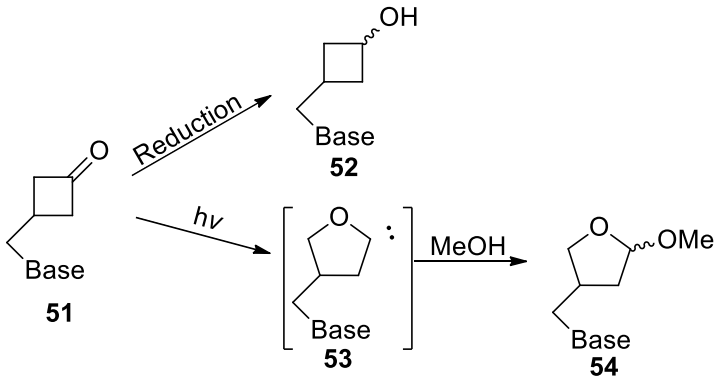


Scheme 8: Proposed synthesis of novel nucleoside analogs from cyclobutanone derivatives

The photochemical ring expansion of cyclobutanones yields oxacarbenes that can insert into alcohols or acidic N-H bonds.[39–44] Photochemical ring expansion of **51** followed by insertion in $H_2O$ or MeOH should give **54,** a furanose nucleoside analog.

# Chapter 2

### *2.0 Results and Discussion*

### *2.1 Synthesis of substrate 49*

The isolation of OXT-A in 1986, from fermentation of *Baccilus megaterium* broth with an oxetanosyl sugar, demonstrated potent inhibition of HSV-1, HSV-2, HCMV, and HIV-1, which motivated chemists to synthesize related analogues.[45] Carbocylic analogues, Cyclobut-A and Cyclobut-G were synthesized to improve metabolic stability.

Similarly, our focus was to add to the library of such oxetanoncin analogues from cyclobutanone precursors. A cyclobutanone with a protected hydroxymethyl group on the β-position, **49** was chosen as the precursor since it is readily synthesized and could be used for a variety of novel nucleoside analogues. Ketone **49** can be prepared from a [2+2] cylcoaddition of allyl benzoate **55**[46] with dichloroketene, generated *in situ* from dechlorination of TCAC with Zn-Cu couple followed by reduction with Zn powder (Eq.3).[47]

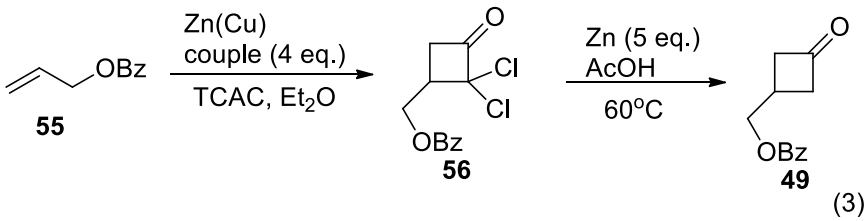

(3)

### *2.2 Debenzoylation of ketoester* **49**

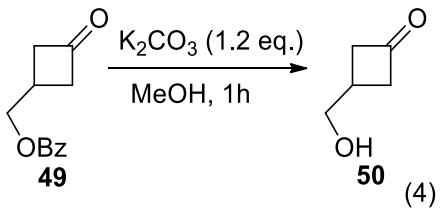

(4)

Debenzoylation of **49** using a saturated solution of NaOMe in methanol[48,49] yielded the deprotected alcohol **50** in minute quantities with the remaining being indiscriminate

decomposition products as evident from the streaking baseline on TLC (EtOAc). We decided to use $K_2CO_3$, a milder base, at room temperature which afforded **50** in 75 % yields (Eq.4). We proposed the possibility of decomposition of **50** in basic conditions. This was supported by the observed decrease in yield to 47% when the reaction time was extended to 3 h.

The structure of **50** was confirmed by the disappearance of the benzoyl proton signals in the aromatic region of the $^1$HNMR spectrum as well as a shift in the bridging methylene peaks from 4.50 ppm in the ester to 3.75 ppm for the alcohol. The shift of the carbonyl peak, of 12 $cm^1$, from 1787 to 1775 $cm^1$ in the IR spectrum is also evidence of this transformation.

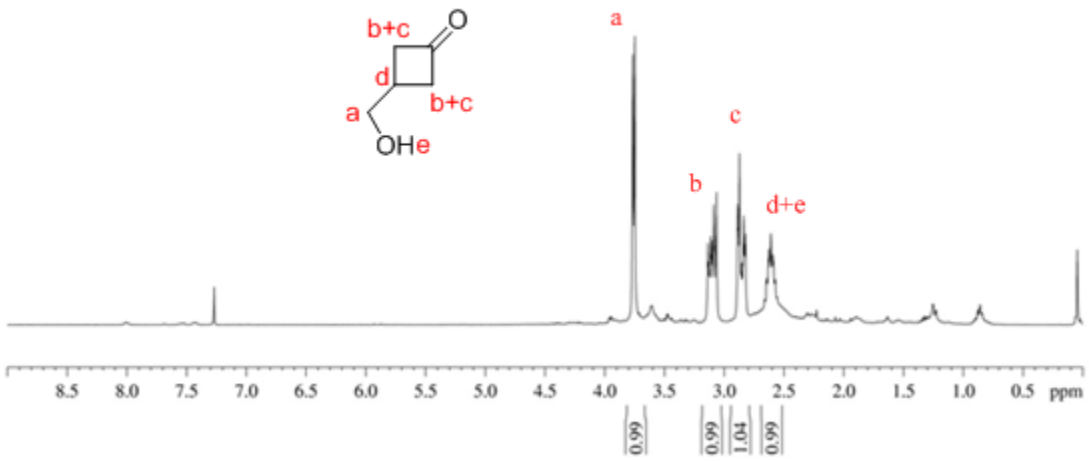


Figure 5 – $^1$H NMR spectrum of alcohol **50**

### *2.3 Triflation of alcohol* **50**

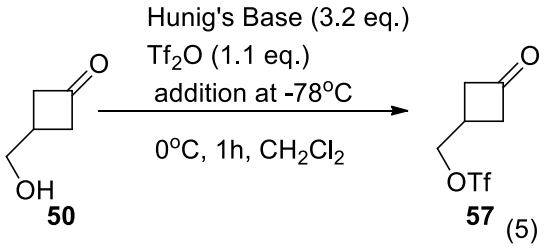

(5)

The addition of Hunig's base followed by a dropwise addition of trifluoromethanesulfonic anhydride ($Tf_2O$) to a solution of **50** in $CH_2Cl_2$, afforded the triflate **57** in quantitative yields (Eq.5). The triflate was not isolated or characterized due to its unstable nature. The structure assignment was confirmed by the observation of deshielding of the methylene protons at $\delta$ 3.75 ppm (d, $J$ = 6.2 Hz, 2H) for the alcohol **50** to $\delta$ 4.68 ppm (d, $J$ = 6.1, 2H) after triflation in the $^1$H NMR spectrum of **57**. The triflate was highly reactive and not sufficiently stable to run 2-D NMR experiments. Decomposition occurred minutes after preparation.

Triflation did not occur when trifluorosulfonyl chloride was used as the triflating agent, and when other conventional bases such as pyridine and trimethylamine were used.

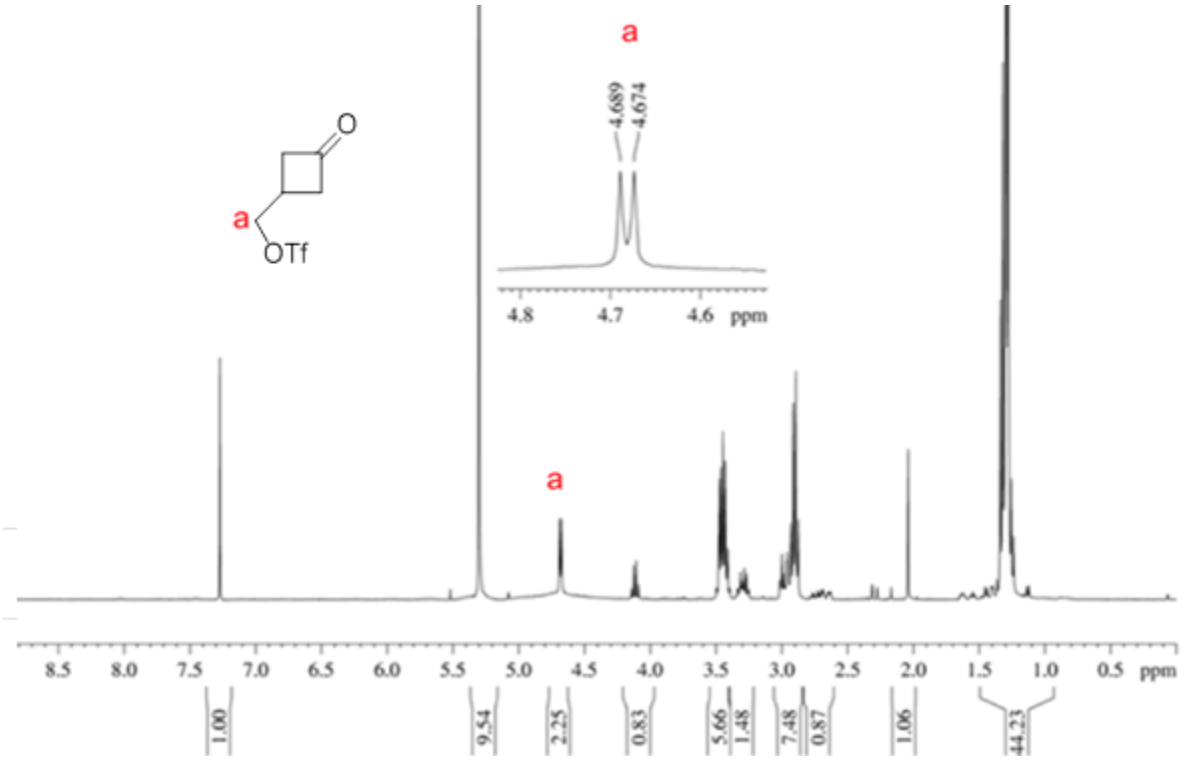


Figure 6 – $^{1}$H NMR spectrum of crude triflate **57**

### *2.4 N-Alkylation of triflate 57*

The introduction of nucleobases via $S_N2$ attack of the heterocyclic salts on alkyl sulfonates, is well documented.[6–13] The pKa of purines and pyrimidines is generally between 8 to 10 and their salts can be readily prepared via deprotonation by inorganic bases such as carbonates, hydroxides, hydrides etc. [6–13,49] Thus, we proposed the use of a 6-chloropurinyl salt, previously prepared in our lab with similar cyclobutanone derivatives. The 6-chloropurinyl salt was prepared by stirring with potassium hydroxide in acetonitrile with 5% molar tris[2-(2-methoxyethoxy)ethyl]amine (TDA-1). Subsequent addition of the crude solution of triflate **57**, afforded a total of 88% *N*-alkylated products as the *N*-9 **60** and *N*-7 **61** ketones in 51% and 37% yields, respectively (Eq.6). Previous attempts at *N*-alkylation involved mesylation and tosylation

of **50** followed by addition to a solution of the 6-chloropurinyl salt. The yields were very low (< 4%) even under elevated temperatures of 60 $^{o}$C and prolonged reaction time of 24 h.

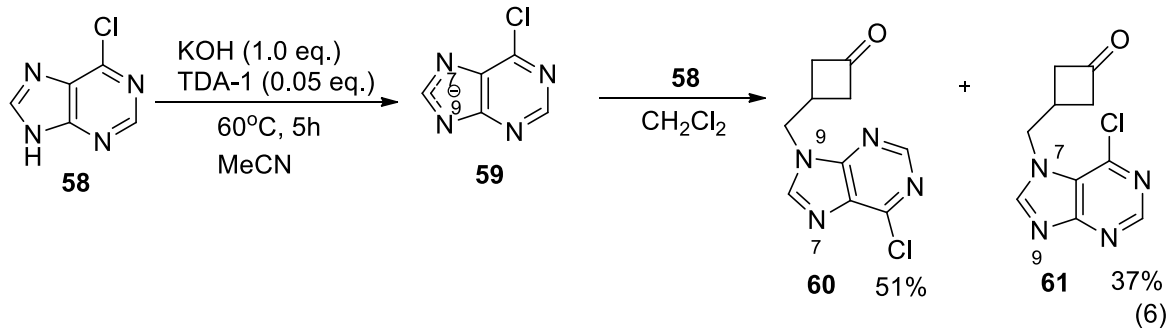

(6)

The observation of *N*-7 and *N*-9 alkylations is known with purines due to the negative charge distribution for the purinyl and 6-purinyl anions as described previously. The larger negative charge (-0.59) for the 6-chloropurinyl anion **59** resides at *N*-9 and the smaller charge (-0.37) resides at *N*-7 (Scheme 9).[21]

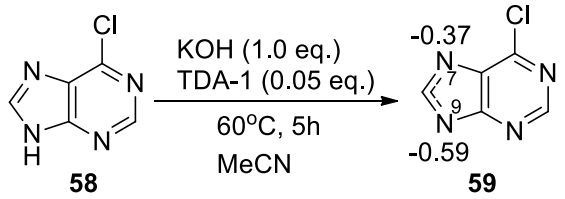

Scheme 9: Computational charge density of 6-chloropurinyl anion

The TLC of the crude solution showed two major UV-active spots with $R_f$ values of 0.45 and 0.22 (5% MeOH in $CHCl_3$). In previous studies, *N*-alkylation of purine bases to similar cyclobutanones often yielded the *N*-7 alkylated products as the more polar component. The methylene protons adjacent to *N*-7 are more deshielded relative to the corresponding protons of the *N*-9 alkylated products in the $^{1}$H NMR spectra. The methylene protons for the alcohol **50** ($\delta$ 3.75, d, $J$ = 6.2 Hz, 2H) and triflate ($\delta$ 4.68, d, $J$ = 6.1, 2H) were replaced by a set of two new methylene peaks at $\delta$ 4.54 (d, $J$ = 7.6 Hz, 2H) and $\delta$ 4.73 (d, $J$ = 7.6, 2H), with similar coupling constants. The relative ratio was determined to be 1:0.68 by integration. Also two pairs of aromatic peaks at δ 8.78 (s, 1H), 8.17 (s, 1H) and δ 8.92 (s, 1H), 8.32 (s, 1H) with similar

relative integral areas of 1:0.6-0.7 were observed. This is close to the calculated ratio of charge localization on *N*-9 and *N*-7 (-0.59:-0.37 ≈ 1:0.63). Furthermore, the IR spectrum showed two carbonyl peaks, at 1779 $cm^{-1}$ and 1777 $cm^{-1}$ typical of cyclobutanones. Thus, it was proposed that the major product was the *N*-9 coupled ketone **60** and the minor product was the *N*-7 coupled ketone **61**. The major product was separated and confirmed to be **60** based on 1D ($^{1}H$ NMR and $^{13}C$ NMR) and 2D NMR (HSQC and HMBC) experiments.

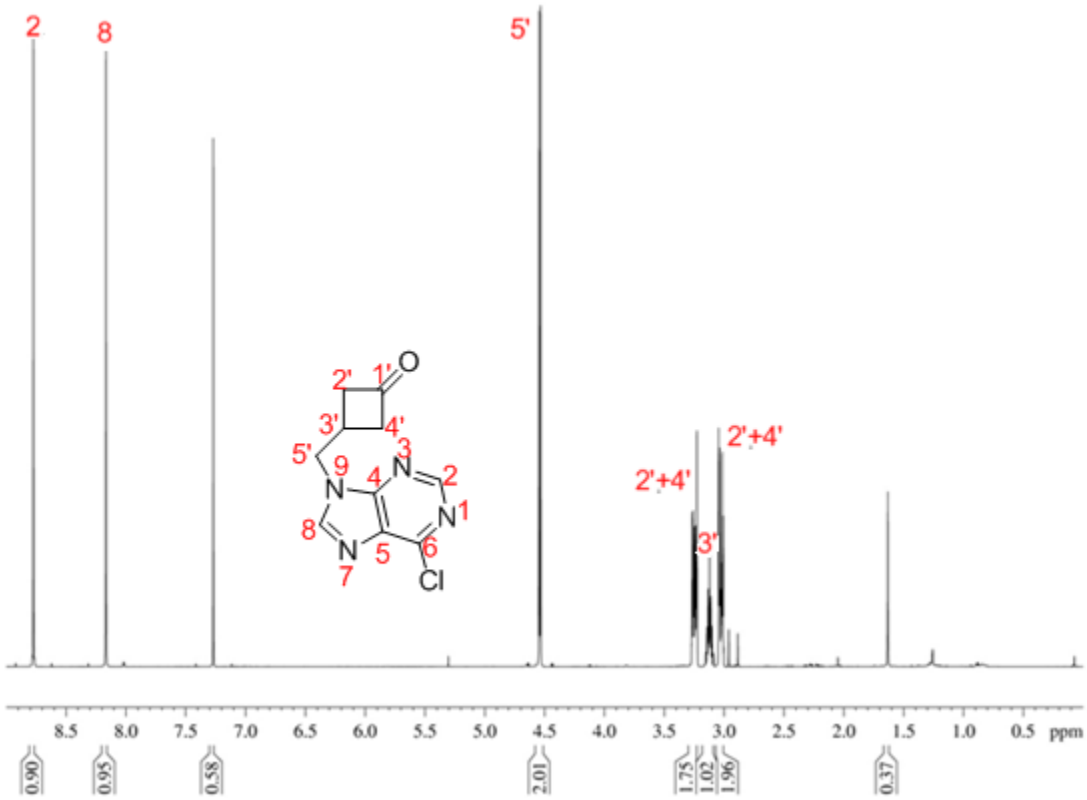


Figure 7 – $^{1}H$ NMR spectrum of *N*-9 ketone **60**

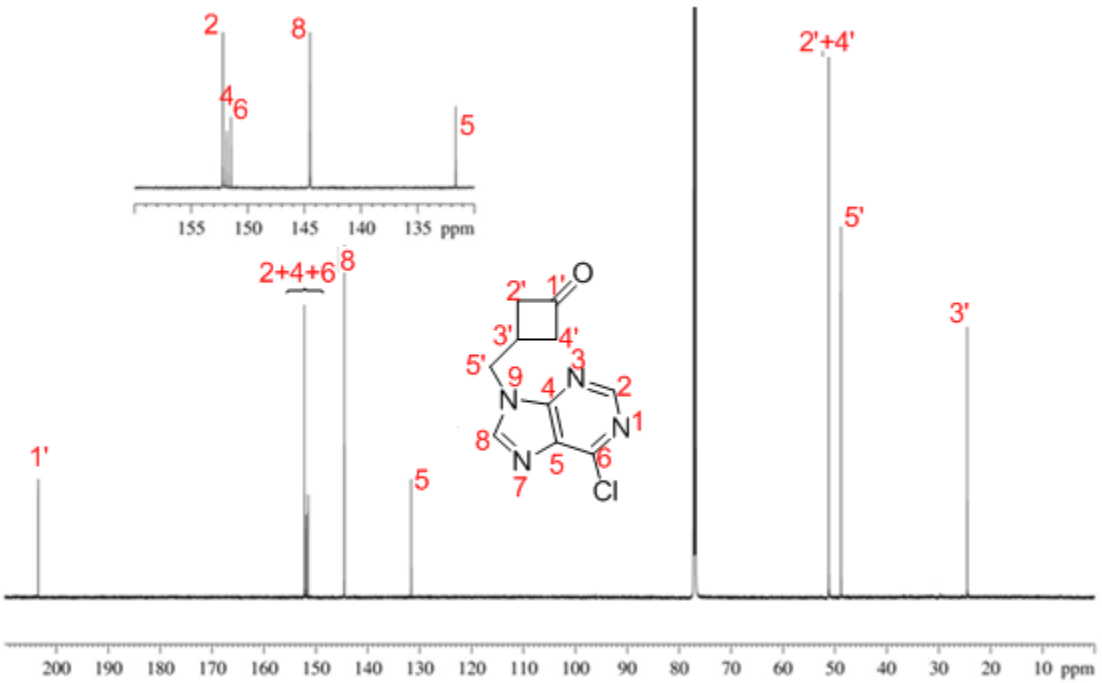


Figure 8 – $^{13}$C-NMR spectrum of *N*-9 coupled ketone **60**

The *N*-9 substituted derivatives can be distinguished from *N*-7 isomers using 2D NMR spectroscopy such as HSQC and HMBC. The regioisomers can be distinguished by first identifying the aromatic protons and the carbons on the purine ring, followed by confirmation of the relationship between the bridging methylene protons, H-5', and the purinyl carbon and nitrogen atoms.

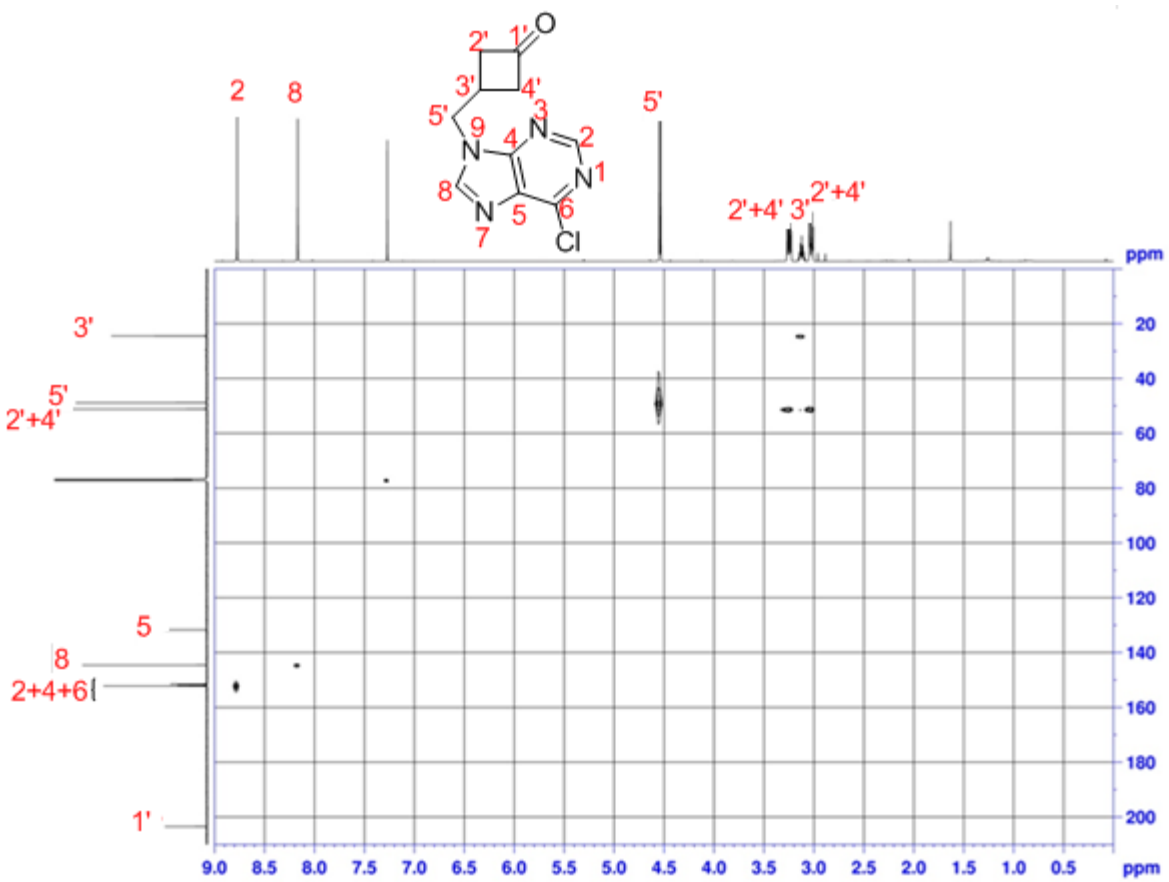


Figure 9 – $^{1}H$-$^{13}C$ HSQC of *N*-9 coupled ketone **60**

The use of HSQC spectroscopy allowed for facile distinction between secondary, tertiary and quaternary carbons. This coupled with HMBC spectroscopy allowed for the identification of C-4 and C-5 its relationship to C-5', and thus the connectivity to *N*-7 or *N*-9.

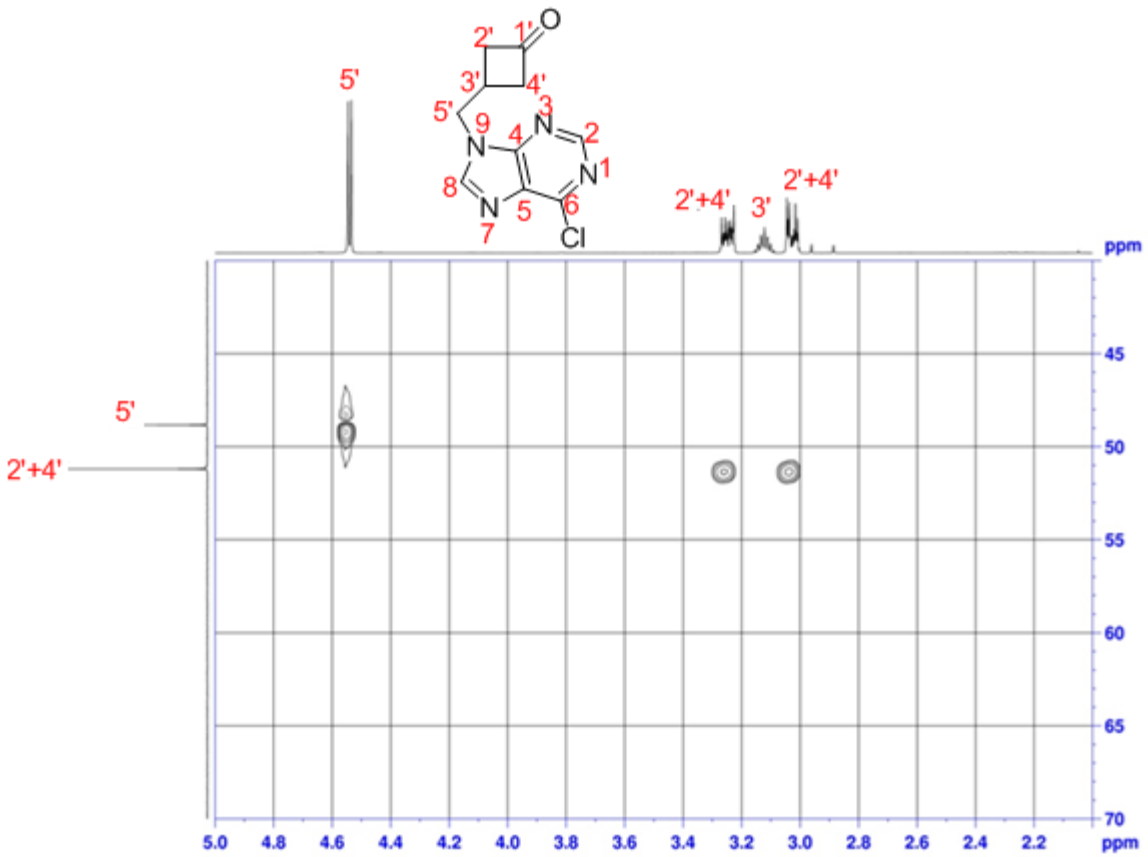


Figure 10 – Magnified $^{1}$H-$^{13}$C HSQC of *N*-9 coupled ketone **60**

The HSQC spectrum of ketone **60** (Figure 10) shows a correlation of two methylene groups H-2' and H-4' with the signal at $\delta$ 51.2 ppm, corresponding to two carbon atoms, C-2' and C-4' in the $^{13}$C NMR spectrum. This is supported by the inherent $C_{2v}$ symmetry that results in the two carbon atoms being in an equivalent magnetic environment, whereas the cis- and trans-protons are in different chemical environments, giving two distinct signals in the $^{1}$H NMR spectrum.

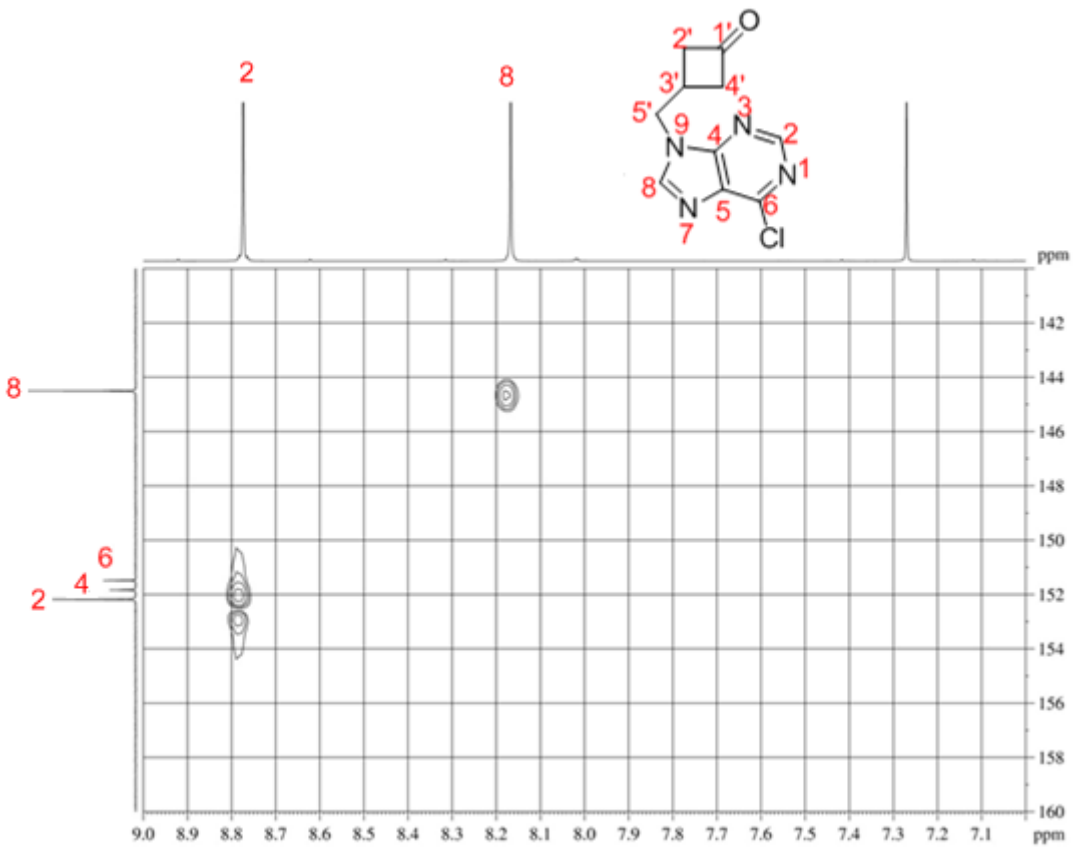


Figure 11 – Magnified $^{1}$H-$^{13}$C HSQC of aromatic peaks of *N*-9 coupled ketone **60**

The aromatic protons, H-8 and H-2, can be distinguished from one another based on the correlation of H-5' with C-8 in the $^{1}$H-$^{13}$C HMBC spectrum, which also shows coupling to H-8 in the HSQC spectrum. The C-4 peak can be characterized since it correlates to both H-8 and H-2 in the HMBC spectrum.

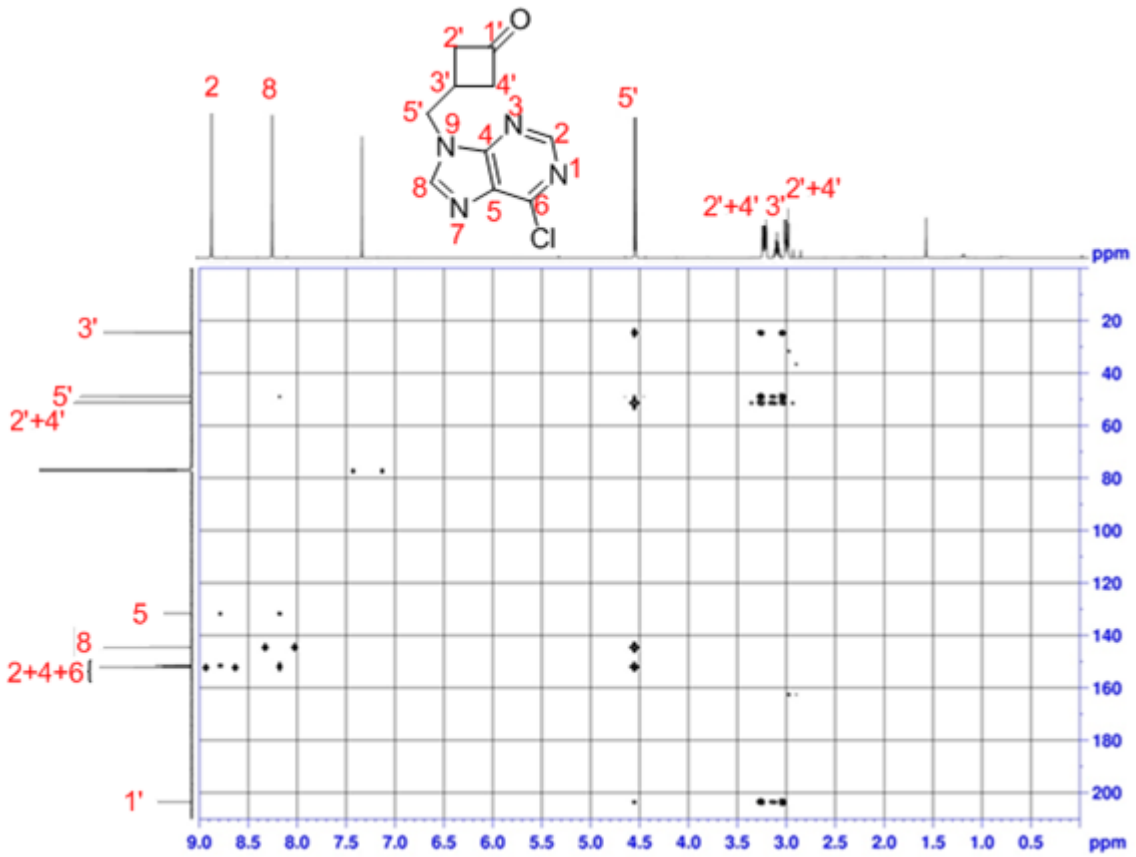


Figure 12 –$^{1}$H-$^{13}$C HMBC of *N*-9 coupled ketone **60**

The HMBC spectrum can be used to characterize the carbons on the 6-chloropurine ring, which in turn gives information about connectivity to the cyclobutanone ring, and thus the regiochemistry of alkylation at either *N*-7 or *N*-9. The signals associated with C-5 and C-6 can be characterized by their correlations in the HMBC spectrum to H-8 and H-2, respectively.

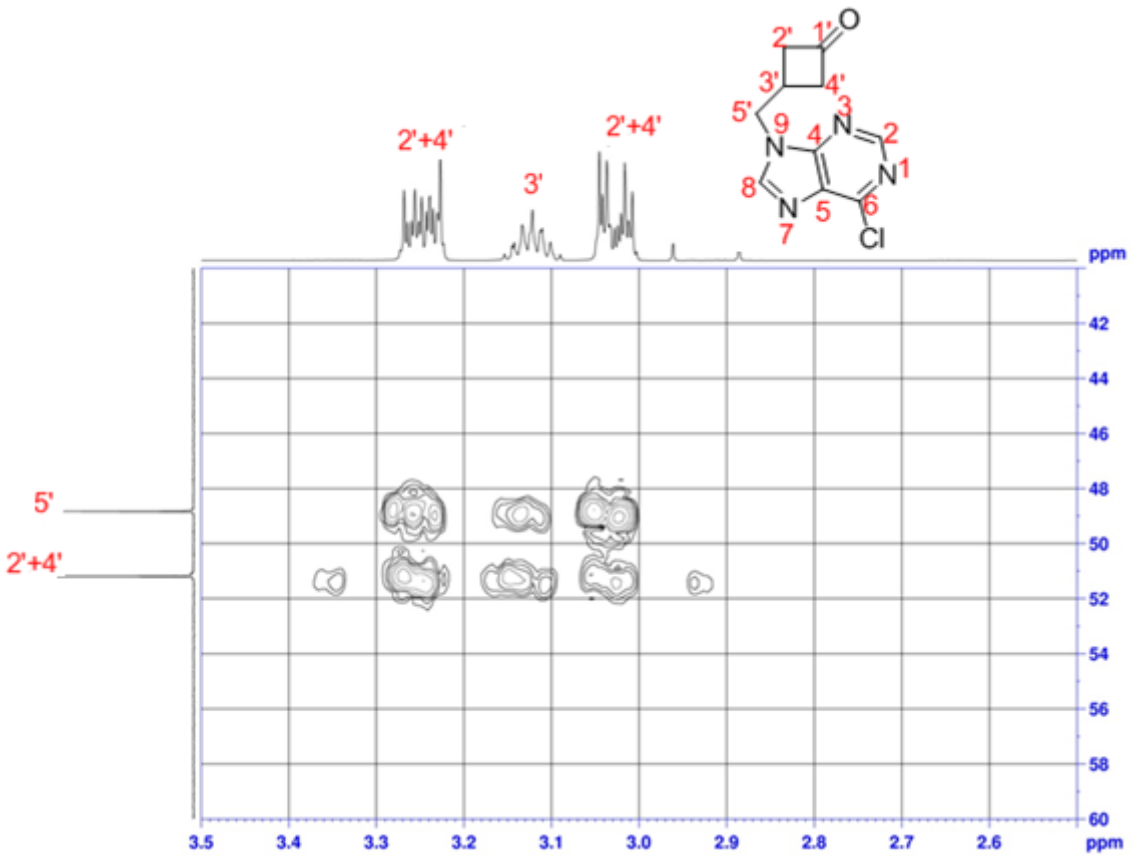


Figure 13 –Magnified $^{1}H$-$^{13}C$ HMBC of *N*-9 coupled ketone **60**

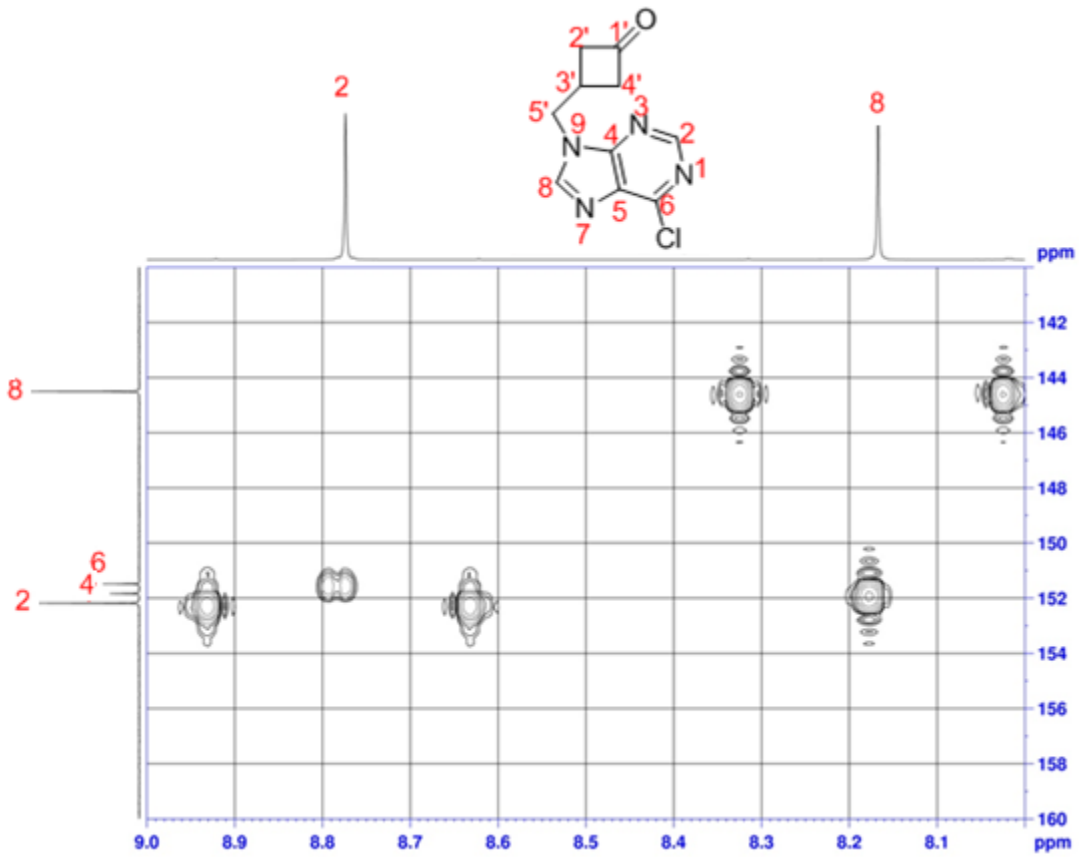


Figure 14 –Magnified $^{1}$H-$^{13}$C HMBC of aromatic region of *N*-9 coupled ketone **60**

As expected, *N*-9 alkylated ketone **60** shows a correlation of H-5' with C-4 (Figure 14).

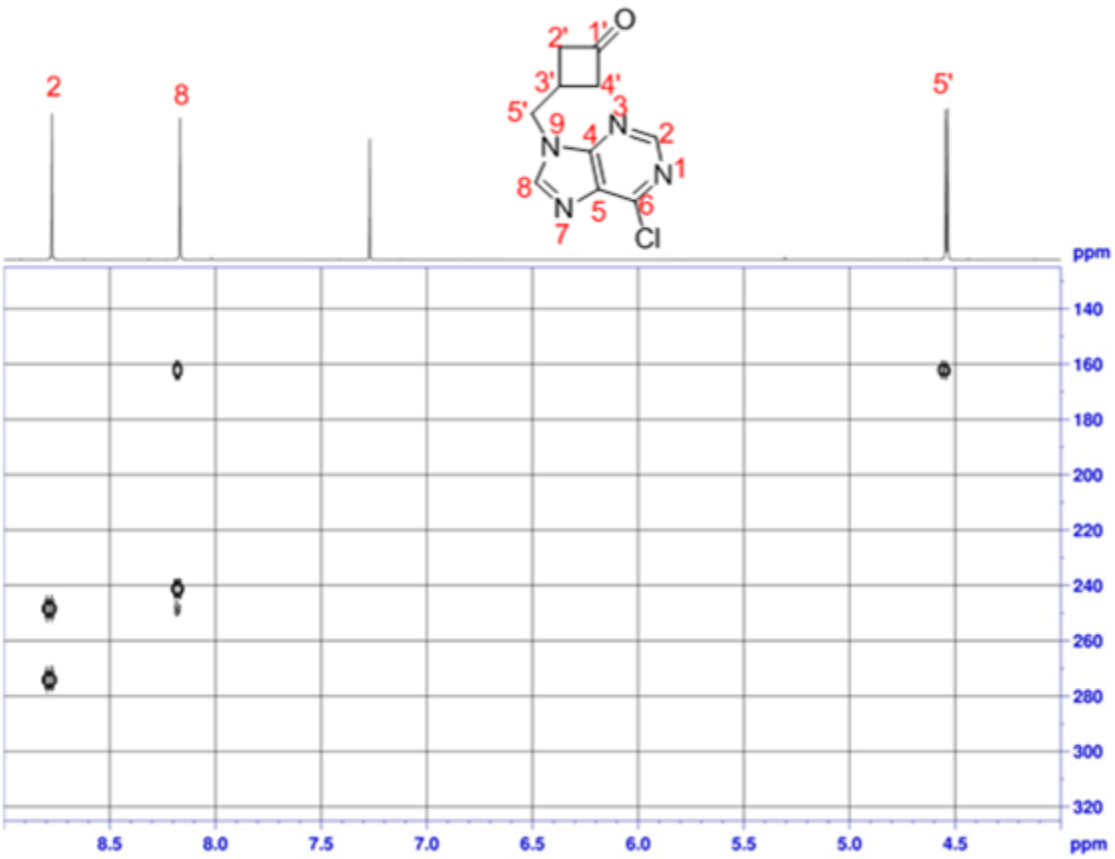


Figure 15 –$^{1}$H-$^{15}$N HMBC of *N*-9 coupled ketone **60**

Furthermore, a $^{15}$N NMR study[50] of *N*-7 and *N*-9 substituted purine derivatives showed the shielding of the alkylated nitrogen by more than $\delta$ 80 ppm. $^{1}$H-$^{15}$N HMBC showed a correlation between H-5' and *N*-9 where *N*-9 was shielded by a factor of approximately $\delta$ 80 ppm relative to *N*-7. The HRMS spectra showed peaks at *m/z* of 239.0510 and 237.0539, with intensities typical of the isotopic abundance of $^{37}$Cl and $^{35}$Cl (1:3) and an error of less than 1 ppm. A fragment at 155.0122 corresponding to the protonated of 6-chloropurine was also observed in the MSMS for the parent ion peak of *m/z* 237.0539. Furthermore, the X-ray structure of the alcohol **62** obtained from reduction of ketone **60** was consistent with alkylation at *N*-9 (*vide infra*).

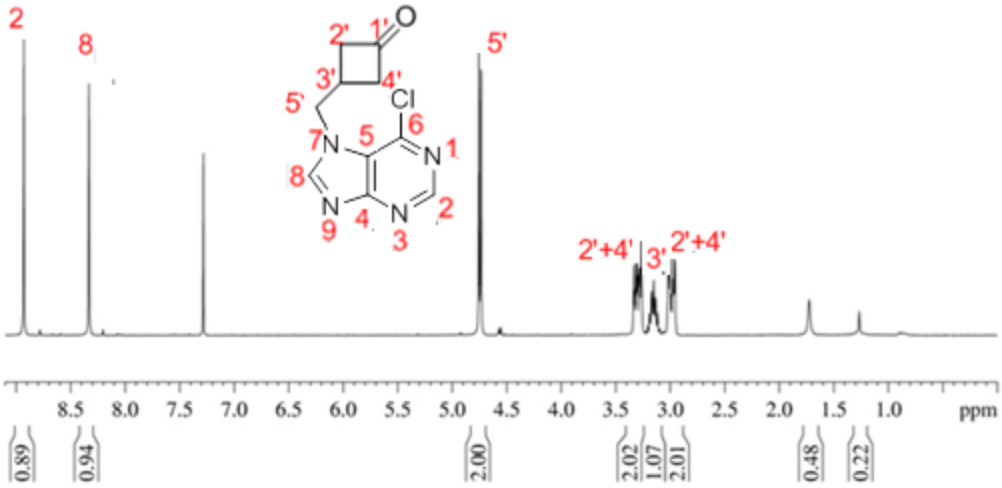


Figure 16 – $^{1}$H NMR spectrum of *N*-7 coupled ketone **61**

The $^{1}$H NMR spectrum of **61** (Figure 16) indicates the presence of protons resembling those for **60** in terms of splitting and chemical shifts. The proton at H-2 is generally more deshielded than H-8 as seen for both ketones **60** and **61.** Thus, the $^{1}$H NMR spectrum is a clear indicator of the regioisomer **60**.

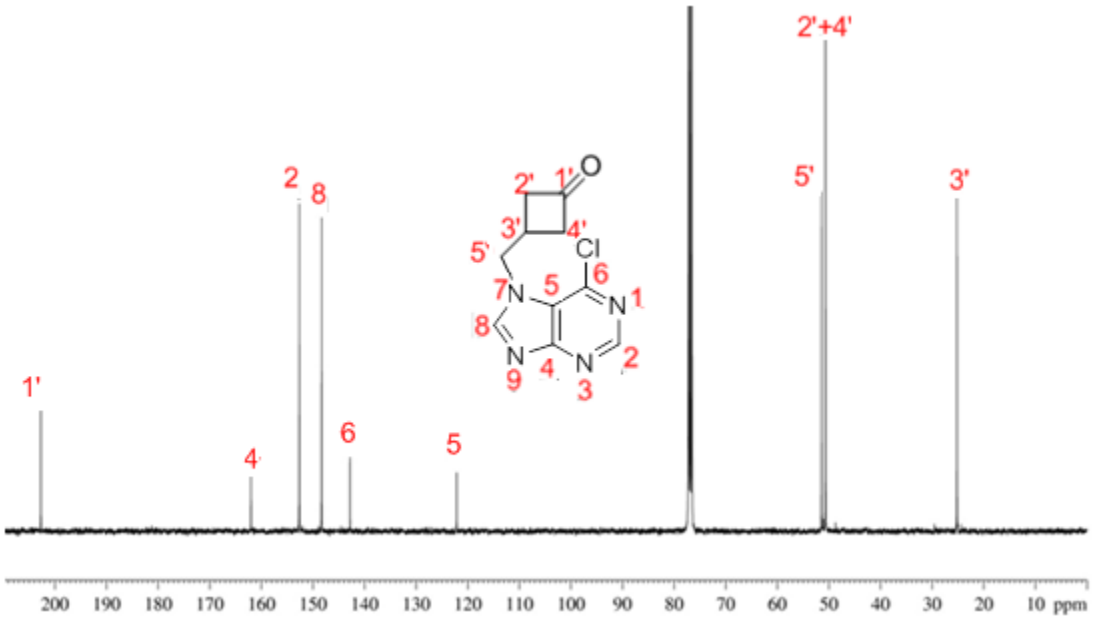


Figure 17 – $^{13}$C NMR spectrum of *N*-7 coupled ketone **61**

The $^{13}$C-NMR spectrum of **61** further indicated the presence of at least ten distinct carbon centers, with the aromatic carbon signals appearing at δ 162.0, 152.6, 148.3, 122.2 ppm and a carbonyl carbon at δ 202.7 ppm. One of the aromatic carbons, C-5, shows a greater shielding (δ 122.8 ppm) relative to C-5 of the *N*-9 ketone **60** (δ 131.6 ppm). The results were consistent with trends found in the literature.[51–53]

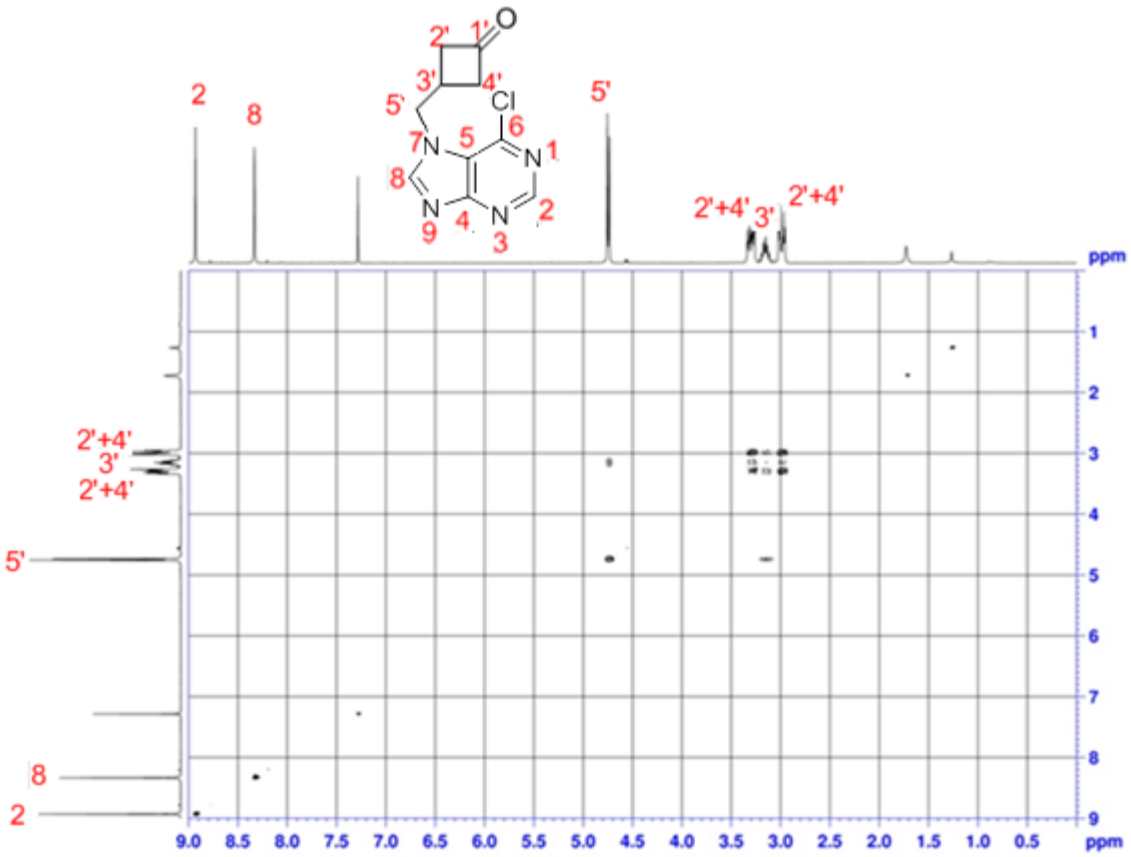


Figure 18 –$^{1}$H-$^{1}$H COSY of *N*-7 coupled ketone **61**

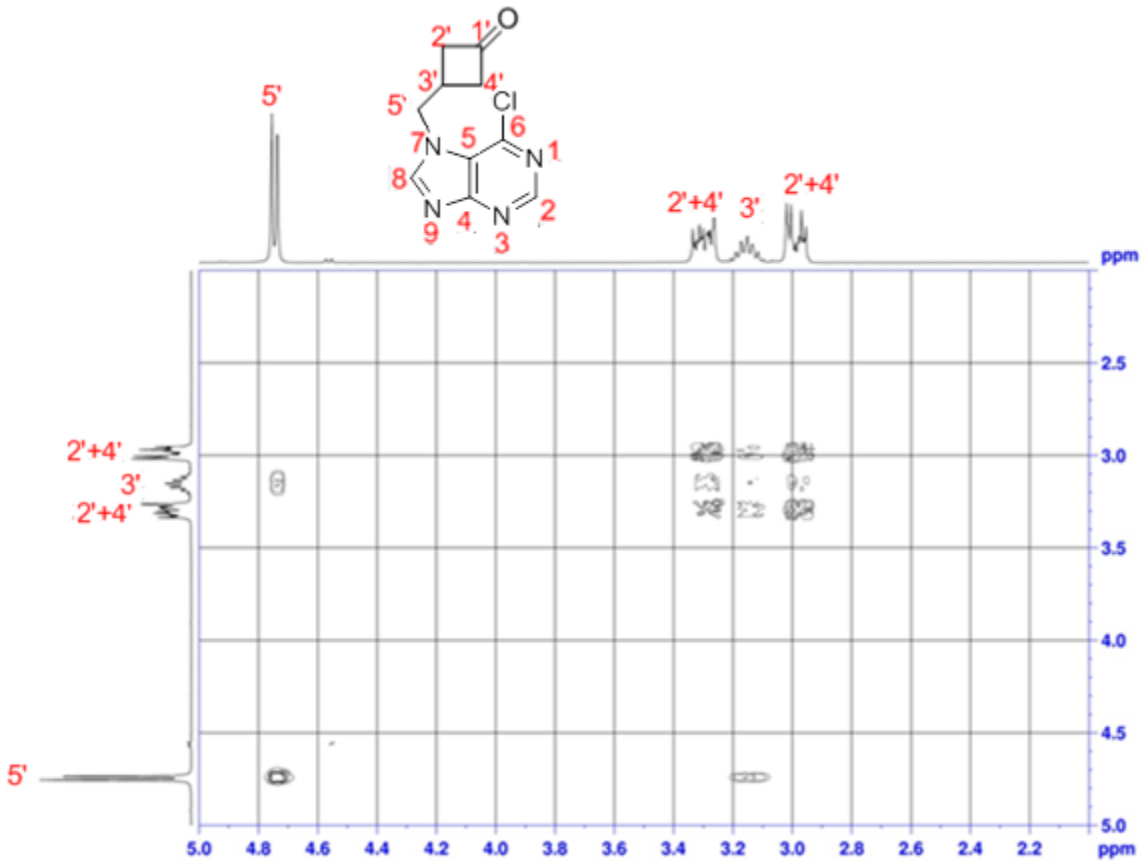


Figure 19 –Magnified $^{1}$H-$^{1}$H COSY of cyclobutanone peaks of the *N*-7 coupled ketone **61**

The COSY spectrum very clearly exhibits the spin-system of H-5', H-3', H-2' and H-4' as is associated with cyclobutanones indicating that it did not decompose under basic conditions of the *N*-alkylation step or under prolonged elution times under flash column chromatography.

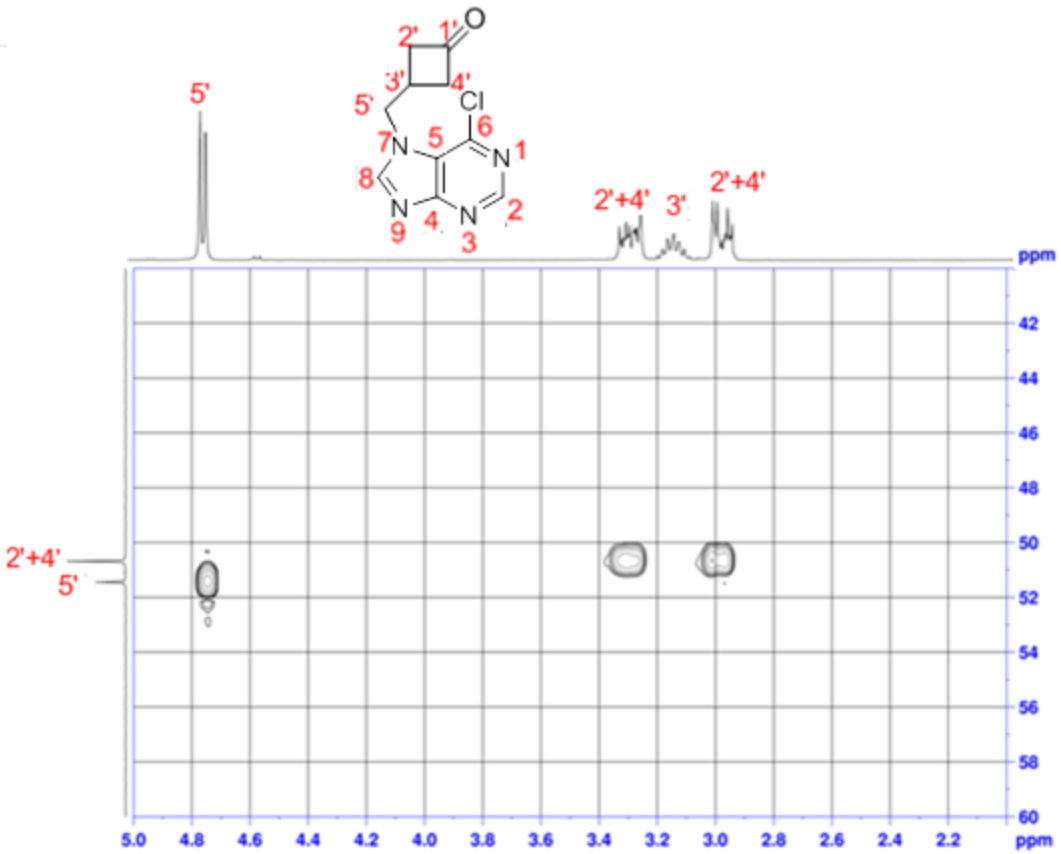


Figure 20 –Magnified $^{1}H$-$^{13}C$ HSQC of cyclobutanone peaks of the *N*-7 coupled ketone **61**

HSQC shows two correlations of H-2' and H-4' to one carbon peak, C-2' and C4' which is supported by the $C_2$ symmetry of the cyclobutanone, rendering the two carbon atoms equivalent.

Table 1: Comparison of $^{1}$H NMR and $^{13}$C-NMR shifts of **60** and **61** in ppm

| Atom-position | *N*-9 ketone **6** | *N*-7 ketone **61** |
|---|---|---|
| C-5’ | 3.27 | 3.32 |
| C-4 | 151.8 | 162.0 |
| C-5 | 131.6 | 122.2 |
| C-8 | 144.5 | 148.3 |
| H-8 | 8.17 | 8.32 |

The structural assignments of the *N*-7 and *N*-9 regioisomers was also supported by trends reported in the literature,[51–53] in terms of shielding and deshielding of specific nuclei. The C-5 signal is expected to be shielded for the *N*-7 isomer **61** relative to the *N*-9 isomer **60** due to steric congestion between the C-6 substituted chlorine and *N*-7, the site of alkylation. Furthermore, C-5’, C-4, C-8 and H-8 are expected to be upfield for the *N*-9 isomer relative to the *N*-7 isomer. The chemical shifts summarized in table 1 demonstrates that the data are consistent with those reported in the literature.

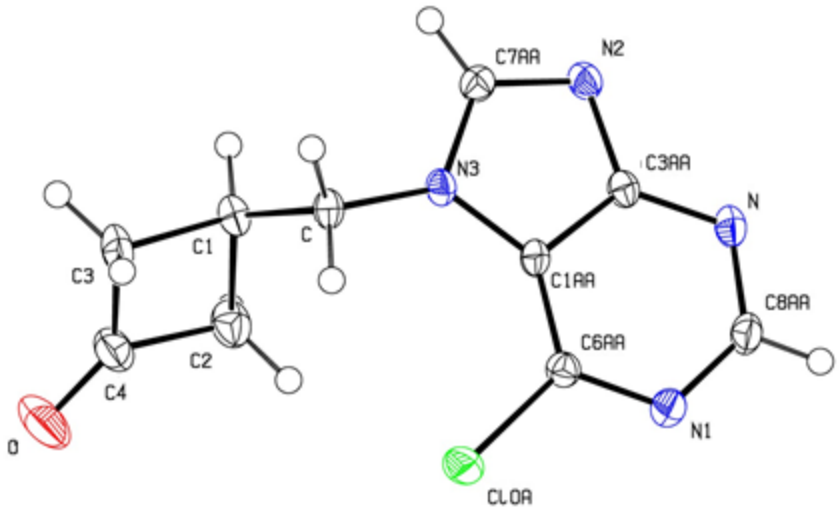


Figure 21- Crystal structure of *N*-7 ketone **61**

The crystal structure further confirmed the connectivity of the cyclobutanone ring with *N*-7. The HRMS spectra further supported the molecular composition of **61** with the 3:1 isotopic pattern for $^{35}Cl$ and $^{37}Cl$ (m/z of 237.0538 and 239.0510 for $M^+$) and fragmentation yielding the protonated 6-chloropurine (*m/z* of 155.0122) in the MSMS spectrum. The IR spectrum exhibits a sharp peak at 1777 $cm^{-1}$, indicative of a cyclobutanone. Thus, all of the evidence conclusively support the assignment of structure and regiochemistry for the *N*-7 and *N*-9 ketones **60** and **61**.

### *2.5 Reduction of Cyclobutanones 60 and 61*

Initial attempts to reduce ketones **60** and **61**, with sodium borohydride and lithium aluminum hydride, yielded two products as evident from TLC with very similar $R_f$ values and could not be separated. It was assumed that both cis and trans alcohols were being formed for both regioisomers, **60** and **61.** Thus, we assumed that we could obtain facial selectivity by altering, the reagents, solvent and temperature.

Table 2: Reaction conditions and results for reduction of ketones **60** and **61**

| **Regents** | **Solvents** | **Temperature** | ***N*-7 ketone (61)** | ***N*-9 ketone (60)** |
|---|---|---|---|---|
| $NaBH_4$ | MeOH | r.t | Quantitative conversion to cis and trans alcohols | Quantitative conversion to cis and trans alcohols |
| $LiAlH_4$ | $CH_2Cl_2$ | 0 $^oC$ | Sluggish reaction (24 h +), very low product conversion | Slow reaction (24 h +) cis and trans alcohol |

| | | | | |
|---|---|---|---|---|
| $LiAlH_4$ | $CH_2Cl_2$ | r.t | Sluggish reaction (24 h +), very low product conversion | Sluggish reaction (24 h +), very low product conversion |
| $LiAlH_4$ | $Et_2O$ | 0 $^oC$ | Fast reaction, quantitative conversion to cis and trans alcohols | Fast reaction, quantitative conversion to cis and trans alcohols |
| $NaBH_4$ | | 0 $^oC$ | Quantitative conversion to cis and trans alcohols | Quantitative conversion to cis and trans alcohol |
| $NaBH_3CN$ | MeOH | r.t | Sluggish reaction; trace cis and trans alcohol | Sluggish reaction; trace cis and trans alcohol |
| $LiAl(OtBu)_3H$ | $Et_2O$ | -78 for 2 h then r.t overnight | Quantitative conversion to cis alcohol | Quantitative conversion to cis alcohol |

Reduction by sodium borohydride and lithium aluminum hydride produced two products, in cases where the ketones reacted completely as was noted by the emergence of two methylene H-5' peaks in the $^1H$ NMR spectra of the mixture and two UV-active spots by TLC. We proposed that the activation barrier for trans hydride addition would be lower, forming the cis alcohol, the kinetic product. Thus, the use of lower temperatures and bulkier but stronger reducing agents would increase stereoselectivity. Since milder reducing agents such as sodium

cyanoborohydride produced a very low product conversion we turned to lithium tri-tert-butoxyaluminum hydride which has three bulky alkoxy groups and is a single hydride donor. Thus we attempted the reduction of ketones **60** and **61** at -78 °C in $Et_2O$ which successfully gave one stereoisomer quantitatively (Eq.7 & 8). We reasoned that a greater activation barrier for a cis-hydride addition would be required due to steric congestion of the bulky tert-butoxy groups and 6-chloropurine in the transition state. Not surprisingly, trans-addition was observed yielding cis alcohols **62** and **63**.

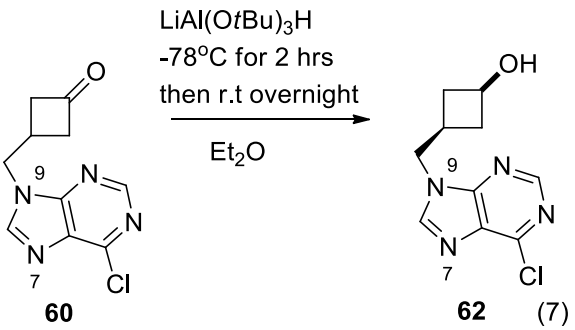


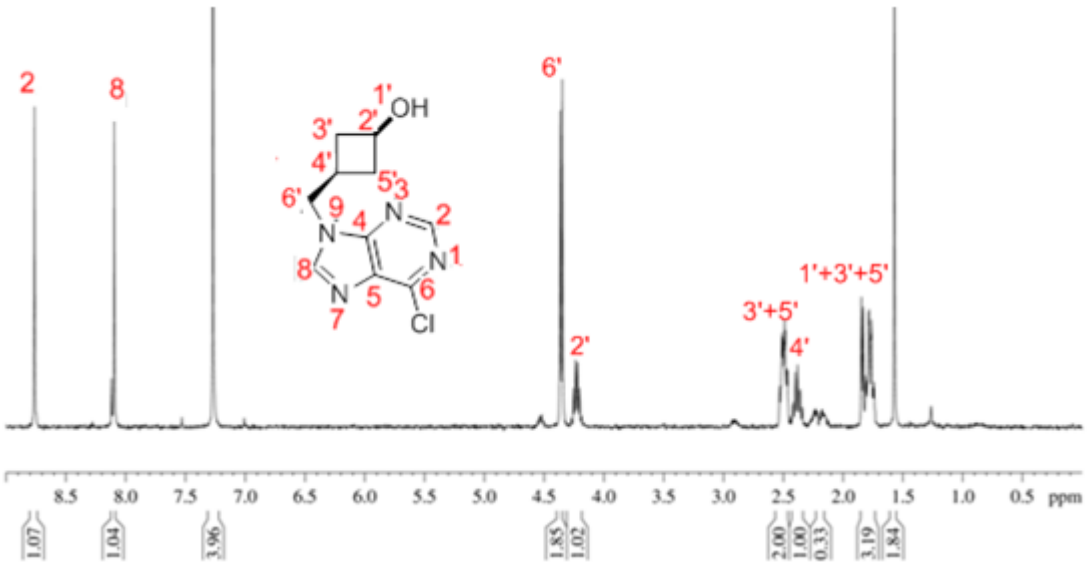


Figure 22 – $^1$H NMR spectrum of *N*-9 alcohol **62**

The NMR spectrum of the cis *N*-9 alcohol **62** (Figure 22) was consistent with the proposed stereoselective reduction based on the methylene shift of δ 0.18 ppm from ketone **60**

(δ 4.55 ppm, d) to **62** (δ 4.37 ppm, d). Furthermore, a new proton peak (δ 4.27-4.19 ppm, m) indicated the hydride attack on the carbonyl carbon, C-1', that was coupled with the adjacent hydrogen atoms on the cyclobutane ring.

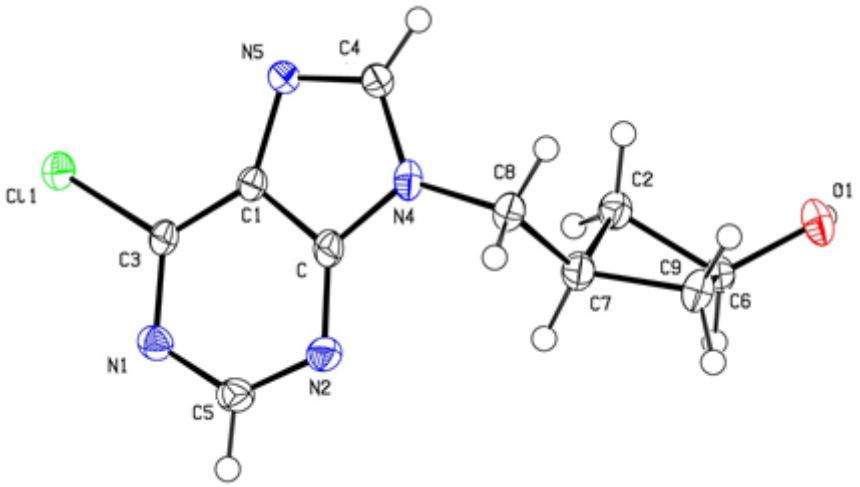


Figure 23- Crystal structure of *N*-9 alcohol **62**

The crystal structure confirmed a cis cyclobutanol **62** (Figure 23) and confirmed a trans hydride addition with $LiAl(OtBu)_3H$. The HRMS spectra also supported the molecular composition of **62** and depicts clearly the isotopic signature of $^{35}Cl$ (*m/z* of 239.0694 for $M^+$) and $^{37}Cl$ (*m/z* of 241.0655 for $M^+$) also showing fragment ions for 6-chloropurine (*m/z* of 155.0118 and *m/z* of 157.0089) in the MSMS spectra for each parent ion. Furthermore, the IR spectrum showed an absence of the carbonyl peak (1779 $cm^{-1}$) of **60** and an emergence of a broad hydroxyl peak (3358 $cm^{-1}$). Thus, all of the evidence was consistent with the assigned regio- and stereochemistry for **62**.

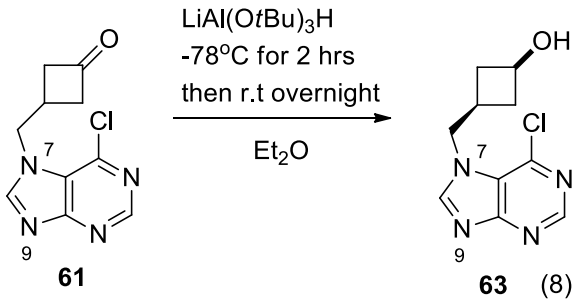


Similarly, reduction of the *N*-7 regioisomer **61** with LiAl(O*t*Bu)$_3$H was also expected to give a cis-alcohol as the kinetic product. The reduction produced one product that was more polar than its ketone counterpart as was evident by TLC.

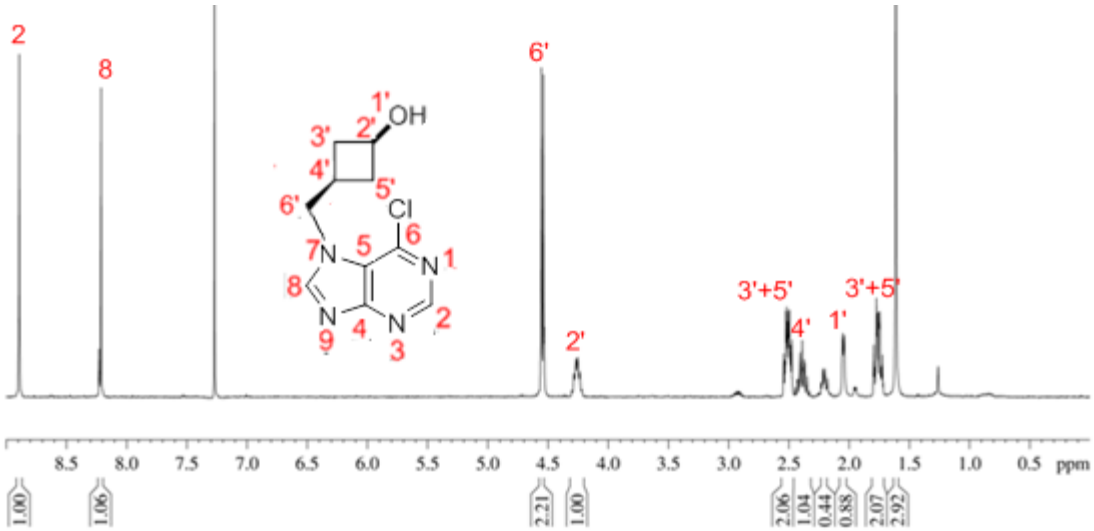


Figure 24- $^1$H NMR spectrum of *N*-7 alcohol **63**

The $^1$H NMR spectrum (Figure 24) showed the characteristic additional hydrogen peak, H-2', (δ 4.30-4.22 ppm, m) and a methylene (H-6') shift of δ 0.18 ppm, from ketone **61** (δ 4.73 ppm) to the alcohol **63** (δ 4.55 ppm)**.** The difference in chemical shift of the methylene peaks, H-6', was exactly the same as that observed between **60** to **62.** This indicated a cis-configuration, since trans and cis alcohols give different chemical shifts as seen by the $^1$H NMR spectra of the crude material for reduction of **60** and **61** by $NaBH_4$. The HRMS data is also consistent with the molecular composition of **63** and also exhibits a clear isotopic chlorine

pattern for $^{35}Cl$ (*m/z* of 239.0694 for $M^+$) and $^{37}Cl$ (*m/z* of 241.0665 for $M^+$). The carbonyl peak of the *N*-7 ketone **61** (1777 $cm^{-1}$) was also absent and a new hydroxyl peak (3443 $cm^{-1}$) emerged in the IR spectrum. The $^{13}C$-NMR spectrum showed the disappearance of the characteristic cyclobutanone carbonyl peak (δ 207.8ppm).

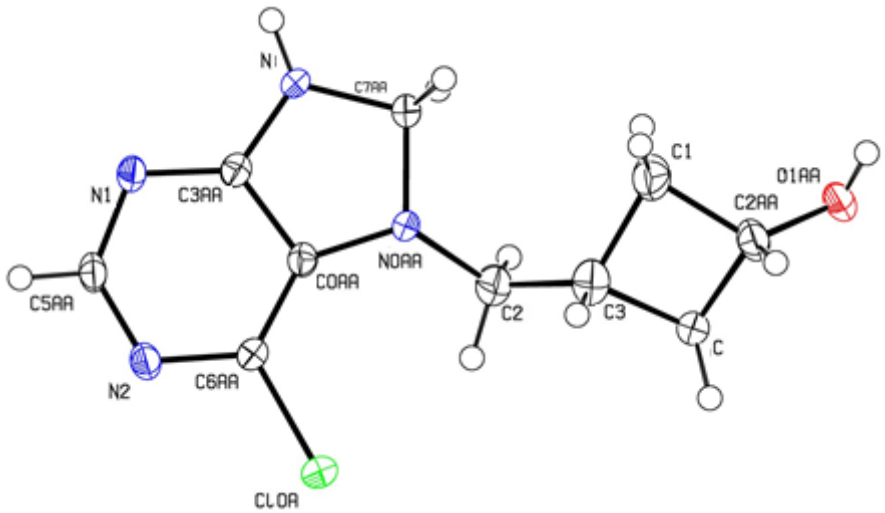


Figure 25- Crystal structure of *N*-7 alcohol **64**

The crystal structure of **63** could not be obtained since crystals of adequate size and uniformity could not be grown even after considerable effort. However, in an attempt to grow crystals of the cis alcohol alkylated at the *N*-7 position, another experiment involving the reduction of ketone initially with $LiAl(OtBu)_3H$, followed by addition of excess $NaBH_4$ yielded the over-reduced alcohol **64** as confirmed by X-ray crystallography (Figure 25). Similar over-reductions of purine derivatives have been reported, where electron deficient purines are converted to dihydropurine with $NaBH_4$.[54] We speculate that the reason for over-reduction of the *N*-7 ketone **61** but not **60** may be associated with steric interaction of 6-chloropurine and the cyclobutanone ring, increasing the strain in the *N*-7 coupled ketone. This compound was easier to crystalize than its precursor **63** and confirmed the reduction of **61** to occur in a trans manner,

similar to its *N*-9 regioisomer **60,** giving the cis alcohol **63.** In conclusion, all of the evidence acquired supported the molecular composition and stereochemistry of **63**.

### *2.6 Alkylation of purines*

Purine as well as pyrimidine bases can generally alkylate at multiple sites. Introduction of heterocycles via a simple $S_N2$ mechanism limits the regioselectivity of the *N*-alkylation step by the electronic charge density and steric hindrance in proximity to nitrogen. For instance, the parent purinyl anion has a very similar charge distribution for the *N*-7 and *N*-9 position (-0.45:-0.56) and is not sterically hindered due to the lack of substitution on the heterocycle. Thus, it has been shown to give roughly a 1:1 mixture of *N*-7 and *N*-9 alkylated products.[55] Substitution of purine can alter the charge distribution as well as steric hindrance around *N*-7 and *N*-9, thereby allowing greater regioselectivity in alkylation.

In the case of purines, substitution at C-6 and *N*-3 promotes alkylation at *N*-9 and *N*-7 respectively. Substitution at C-6 with chlorine, *peri* to *N*-7, alters the charge distribution of the corresponding anion and localizes the charge density on *N*-9 (ratio of charge localization for *N*-7 to *N*-9 is -0.37:-0.59, respectively) and sterically hinders the *N*-7 position as can be predicted by it's A-value of 0.52 (free-energy difference between its axial and equatorial conformers of substituted cyclohexane). It also increases the acidity at the *N*-9 center through inductive effects by the *meta* sigma value ($\sigma$) of 0.37 for chlorine. As expected, 6-chloropurine gives the *N*-9 alkylated regioisomer as the major product,[21] as was also the case for alkylation of **57**. Several methods have been developed to promote greater regioselectivity for *N*-alkylation using sterically hindered substituents at C-3 and C-6. Bulky protecting groups such as 2, 3-dicyclohexylsuccinimidyl ($Cy_2SI$) at C-6 affords *N*-9 alkylated acylic and cyclic products

regioselectively with various substituted purine derivatives.[56] Similarly, the formation of *N*-7 products is favoured in the case of 6-chloro-3-deaza-3-methyl, a C-3 substituted purine.[57]

Others have established the use of microwave excitation to give regioselective alkylation with purines as well as pyrimidines. Khalaf-Nezhad et al. have developed an efficient and rapid synthesis of carboacyclic nucleoside analogues using microwave assisted Michael addition of α,β-unsaturated esters with adenine and pyrimidine derivatives under solvent-free conditions.[58] They report the use of tetrabutylammonium bromide (TBAB) as a facilitating agent that absorbs microwave irradiation homogenizing the reaction media (Scheme 10).

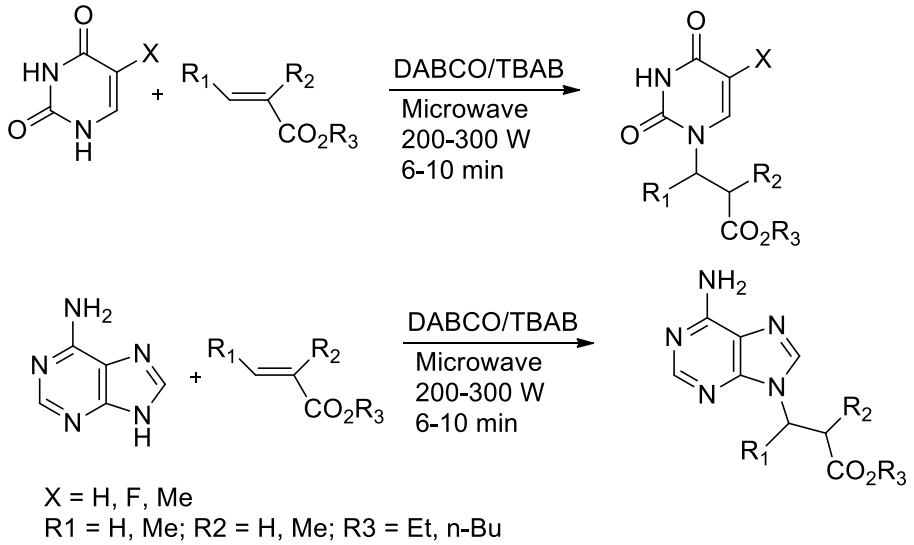


Scheme 10: Microwave assisted regioselective alkylation of purines and pyrimidines with α,β- unsaturated esters

Similarly, Xia et al. have confirmed the use of microwave excitation to prepare carboacyclic nucleoside analogues from alkyl halides and purine and pyrimidine nucleobases in water, under short reaction times (Scheme 11).[59]

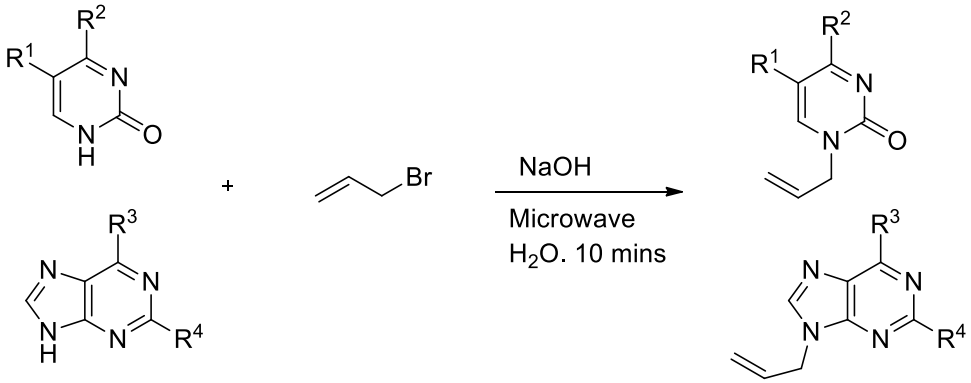


$R^1$ = H, F, Cl, Br, I, $CH_3$; $R^2$ = $NH_2$, OH

$R^3$ = Cl, $NH_2$, ArNH, morpholinyl; $R^4$ = Cl, H

Scheme 11: Microwave assisted regioselective alkylation of purines and pyrimidines with allyl bromide

Our initial attempts towards *N*-alkylation of nucleobases were to carry these our under neutral conditions. The Mitsunobu reaction of several nucleobases with various solvents, produced products which exhibit NMR spectra showing multiple alkylation sites. However, these products were either too close in $R_f$ values to separate or no *N*-alkylation was the outcome (Table 3).

Table 3: Summary of Mitsunobu reaction of **50** with various nucleobases and solvents at room temperature.

| **Solvent** | **Time duration (h)** | **Base** | **Results** |
|---|---|---|---|
| $CH_2Cl_2$ | 8 | 5-iodouracil | < 1 % *N*-alkylation |
| $CH_2Cl_2$ | 18 | Uracil | No *N*-alkylation |
| $CH_2Cl_2$ | 18 | 6-chloropurine | No *N*-alkylation |
| $CH_2Cl_2$ | 18 | Adenine | No *N*-alkylation |
| DMF | Overnight | 5-iodouracil | Unable to isolate or identify *N*-alkylation |
| DMF | Overnight | Uracil | Unable to isolate or identify *N*-alkylation |
| DMF | Overnight | Adenine | Unable to isolate or identify *N*-alkylation |

| | | | |
|---|---|---|---|
| DMF | Overnight | Cytosine | Unable to isolate or identify *N*-alkylation |
| DMF | Overnight | Guanine | Unable to isolate or identify *N*-alkylation |
| THF | Overnight | 6-chloropurine | No *N*-alkylation |

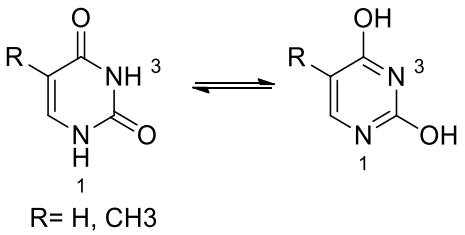


The general procedure (Scheme 12) for the Mitsunobu reaction involves the use of an azodicarboxylate, such as diethyl azodicarboxylate (DEAD) or diisopropyl azodicarboxylate (DIAD), and triphenylphosphine to displace the OH group of the alcohol by $S_N2$ reaction. One of the last steps in the mechanism involves the deprotonation of the nucleophile to create an anion, which then attacks the phosphinium oxide to produce the $S_N2$ product and triphenylphosphine oxide.

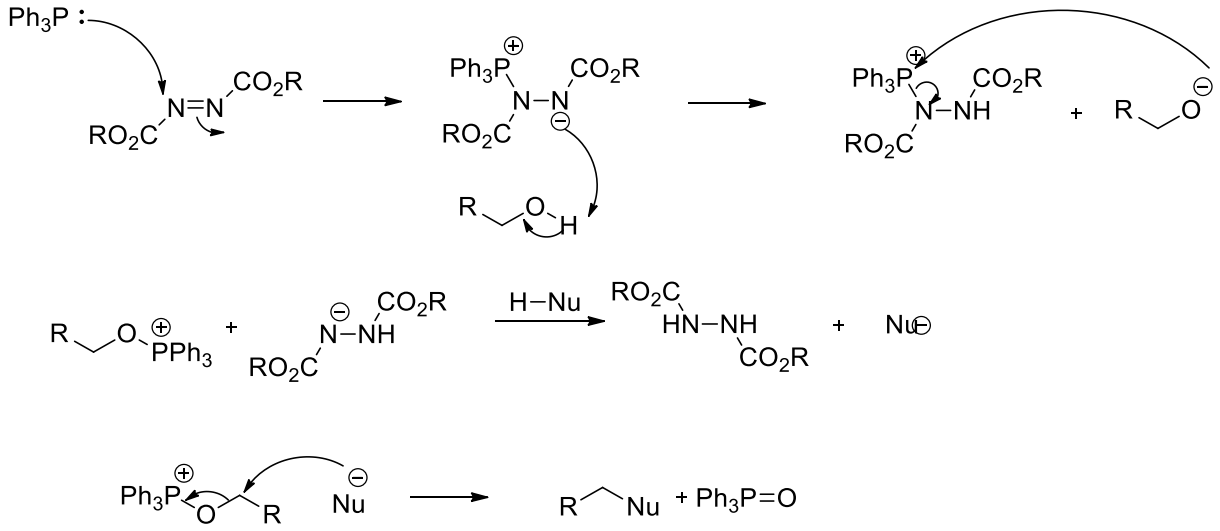

Scheme 12: Mechanism of Mitsunobu reaction

In general, the factors that affect the distribution of *O*-vs. *N*-alkylated products include the importance of the individual resonance structures. Other factors include tautomer distribution, solvent and the nature of the electrophile.[20,60–63] The relative stabilities of the resonance structures that contain the negative charge on oxygen vs. nitrogen are speculated to be the cause of the *O*-vs. *N*-alkylation distribution.[20]

# Chapter 3

### *3.0 Photolysis of 60 and 61*

As previously stated, cyclobutanones can undergo a number of photochemical transformations. Three main photochemical pathways include ring-expansion, cycloelimination and decarbonylation forming a furanose ring, an alkene, and a cyclopropane respectively (Scheme 6). The objective for photolysis of **60** and **61** was to form ring expansion products as isonucleoside analogs.

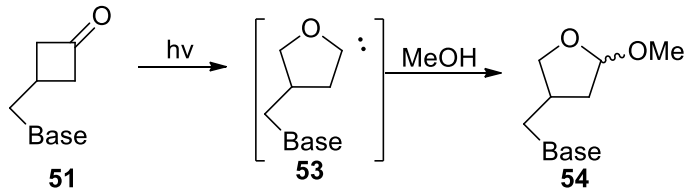


The photolysis of both *N*-7 and *N*-9 ketones, **60** and **61**, under various conditions did not yield any ring expansion products (Scheme 13).

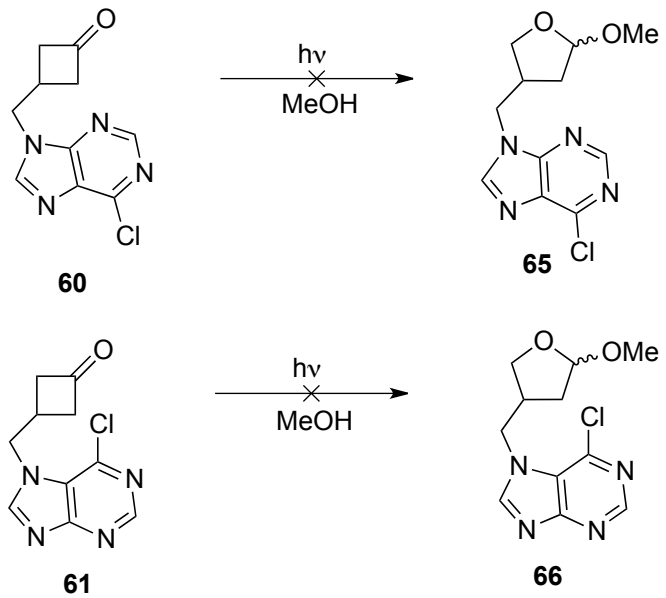


Scheme 13: Photolysis of **60** and **61** under varying conditions to promote ring expansion

Previous studies[26] have shown that polar solvents, such as acetonitrile and methanol, promote ring expansion, whereas non-polar solvents promote cycloelimination. Decarbonylation is promoted by the presence of triplet photosensitizers such as acetone and electron-donating groups on the α-position.[26,30] Thus, attempts at photolysis of *N*-9 and *N*-7 coupled ketones **60** and **61**, respectively, to promote ring expansion products (Scheme 8) were conducted with methanol. Initial experiments included the use of pyrex glass tubes. However, *N*-9 coupled ketone **60** showed very little product conversion even after 5 h of irradiation. Thus, further experiments were conducted in quartz tubes since quartz is transparent down to 200 nm of light. The carbonyl chromophore is excited at 300 nm. Both ketones displayed similar trends in their reactivity. Exposure to only 15 minutes gave a small amount of product conversion as observed by the disappearance of the cyclobutanone peaks ($\delta$ 3.0-3.28 ppm for **60** and $\delta$ 2.94-3.25 ppm for **61**) and the appearance of more shielded peaks ($\delta$ 1.95-2.75 ppm for photolysis of **60** and $\delta$ 1.91-2.40 ppm for photolysis of **61**) in their NMR spectra. TLC indicated only one major non-polar UV active spot for photolysis of both regioisomers. Prolonged irradiation for 1 h gave NMR spectra of the crude that showed a product conversion of more than 60% as seen by the relative integration ratios of the methylene protons. Attempts at isolation of the product were unsuccessful even after purification by column chromatography, followed by preparative TLC. The products formed were neither cycloelimination products (Scheme 14), as seen by the absence of alkene protons, nor ring-expansion products as noted by the absence of a singlet for the three methoxy protons.

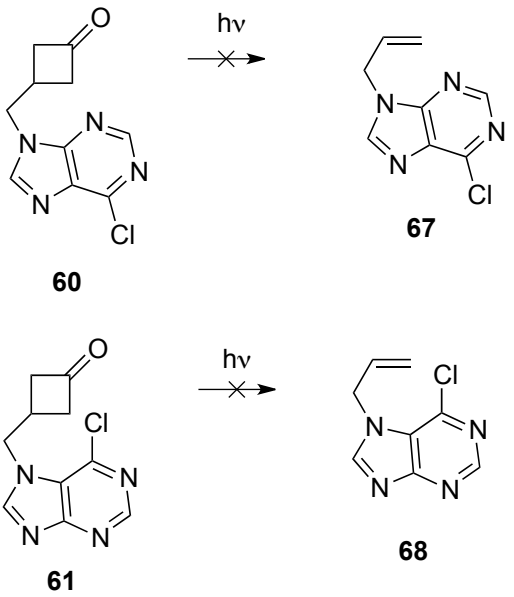


Scheme 14: Cycloelimination derived alkene products from photolysis of **60** and **61**

We speculate the possibility of the products being cyclopropanes, **69** and **70** (scheme 15), since methylene NMR peaks were more deshielded. Since the formation of cyclopropanes usually occurs by decarbonylation of cyclobutanones in their excited triplet state, we speculate that perhaps 6-chloropurine may be acting as a triplet sensitizer. Prolonged irradiation led to decomposition of the ketones as seen by broad NMR signals appearing throughout the aliphatic region that did not have integration ratios related to any of the peaks around $\delta$ 4-5 ppm of the bridging methylene protons, or to the aromatic peaks. The *N*-7 ketone **61** showed more rapid product conversion than **60**, perhaps due to its inherent strain leading to greater reactivity and decomposition.

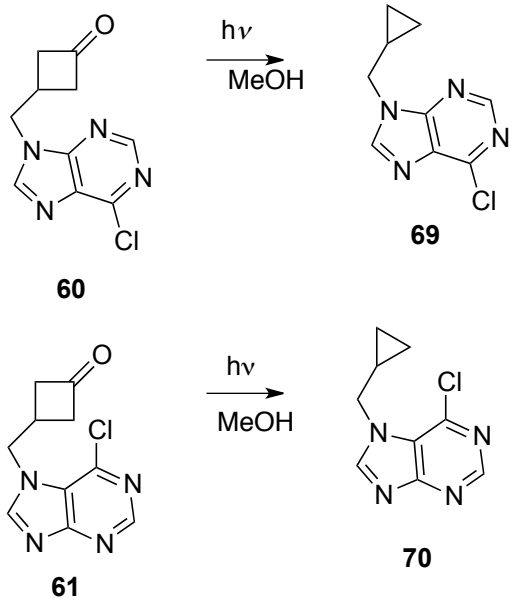


Scheme 15: Proposed cylopropane derivatives **69** and **70** from decarbonylation of **60** and **61**

In conclusion, photolysis of ketones **60** and **61** did not produce their expected ring-expansion counterparts **65** and **66** but rather formed non-polar products that could not be completely characterized.

# Chapter 4

### *4.1 Conclusions and Comments*

Cyclobutanones bearing a hydroxymethyl **50** can be readily prepared from a [2+2] cycloaddition of a protected allyl alcohol and dichloroketene, generated *in situ*, followed by dechlorination and deprotection. Compound **50** can be used to synthesize nornucleoside and isonucleoside analogs by a variety of methods. The Mitsunobu reactions were employed in an attempt at *N*-alkylation under neutral conditions. The products of *N*-alkylations however, were either not formed or were not able to be separated since the $R_f$ values were too close and multiple alkylations occurred as observed by the $^1$H NMR spectra. Thus, activated alcohols were used in an $S_N2$ protocol under basic conditions, with 6-chloropurine as the nucleobase. Substitution of the triflated ketone **57** with a 6-chloropurinyl salt afforded the *N*-9 and *N*-7 regioisomers, **60** and **61** respectively, in reasonable yields. The relative distribution of the *N*-9 and *N*-7 coupled ketones were rationalized on the basis charge distribution calculations calculated on *N*-9 and *N*-7 as well as the steric congestion by chlorine, being *peri* to *N*-7, for the 6-chloropurinyl anion **59**. Both regioisomers were confirmed by HRMS, IR and NMR spectroscopy. A crystal structure of **61** was also obtained.

Initial attempts at reduction of ketones **60** and **61** with $LiAlH_4$, $NaBH_4$ and $NaBH_3CN$ were unsuccessful and produced both cis and trans isomers as seen by TLC and $^1$H NMR. These could not be separated by column chromatography. It was speculated that the transition states for trans vs. cis hydride addition would have different energies with the use of a bulky hydride donor such as $LiAl(O\textit{t}Bu)_3H$. The reaction successfully provided *N*-9 and *N*-7 cis-alcohols **62** and **63** respectively. The alcohols were characterized by HRMS, IR and NMR spectroscopy, and

a crystal structure of **62** also confirmed a trans hydride addition. Attempts at crystallizing **63** sutiable for x-ray diffraction were unsuccessful. However, in an attempt to grow single crystals of *N*-7 alkylated cis alcohol, the over-reduced cis alcohol **64** with reduced aromaticity was formed as confirmed by x-ray crystallography. This was obtained when excess $NaBH_4$ was added after the addition of $LiAl(OtBu)_3H$. We speculated the reason for over-reduction of *N*-7 coupled ketone **61** and not **60** may be associated with steric interaction from the cyclobutanone and 6-chloropurine, where chlorine is *peri* to *N-7*. A crystal structure of **64** supported the reduction of **61** with $LiAl(OtBu)_3H$ to occur in a trans fashion yielding the cis alcohol **63**.

Photolysis of **60** and **61** in MeOH which is known to promote ring-expansion, showed products that were less polar and showed more shielded proton signals relative to the ketones in their NMR spectra. The products were speculated to be the decabonylated cyclopropanes **69** and **70**.. The possibility of cycloelimination derived alkene products since no vinyl peaks were observed. Ring-expansion was also ruled out since no methoxy peaks were observed in their NMR spectra. The unusual photodecarbonylation under non-sensitized condtions were rationalized in terms of intramolecular triplet photosensitization by the purine chromophore.

### *4.2 Future Directions*

Derivative **50** can also be used to make other analogs. Since triflate **57** was extremely unstable to moisture, reactions involving polar solvents such as DMSO and DMF for alkylation of other polar nucleobases were not practical. It is possible to introduce other nucleobases to **50** via halogenation by the Appel reaction[64] to make **71**, followed by displacement of the halogen to give **51**. It can then be reduced to make other analogs, or photolysed in the presence of a photosensitizer (Scheme 16).

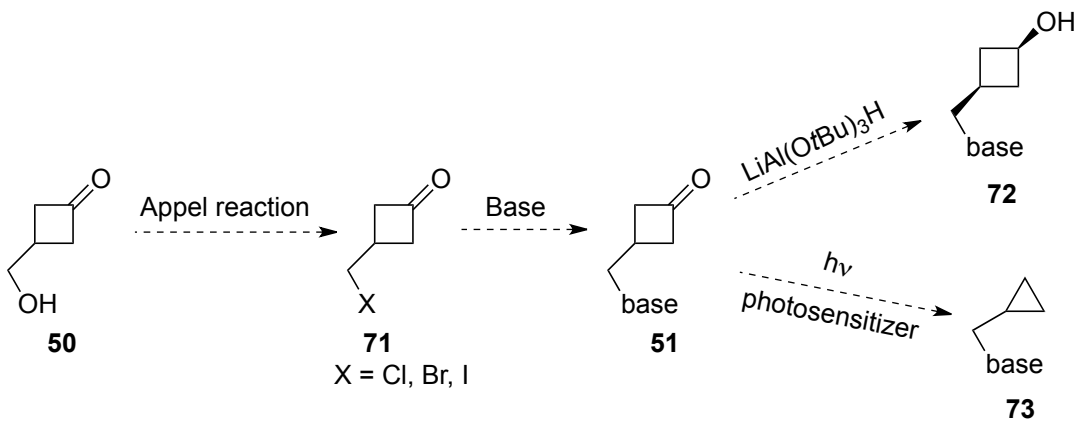


Scheme 16: Proposed synthesis of other *N*-alkylated cyclobutanones and their subsequent reduction and photolysis

The use of halogenated ketone **71** may serve as a more viable alternative to triflate **57** and should be more resistant to hydrolysis since the triflate is a better leaving group than the halogens. This should allow the use of other more polar solvents such as DMF and DMSO, in which nucleobases are more soluble helping to overcome the solubility issues associated with purines and pyrimidines. The use of microwave irradiation may also assist in homogenizing the reaction media and the use of other pyrimidine and purine nucleobases in a regioselective *N*-alkylation.[58,59] The reasons for enhanced regioselectivity is not known. Furthermore, the soft nature of leaving groups such as iodide and bromide may also complement the nature of the soft purinyl anion and further promote *N*-alkylation according to the HSAB theory. Subsequently, derivative **51** can be reduced stereoselectively by $LiAl(O\mathit{t}Bu)_3H$ to yield cyclobutane analogs of various nucleobases. The photolysis of **51** where other purine or pyrimidine nucleobases are attached, may also be of great interest since it could give further insight to the photochemical reactivity of cyclobutanones. Further experiments to determine the possibility of an intramolecular triplet photosensitization can be conducted using an added triplet photosensitizer as a control. Determining the conditions that may promote intramolecular triplet

photosensitization could also be of great importance in understanding the potential trends in the photochemical reactivity of these cyclobutanones.

Ketone **51** can also be used to make five-membered ring analogs by ring-expansion by homologation with diazomethane or Baeyer-Villiger oxidation (Scheme 17).

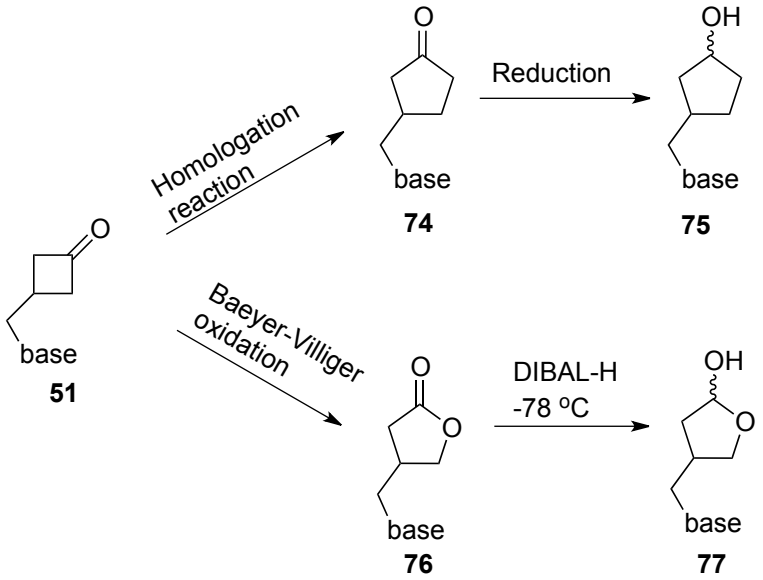


Scheme 17: Proposed synthesis of other five-membered ring analogs

Cyclobutanones are known to undergo ring-expansion by homologation[65] quite readily with diazomethane, generally generated *in situ*.[66] Due to the inherent symmetry of **51**, only **74** is expected, with the stereochemistry of **75** being determined in the reduction step. Similarly the Baeyer-Villiger oxidation should also form one product **76** with the stereochemistry of **77** being governed in reduction to lactol **77** under controlled conditions to prevent ring-opening.[67]

# Chapter 5

### *5.0 Experimental*

### *5.1 General Experimental*

All chemicals were from Sigma Aldrich Co. and not further purified. All solvents were dried and distilled prior to use. Reactions were carried out in oven or flame-dried glassware under argon unless stated otherwise. The melting points (mp) were measured on a Fisher-Johns melting point apparatus and are uncorrected. FT-IR spectra were recorded on a Bruker Alpha Platinum-ATR as a thin layer of liquid or a thin film of solid introduced by dissolving the substrate in chloroform or dichloromethane and applying as a thin layer, followed by evaporation. The mass spectrometry analyses was performed at York University Centre for Research in Mass Spectrometry on an Orbitrap Elite Hybrid Ion Trap-Orbitrap Mass Spectrometer (ThermoFisher, Waltham, MA) using an electrospray ionization source and helium as the collision gas with 50/50 water/methanol solution. UV-vis spectra were determined using methanol as solvent on an Ultrospec 4300 pro UV spectrometer. X-ray diffraction was carried out using a Bruker APEX II CCD diffractometer at the University of Western Ontario (UWO) using graphite-monochromated Mo Kα ($\lambda$ = 0.71073 $A^o$) for ketone **61** and CuKα($\lambda$ = 1.54178 $A^o$) for the alcohol **62.**

The1D and 2D- NMR spectra were recorded on Bruker AV 300, Bruker 400 or Bruker 700 spectrometer. The $^1$HNMR spectra are referenced relative to the solvent residual proton signals of $CDCl_3$ ($\delta$ 7.27), $CD_3OD$ ($\delta$ 3.31) and DMSO-$d_6$ ($\delta$ 2.50). The chemical shifts are reported as delta ($\delta$) values downfield from tetramethylsilane (TMS, $\delta$ = 0) in parts per million (ppm). Data from 1D –H NMR are reported in the following order: chemical shifts ($\delta$ in

ppm), multiplicity (s = singlet, d = doublet, t = triplet, dd = doublet of doublets, q = quartet, m = multiplet), coupling constant (*J* in Hz), and lastly relative integration (number of protons).

Photolyses were carried in quartz tubes strapped around a water-cooled quartz immersion well containing a 450-W Hanovia medium pressure mercury arc lamp. This set-up was immersed in an ice-water bath. Samples were purged with argon for 15 minutes, prior to irradiation.

Analytical thin layer chromatography (TLC) was done using commercial Machery-Nagel 60 F 254 silica gel coated aluminum sheets and visualization of spots was carried out with $KMnO_4$ and/or under UV light (254 nm). Glass plates coated with Silicycle silica gel 60 F 254 (40-63 μm particle size) were used for preparative TLC, and Silicycle silica gel (60-200 μm particle size) used for column chromatography.

***5.2 Specific Experimental Procedure and Data***

**Debenzoylation of ketone 49**

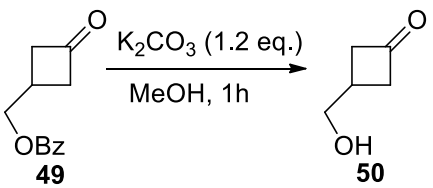


1.66 g (12.0 mmol) of $K_2CO_3$ was added to a solution of 1.00 g (10.0 mmol) of **49**[30] in 20 mL methanol and the mixture was stirred for 1 h at room temperature. A solution of saturated aqueous solution of $NaHCO_3$ (10 mL) was added and the mixture was stirred for an additional 15 min. The solvent was evaporated under vacuum, and the sample was purified by flash column chromatography using ethyl acetate to provide **50** in 70% yield. Its complete characterization was not carried out, since it was a known compound.[43,68]

Data for **50**

$^1$H NMR (400 MHz, $CDCl_3$) δ 3.75 (d, *J* = 6.2 Hz, 2H), 3.14-3.06 (m, 2H), 2.88-2.82 (m, 2H), 2.69-2.56 (m, 1H)

IR ν = 1775 $cm^{-1}$

**Triflation of alcohol 50**

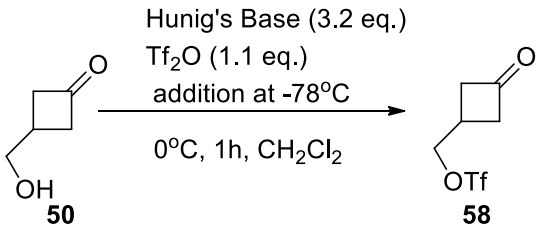


A solution of 0.100 g (1.00 mmol) **50** in 10 mL of dry $CH_2Cl_2$ was cooled to -78 °C before adding 0.56 mL (3.20 mmol) of Hunig's base, followed by 0.17 mL (1.01 mmol) of trifluoromethanesulfonic anhydride. The mixture was stirred for 10 mins, warmed to 0 °C and stirred for 1 h providing quantitative conversion to **57**. The mixture was not purified and immediately used for the next step.

***N*-Alkylation of 6-chloropurine**

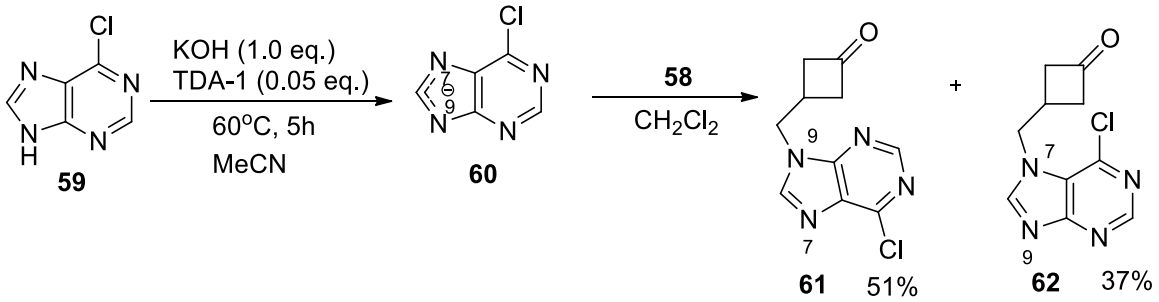


A mixture consisting of 0.866 g (5.61 mmol) of 6-chloropurine **5**, 0.314 g (5.61 mmol) of potassium hydroxide, 0.091 g (0.28 mmol) of tris[2-(2-methoxyethoxy)ethyl]amine, and 2 g of magnesium sulfate was added to 100 mL of anhydrous acetonitrile. This mixture was stirred overnight, then heated to 60 °C for 5 h and then cooled to room temperature. Triflate **57**

1.303 g (5.61 mmol) was added directly as a crude solution from the previous step, and the reaction mixture was stirred overnight. The insoluble material was filtered off, and the solvent removed under vacuum. The residue was purified using 5% methanol and 5% triethylamine in chloroform. The two UV active spots in the TLC were collected and further purified by flash column chromatography using ethyl acetate to provide 0.671 g (51%) of *N*-9 alkylated derivative **60** and 0.495 g (37%) of *N*-7 alkylated derivative **61.**

Data for **60**

$^{1}$H NMR (700 MHz, $CDCl_3$) δ 8.78 (s, 1H), 8.17 (s, 1H), 4.54 (d, $J$ = 7.6 Hz, 2H), 3.28-3.22 (m, 2H), 3.15-3.09 (m, 1H), 3.04-3.00 (m, 2H)

$^{13}$C NMR (700 MHz, $CDCl_3$) δ 203.5, 152.2, 151.8, 151.5, 144.5, 131.6, 51.2, 48.9, 24.5

IR ν = 3446, 3075, 2926, 1779 $cm^{-1}$

HRMS Calculated for $C_{10}H_{10}ON_4Cl$ ($M^+$) *m/z* 237.0539, 239.0510, found 237.0539, 239.0513

Melting point : 67.1-69.3 $^{o}$C

Data for **61**

$^{1}$H NMR (400 MHz, $CDCl_3$)

δ 8.92 (s, 1H), 8.32 (s, 1H), 4.73 (d, $J$ = 7.6, 2H), 3.32-3.25 (m, 2H), 3.21-3.08 (m, 1H), 3.01-2.94 (m, 2H)

$^{13}$C NMR (400 MHz, $CDCl_3$) δ 202.7, 162.0, 152.6, 148.3, 142.8, 122.2, 51.4, 50.7, 25.2

IR ν = 3443, 3104, 3069, 2854, 1777 $cm^{-1}$

HRMS Calculated for $C_{10}H_{10}ON_4Cl$ ($M^+$) *m/z* 237.0538, 239.0510, found 237.0538, 239.0512

Melting point: 115.4-117.7 $^{o}$C

**Reduction of *N*-9 Ketone 60**

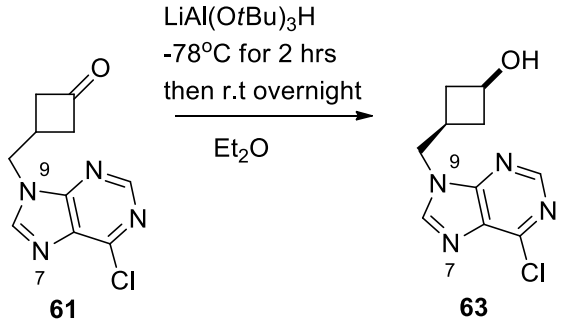


A of solution of 50 mg (0.21 mmol) of **60** in 10mL of $Et_2O$ was cooled to -78 $^oC$ and 81mg (0.32 mmol) of lithium tri-tert-butoxyaluminum hydride was added. The mixture was allowed to warm to room temperature after 2.5 h and was left to stir overnight, to provide quantitative conversion to the cis-cyclobutanol **62**.

Data for **62**

$^1H$ NMR (400 MHz, $CDCl_3$) δ 8.76 ( s, 1H), 8.10 (s, 1H), 4.36 (d, $J$ = 7.0, 2H) , 4.27-4.19 (m, 1H), 2.53-2.47 (m, 2H), 2.44-2.34 (m, 1H), 1.81 (d, $J$ = 5.6, 1H), 1.81-1.74 (m, 2H)

IR ν = 3358, 3113, 3075, 2973, 2929, 2853 $cm^{-1}$

HRMS Calculated for $C_{10}H_{20}ON_4Cl$ ($M^+$) *m/z* 239.0694, 241.0665, found 239.0689, 241.00661

UV $\lambda_{max}$ = 206 nm, ε = 10676 $M^{-1}cm^{-1}$

Melting point: 173.5-175 $^oC$

**Reduction of N-7 Ketone 61**

A of solution of 50 mg (0.21 mmol) of **61** in 10 mL of $Et_2O$ was cooled to -78 $^oC$ and 81 mg (0.32 mmol) of lithium tri-tert-butoxyaluminum hydride was added. The mixture was allowed to warm to room temperature after 2.5 h and was left to stir overnight, to provide quantitative conversion to the cis-cyclobutanol **63**.

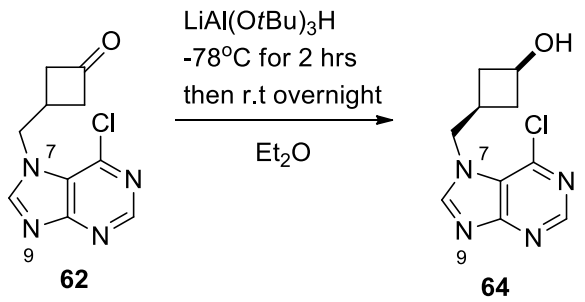


Data for **63**

$^{1}$H NMR (400 MHz, $CDCl_3$) δ 8.89 ( s, 1H), 8.21 (s, 1H), 4.55 (d, $J$ = 7.0, 2H) , 4.30-4.22 (m, 1H), 2.54-2.48 (m, 2H), 2.45-2.33 (m, 1H), 2.05 (d, $J$ = 5, 1H), 1.79-1.72 (m, 2H)

$^{13}$C NMR (400 MHz, $CDCl_3$) δ 161.8, 152.4, 148.6, 142.9, 122.2, 62.9, 52.3, 36.9, 26.7

IR ν = 3364, 3102, 3068, 2974, 2934, 2857 $cm^{-1}$

UV $\lambda_{max}$ = 208 nm, ε = 19487 $M^{-1}cm^{-1}$

Melting point: 175.6-177.6 $^{o}$C

## 5.3 References


(1) Périgaud, C.; Gosselin, G.; Imbach, J. L. *Nucleosides and Nucleotides* **1992**, *11* (2–4), 903–945.

(2) Shelton, J.; Lu, X.; Hollenbaugh, J. A.; Cho, J. H.; Amblard, F.; Schinazi, R. F. *Chem. Rev.* **2016**, acs.chemrev.6b00209.

(3) Shah, P.; Westwell, A. D. *J. Enzyme Inhib. Med. Chem.* **2007**, *22* (5), 527–540.

(4) Khandazhinskaya, A. L.; Matyugina, E. S. *Russ. Chem. Bull. Int. Ed.* **2014**, *63* (5), 1069–1080.

(5) Jalandhar, T. *Curr. Top. Med. Chem.* **2016**, *16* (November), 3258–3273.

(6) Tuncbilek, M.; Ates-Alagoz, Z.; Altanlar, N.; Karayel, A.; Ozbey, S. *Bioorg. Med. Chem.* **2009**, *17* (4), 1693–1700.

(7) Holý, A.; Dvořáková, H.; Jindřich, J.; Masojídková, M.; Buděšínský, M.; Balzarini, J.; Andrei, G.; De Clercq, E. *J. Med. Chem.* **1996**, *39* (20), 4073–4088.

(8) Kværnø, L.; Kumar, R.; Dahl, B. M.; Olsen, C. E.; Wengel, J. *J. Org. Chem.* **2000**, *65* (17), 5167–5176.

(9) Wainwright, P.; Maddaford, A.; Zhang, X.; Billington, H.; Leese, D.; Glen, R.; Pryde, D. C.; Middleton, D. S.; Stephenson, P. T.; Sutton, S. *Nucleosides Nucleotides Nucleic Acids* **2013**, *32* (9), 477–492.

(10) Nair, V.; Jeon, G.-S. *Arkivoc* **2004**, *2004* (xiv), 133–140.

(11) Ahmad, S.; Bisacchi, G. S.; Field, A. K.; Jacobs, G. A.; Tuomari, A. V.; McGeever-Rubin, B.; Vite, G. D.; Zahler, R. *Bioorganic Med. Chem. Lett.* **1993**, *3* (6), 1215–1218.

(12) Grice, I. D.; Whelan, C.; Tredwell, G. D.; Von Itzstein, M. *Tetrahedron Asymmetry* **2005**, *16* (8), 1425–1434.

(13) Wu, T.; Nauwelaerts, K.; Van Aerschot, A.; Froeyen, M.; Lescrinier, E.; Herdewijn, P. *J. Org. Chem.* **2006**, *71* (15), 5423–5431.

(14) Guo, H. M.; Wu, Y. Y.; Niu, H. Y.; Wang, D. C.; Qu, G. R. *J. Org. Chem.* **2010**, *75* (11), 3863–3866.

(15) Lu, W.; Sengupta, S.; Petersen, J. L.; Akhmedov, N. G.; Shi, X.; Bennett, C. E.; Virginia, W.; Uni, V.; Virginia, W. *J. Org. Chem.* **2007**, *72* (13), 5012–5015.

(16) Zhou, J.; Shevlin, P. B. *Synth. Commun.* **1997**, *27* (20), 3591–3597.

(17) Hubert, C.; Alexandre, C.; Aubertin, A. M.; Huet, F. *Tetrahedron* **2002**, *58* (19), 3775–3778.

(18) Quezada, E.; Viña, D.; Delogu, G.; Borges, F.; Santana, L.; Uriarte, E. *Helv. Chim. Acta* **2010**, *93* (2), 309–313.

(19) Barral, K.; Courcambeck, J.; Pèpe, G.; Balzarini, J.; Neyts, J.; De Clercq, E.; Camplo, M. *J. Med. Chem.* **2005**, *48* (2), 450–456.

(20) Choo, H.; Chong, Y.; Chu, C. K. **2001**, No. 4, 2000–2002.

(21) Ebead, A.; Fournier, R.; Lee-Ruff, E. *Nucleosides. Nucleotides Nucleic Acids* **2011**, *30* (6), 391–404.

(22) Lee-Ruff, E.; Mladenova, G. *Chem. Rev* **2003**, *103*, 1449–1483.

(23) Mladenova, G.; Lee-Ruff, E. *Tetrahedron Lett.* **2007**, *48* (15), 2787–2789.

(24) Ramnauth, J.; Lee-Ruff, E. *Can. J. Chem.* **1999**, *77* (416), 1245–1248.

(25) Lee-Ruff, E. In *The Chemistry of Cyclobutanones*; Rappoport, Z., Liebman, J.L., Ed.; J. Wiley & Sons; Chichester, UK, 2005; Part 1, pp 281-355

(26) Hayes, I. E. E.; Kazarians-Moghaddam, H.; Lee-Ruff, E. *Struct. Chem.* **1991**, *2*, 87–95.

(27) Ramnauth, J.; Lee-Ruff, E. *Can. J. Chem.* **1997**, *75*, 518–522.

(28) Wilsey, S.; Bearpark, M. J.; Bernardi, F.; Olivucci, M.; Robb, M. A. *J. Am. Chem. Soc.* **1996**, *118* (18), 4469–4479.

(29) Pan, S.; Amankulor, N. M.; Zhao, K. *Tetrahedron* **1998**, *54* (24), 6587–6604.

(30) Ramnauth, J.; Lee-Ruff, E. *Can. J. Chem.* **2001**, *79* (2), 114–120.

(31) Ghazi, H., Synthesis of Fluorinated Nucleosides. M.Sc. Dissertation, York University, Toronto, ON, 2000.

(32) Csuk, R.; Kern, A. *Tetrahedron* **1999**, *55* (28), 8409–8422.

(33) Qui, Y. L.; Ksebati, M. B.; Zemlicka, J. *Nucleosides Nucleotides Nucleic Acids* **2000**, *19* (1–2), 31–37.

(34) Jacobs, G. A.; Tino, J. A.; Zahler, R. *Tetrahedron Lett.* **1989**, *30* (50), 6955–6958.

(35) Guan, H. P.; Ksebati, M. B.; Kern, E. R.; Zemlicka, J. *J. Org. Chem.* **2000**, *65* (17), 5177–5184.

(36) Crimmins, M. T.; King, B. W.; Zuercher, W. J.; Choy, A. L. *J. Org. Chem.* **2000**, *65* (25), 8499–8509.

(37) Besada, P.; Terán, C.; Santana, L.; Teijeira, M.; Uriarte, E. *Nucleosides And Nucleotides* **1999**, *18* (4–5), 725–726.

(38) Bridwell-Rabb, J.; Kang, G.; Zhong, A.; Liu, H.-W.; Drennan, C. L. *Proc. Natl. Acad. Sci. U. S. A.* **2016**, 201613610.

(39) Lee-Ruff, E.; Xi, F.; Qie, J. H. *J. Org. Chem.* **1996**, *61*, No. 4, 1547–1550.

(40) Lee-Ruff, E.; Ostrowski, M.; Ladha, A.; Stynes, D. V; Vernik, I.; Jiang, J.-L.; Wan, W.-Q.; Ding, S.-F.; Joshi, S. *J. Med. Chem.* **1996**, *39*, 5276–5280.

(41) Lee-Ruff, E.; Margau, R. *Nucleosides, Nucleotides and Nucleic Acids* **2001**, *20*, 185–196.

(42) Zhong, J.-H.; Fishman, A.; Lee-Ruff, E. *Org. Lett.* **2002**, *4*, 4415–4417.

(43) Ghazi, H.; Lee-Ruff, E. *J. Florine Chem.* **2005**, *126*, 1565–1569.

(44) Leclerc, J.-P.; Fagnou, K. *Angew. Chemie Int. Ed.* **2006**, *45*, 7781–7786.

(45) Liang, Y.; Hnatiuk, N.; Rowley, J. M.; Whiting, B. T.; Coates, G. W.; Rablen, P. R.; Morton, M.; Howell, A. R. *J. Org. Chem.* **2011**, *76* (24), 9962–9974.

(46) Szeja, W. *Synth. Commun.* **1980**, *5*, 402–403.

(47) Krepski, L. R.; Hassner, A. *J. Org. Chem.* **1978**, *43* (14), 2879–2882.

(48) Jaffer, M.; Ebead, A.; Lee-Ruff, E. *Molecules* **2010**, *15* (6), 3816–3828.

(49) Afifi, H.; Ebead, A.; Pignatelli, J.; Lee-Ruff, E. *Nucleosides, Nucleotides and Nucleic Acids* **2015**, *34* (11), 786–798.

(50) Marek, R.; Brus, J.; Tousek, J.; Kovacs, L.; Hockova, D. *Magn. Reson. Chem.* **2002**, *40*, 353–360.

(51) Hockova, D.; Budesinsky, M.; Marek, R.; Marek, J.; Holy, A. *European J. Org. Chem.* **1999**, 2675.

(52) Rustellet, A.; Alibes, R.; March, P.; Figueredo, M.; Font, J. *Org. Lett.* **2007**, *9*, 2827.

(53) Kjellberg, J.; Johansson, N. G. *Tetrahedron* **1986**, *42* (23), 6541–6544.

(54) Aarhus, T. I.; Fritze, U. F.; Hennum, M.; Gundersen, L. L. *Tetrahedron Lett.* **2014**, *55* (42), 5748–5750.

(55) Ebead, A. Synthesis of Cyclobutane Nucleosides and Related Analogues. Ph.D Dissertation, York University, Toronto, ON, 2011.

(56) Pal, A.; Salandria, K. J.; Arico, J. W.; Schlegel, M. K.; McLaughlin, L. W. *Chem. Commun. (Camb).* **2013**, *49* (28), 2936–2938.

(57) Irani, R. J.; SantaLucia, J. *Nucleosides, Nucleotides and Nucleic Acids* **2002**, *21* (11–12), 737–751.

(58) Khalafi-Nezhad, A.; Zarea, A.; Soltani Rad, M. N.; Mokhtari, B.; Parhami, A. *Synthesis (Stuttg).* **2005**, No. 3, 419–424.

(59) Xia, R.; Sun, L.-P. *Nucleosides, Nucleotides and Nucleic Acids* **2016**, *35* (2), 76–82.

(60) Richichi, B.; Cicchi, S.; Chiacchio, U.; Romeo, G.; Brandi, A. *Tetrahedron Lett.* **2002**, *43* (22), 4013–4015.

(61) Torhan, M. C.; Peet, N. P.; Williams, J. D. *Tetrahedron Lett.* **2013**, *54* (30), 3926–3928.

(62) Kocalka, P.; Pohl, R.; Rejman, D.; Rosenberg, I. *Nucleosides, Nucleotides and Nucleic Acids* **2005**, *24* (5–7), 805–808.

(63) Comins, D. L.; Jianhua, G. *Tetrahedron Lett.* **1994**, *35* (7), 968.

(64) Hajipour, A. R.; Mostafavi, M.; Ruoho, A. E. *Org. Prep. Proced. Int.* **2009**, *41* (1), 87–91.

(65) Candeias, N. R.; Paterna, R.; Gois, P. M. P. *Chem. Rev.* **2016**, *116* (5), 2937–2981.

(66) Moore, J. A.; Reed, D. E. *Org. Synth.* **1961**, *41*, 16.

(67) Stephens, B. E.; Liu, F. *J. Org. Chem.* **2009**, *74* (1), 254–263.

(68) Lopp, M.; Paju, A.; Kanger, T.; Pehk, T. *Tetrahedron Lett.* **1996**, *37* (42), 7583–7586.

## 5.4 Appendix

**X-ray Structure data for *N*-7 ketone 61**

**Table 1 Crystal data and structure refinement for 61.**

| | |
|---|---|
| Identification code | elrx02 |
| Empirical formula | $C_{10}H_9ClN_4O$ |
| Formula weight | 236.66 |
| Temperature/K | 273.15 |
| Crystal system | monoclinic |
| Space group | $P2_1/c$ |
| a/Å | 11.9692(4) |
| b/Å | 6.8789(3) |
| c/Å | 12.2719(4) |
| α/° | 90 |
| β/° | 92.920(3) |
| γ/° | 90 |
| Volume/Å$^3$ | 1009.09(7) |
| Z | 4 |
| $\varrho_{calc}$g/cm$^3$ | 1.558 |
| μ/mm$^{-1}$ | 0.361 |
| F(000) | 488.0 |
| Crystal size/mm$^3$ | ? × ? × ? |

| | |
|---|---|
| Radiation | MoKα (λ = 0.71073) |
| 2Θ range for data collection/° | 6.648 to 82.898 |
| Index ranges | $-21 \le h \le 22, -11 \le k \le 11, -22 \le l \le 22$ |
| Reflections collected | 55495 |
| Independent reflections | 6450 [$R_{int} = 0.0599$, $R_{sigma} = 0.0499$] |
| Data/restraints/parameters | 6450/0/145 |
| Goodness-of-fit on $F^2$ | 1.047 |
| Final R indexes [I>=2σ (I)] | $R_1 = 0.0740$, $wR_2 = 0.1552$ |
| Final R indexes [all data] | $R_1 = 0.1217$, $wR_2 = 0.1792$ |
| Largest diff. peak/hole / e $Å^{-3}$ | 1.29/-0.46 |

**Table 2 Fractional Atomic Coordinates ($\times 10^4$) and Equivalent Isotropic Displacement Parameters ($Å^2 \times 10^3$) for elrx02. $U_{eq}$ is defined as 1/3 of of the trace of the orthogonalised $U_{IJ}$ tensor.**

| Atom | *x* | *y* | *z* | U(eq) |
|---|---|---|---|---|
| Cl0A | 2013.0(4) | 7138.3(6) | 290.5(3) | 25.11(10) |
| N2 | 4504.0(11) | 12741(2) | -596.1(11) | 19.5(2) |
| C1AA | 3391.1(11) | 10128(2) | -232.9(10) | 15.6(2) |
| N3 | 3407.1(10) | 11386.5(19) | 645.8(10) | 16.6(2) |
| C3AA | 4086.9(12) | 11007(2) | -991.2(11) | 16.7(2) |
| N | 4306.3(11) | 10196(2) | -1950.4(10) | 20.4(2) |

| | | | | |
|---|---|---|---|---|
| N1 | 3130.6(12) | 7528(2) | -1470.1(11) | 21.4(2) |
| C6AA | 2917.1(12) | 8358(2) | -533.1(12) | 17.4(2) |
| C7AA | 4089.1(13) | 12899(2) | 368.3(12) | 18.8(2) |
| C | 2944.6(12) | 11111(2) | 1724.7(11) | 18.1(2) |
| C1 | 1980.8(12) | 12462(2) | 1918.1(12) | 19.8(3) |
| C8AA | 3823.3(13) | 8486(3) | -2122.8(12) | 21.5(3) |
| C2 | 852.6(14) | 12032(3) | 1271.9(14) | 27.8(3) |
| C3 | 1421.0(15) | 12040(3) | 3013.5(14) | 28.0(3) |
| C4 | 326.1(15) | 11752(3) | 2365.6(16) | 27.9(3) |
| O | -614.8(13) | 11449(3) | 2613.2(17) | 48.0(4) |

**Table 3 Anisotropic Displacement Parameters ($Å^2 \times 10^3$) for elrx02. The Anisotropic displacement factor exponent takes the form: $-2\pi^2[h^2a^{*2}U_{11}+2hka^*b^*U_{12}+\ldots]$.**

| Atom | $U_{11}$ | $U_{22}$ | $U_{33}$ | $U_{23}$ | $U_{13}$ | $U_{12}$ |
|---|---|---|---|---|---|---|
| Cl0A | 28.54(19) | 24.83(19) | 22.37(16) | 1.55(14) | 5.40(13) | -8.20(14) |
| N2 | 21.1(5) | 19.0(5) | 18.9(5) | 1.7(4) | 5.3(4) | -1.7(4) |
| C1AA | 16.3(5) | 18.5(6) | 12.0(5) | 0.4(4) | 1.8(4) | 2.3(4) |
| N3 | 18.6(5) | 18.2(5) | 13.2(4) | 1.0(4) | 3.7(4) | 0.4(4) |
| C3AA | 16.6(5) | 19.3(6) | 14.3(5) | 2.2(4) | 2.1(4) | 1.4(4) |
| N | 20.3(5) | 25.4(6) | 15.7(5) | -0.1(4) | 4.5(4) | 1.6(5) |
| N1 | 21.5(5) | 23.6(6) | 19.1(5) | -3.4(4) | 1.5(4) | -0.4(5) |

| | | | | | | |
|---|---|---|---|---|---|---|
| C6AA | 18.1(5) | 18.3(6) | 15.9(5) | 1.2(4) | 1.0(4) | -0.4(5) |
| C7AA | 20.1(6) | 17.1(6) | 19.4(6) | -1.6(5) | 1.8(4) | 0.4(5) |
| C | 20.9(6) | 21.5(6) | 12.0(5) | 1.5(4) | 3.1(4) | 1.5(5) |
| C1 | 17.9(5) | 24.1(7) | 17.8(6) | 1.8(5) | 4.9(4) | 1.8(5) |
| C8AA | 21.6(6) | 27.6(7) | 15.7(5) | -4.3(5) | 2.9(5) | 1.7(5) |
| C2 | 19.7(6) | 40(1) | 23.5(7) | -0.7(7) | 0.5(5) | 3.8(6) |
| C3 | 25.5(7) | 40.3(10) | 19.1(6) | 0.5(6) | 9.0(5) | 3.0(7) |
| C4 | 21.9(7) | 27.7(8) | 34.9(9) | -0.1(7) | 9.8(6) | -0.1(6) |
| O | 27.5(7) | 56.7(11) | 61.5(11) | 0.2(9) | 19.3(7) | -7.8(7) |

**Table 4 Bond Lengths for elrx02.**

| Atom | Atom | Length/Å | Atom | Atom | Length/Å |
|---|---|---|---|---|---|
| Cl0A | C6AA | 1.7343(15) | N | C8AA | 1.323(2) |
| N2 | C3AA | 1.373(2) | N1 | C6AA | 1.320(2) |
| N2 | C7AA | 1.3111(19) | N1 | C8AA | 1.353(2) |
| C1AA | N3 | 1.3824(18) | C | C1 | 1.510(2) |
| C1AA | C3AA | 1.4157(19) | C1 | C2 | 1.559(2) |
| C1AA | C6AA | 1.385(2) | C1 | C3 | 1.559(2) |
| N3 | C7AA | 1.376(2) | C2 | C4 | 1.524(3) |
| N3 | C | 1.4732(17) | C3 | C4 | 1.511(3) |
| C3AA | N | 1.3404(19) | C4 | O | 1.200(2) |

**Table 5 Bond Angles for elrx02.**

| Atom | Atom | Atom | Angle/° | Atom | Atom | Atom | Angle/° |
|---|---|---|---|---|---|---|---|
| C7AA | N2 | C3AA | 104.07(12) | N1 | C6AA | Cl0A | 116.89(12) |
| N3 | C1AA | C3AA | 105.06(12) | N1 | C6AA | C1AA | 121.13(13) |
| N3 | C1AA | C6AA | 138.36(13) | N2 | C7AA | N3 | 114.68(13) |
| C6AA | C1AA | C3AA | 116.57(12) | N3 | C | C1 | 112.77(12) |
| C1AA | N3 | C | 129.01(13) | C | C1 | C2 | 116.87(14) |
| C7AA | N3 | C1AA | 105.40(11) | C | C1 | C3 | 112.71(13) |
| C7AA | N3 | C | 125.08(13) | C2 | C1 | C3 | 90.24(12) |
| N2 | C3AA | C1AA | 110.78(12) | N | C8AA | N1 | 127.89(14) |
| N | C3AA | N2 | 126.00(13) | C4 | C2 | C1 | 87.84(13) |
| N | C3AA | C1AA | 123.21(14) | C4 | C3 | C1 | 88.28(13) |
| C8AA | N | C3AA | 113.99(13) | C3 | C4 | C2 | 93.47(13) |
| C6AA | N1 | C8AA | 117.16(14) | O | C4 | C2 | 132.9(2) |
| C1AA | C6AA | Cl0A | 121.97(11) | O | C4 | C3 | 133.62(19) |

**Table 6 Torsion Angles for elrx02.**

| A | B | C | D | Angle/° | A | B | C | D | Angle/° |
|---|---|---|---|---|---|---|---|---|---|
| N2 | C3AA | N | C8AA | 178.08(14) | C6AA | C1AA | C3AA | N2 | -179.86(13) |
| C1AA | N3 | C7AA | N2 | 0.34(18) | C6AA | C1AA | C3AA | N | -0.9(2) |
| C1AA | N3 | C | C1 | -113.39(17) | C6AA | N1 | C8AA | N | -1.5(3) |

| | | | | | | | | | | | |
|---|---|---|---|---|---|---|---|---|---|---|---|
| C1AA | C3AA | N | C8AA | -0.7(2) | C7AA | N2 | C3AA | C1AA | 0.69(16) | | |
| N3 | C1AA | C3AA | N2 | -0.50(16) | C7AA | N2 | C3AA | N | -178.22(15) | | |
| N3 | C1AA | C3AA | N | 178.44(13) | C7AA | N3 | C | C1 | 76.08(18) | | |
| N3 | C1AA | C6AA | Cl0A | 2.9(3) | C | N3 | C7AA | N2 | 172.73(13) | | |
| N3 | C1AA | C6AA | N1 | -177.57(16) | C | C1 | C2 | C4 | 118.94(15) | | |
| N3 | C | C1 | C2 | 72.14(17) | C | C1 | C3 | C4 | -122.64(15) | | |
| N3 | C | C1 | C3 | 174.68(14) | C1 | C2 | C4 | C3 | -3.26(15) | | |
| C3AA | N2 | C7AA | N3 | -0.64(18) | C1 | C2 | C4 | O | 175.6(2) | | |
| C3AA | C1AA | N3 | C7AA | 0.11(15) | C1 | C3 | C4 | C2 | 3.26(15) | | |
| C3AA | C1AA | N3 | C | -171.86(13) | C1 | C3 | C4 | O | -175.6(3) | | |
| C3AA | C1AA | C6AA | Cl0A | -178.04(11) | C8AA | N1 | C6AA | Cl0A | 179.13(12) | | |
| C3AA | C1AA | C6AA | N1 | 1.5(2) | C8AA | N1 | C6AA | C1AA | -0.4(2) | | |
| C3AA | N | C8AA | N1 | 2.0(2) | C2 | C1 | C3 | C4 | -3.18(15) | | |
| C6AA | C1AA | N3 | C7AA | 179.24(17) | C3 | C1 | C2 | C4 | 3.15(14) | | |
| C6AA | C1AA | N3 | C | 7.3(3) | | | | | | | |

**Table 7 Hydrogen Atom Coordinates (Å×10$^4$) and Isotropic Displacement Parameters (Å$^2$×10$^3$) for elrx02.**

| **Atom** | ***x*** | ***y*** | ***Z*** | **U(eq)** |
|---|---|---|---|---|
| H7AA | 4243.49 | 13950.1 | 828.32 | 23 |

| | | | | |
|---|---|---|---|---|
| HA | 3531.94 | 11326.29 | 2285.71 | 22 |
| HB | 2692.04 | 9777.18 | 1787.55 | 22 |
| H1 | 2198.68 | 13829.86 | 1858.25 | 24 |
| H8AA | 3979.03 | 7866.27 | -2771.37 | 26 |
| H2A | 554.69 | 13128.63 | 853.69 | 33 |
| H2B | 862.79 | 10865.14 | 828.67 | 33 |
| H3A | 1698.52 | 10878.06 | 3384.14 | 34 |
| H3B | 1423.04 | 13141.31 | 3507.4 | 34 |

**Crystal structure determination of N-7 ketone 61**

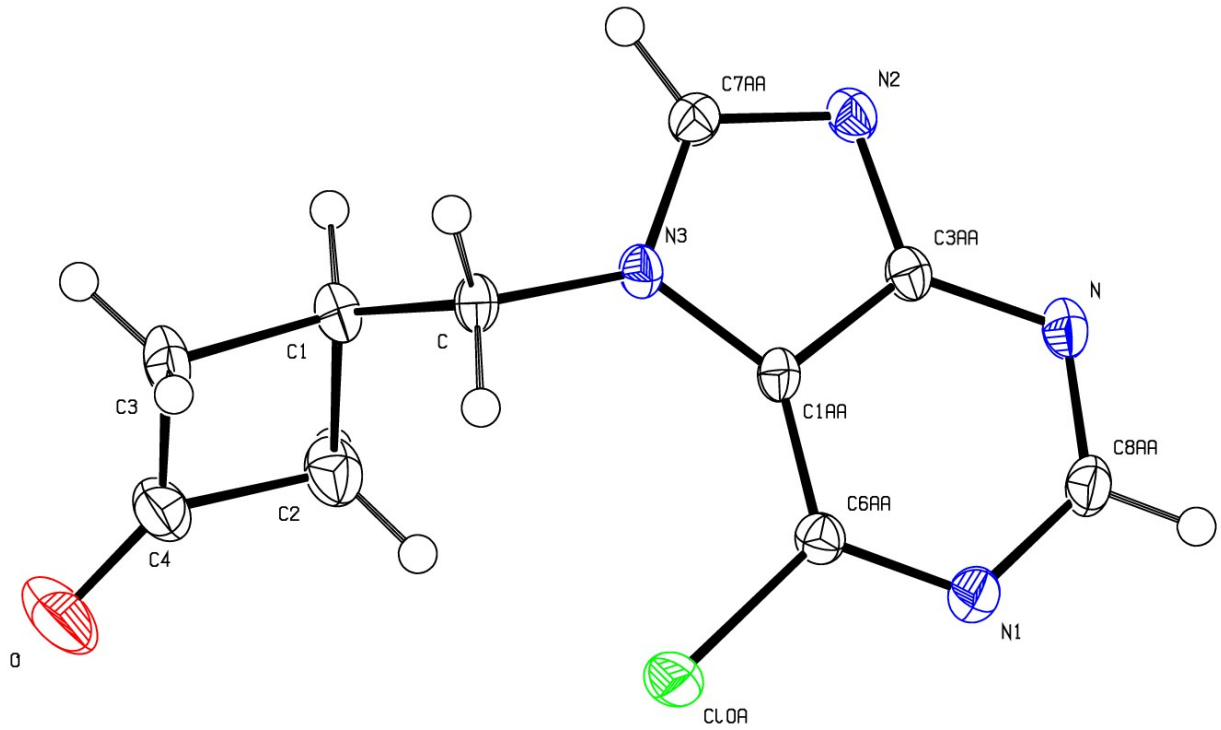


**Crystal Data** for $C_{10}H_9ClN_4O$ ($M$ =236.66 g/mol): monoclinic, space group $P2_1/c$ (no. 14), $a$ = 11.9692(4) Å, $b$ =6.8789(3) Å, $c$ =12.2719(4) Å, $\beta$ = 92.920(3)°, $V$ = 1009.09(7) Å$^3$, $Z$ = 4, $T$ = 273.15 K, μ(MoKα) = 0.361 mm$^{-1}$, *Dcalc* = 1.558 g/cm$^3$, 55495 reflections measured (6.648° ≤ 2Θ ≤ 82.898°), 6450 unique ($R_{int}$ = 0.0599, $R_{sigma}$ = 0.0499) which were used in all calculations. The final $R_1$ was 0.0740 (I > 2σ(I)) and $wR_2$ was 0.1792 (all data).

**X-ray Structure data for *N*-9 alcohol 62**

**Table 1 Crystal data and structure refinement for elrx04.**

| | |
|---|---|
| Identification code | elrx04 |
| Empirical formula | $C_{10}H_{12}ClN_4O$ |
| Formula weight | 239.69 |

| | |
|---|---|
| Temperature/K | 273.15 |
| Crystal system | Monoclinic |
| Space group | $P2_1/n$ |
| a/Å | 12.7276(8) |
| b/Å | 5.9725(4) |
| c/Å | 14.8190(10) |
| α/° | 90 |
| β/° | 108.250(3) |
| γ/° | 90 |
| Volume/Å$^3$ | 1069.81(12) |
| Z | 4 |
| $\rho_{calc}$g/cm$^3$ | 1.488 |
| μ/mm$^{-1}$ | 3.045 |
| F(000) | 500.0 |
| Crystal size/mm$^3$ | 0.504 × 0.211 × 0.073 |
| Radiation | CuKα (λ = 1.54178) |
| 2Θ range for data collection/° | 8.012 to 129.852 |
| Index ranges | $-14 \leq h \leq 14$, $-4 \leq k \leq 7$, $-17 \leq l \leq 17$ |
| Reflections collected | 7082 |
| Independent reflections | 1736 [$R_{int}$ = 0.0448, $R_{sigma}$ = 0.0269] |
| Data/restraints/parameters | 1736/0/147 |
| Goodness-of-fit on $F^2$ | 1.128 |

Final R indexes [I>=2σ (I)] $R_1 = 0.0390$, $wR_2 = 0.0991$

Final R indexes [all data] $R_1 = 0.0468$, $wR_2 = 0.1226$

Largest diff. peak/hole / e $Å^{-3}$ 0.37/-0.35

**Table 2 Fractional Atomic Coordinates ($\times 10^4$) and Equivalent Isotropic Displacement Parameters ($Å^2 \times 10^3$) for elrx04. $U_{eq}$ is defined as 1/3 of of the trace of the orthogonalised $U_{IJ}$ tensor.**

| Atom | *x* | *y* | *z* | U(eq) |
|---|---|---|---|---|
| Cl1 | 6597.9(5) | 2275.9(12) | 2171.9(4) | 26.6(3) |
| O1 | -657.0(13) | 5696(3) | -1925.0(12) | 24.1(5) |
| N1 | 6172.5(16) | 5892(4) | 1134.5(14) | 20.3(5) |
| N2 | 4473.0(17) | 7996(4) | 653.1(14) | 22.2(5) |
| N5 | 3984.2(16) | 3286(4) | 1958.0(14) | 20.5(5) |
| N4 | 3040.8(15) | 6277(4) | 1187.4(13) | 19.5(5) |
| C | 4082.3(19) | 6424(5) | 1100.4(16) | 19.7(6) |
| C1 | 4656.7(19) | 4573(4) | 1581.0(15) | 17.5(5) |
| C2 | 1259.4(19) | 5194(5) | -717.6(16) | 20.7(6) |
| C3 | 5741.9(19) | 4398(5) | 1577.9(16) | 19.2(6) |
| C4 | 3034.0(19) | 4388(4) | 1697.9(16) | 19.3(6) |
| C5 | 5520(2) | 7605(5) | 700.6(17) | 22.4(6) |
| C6 | 444.3(18) | 6481(5) | -1549.4(16) | 18.6(6) |
| C7 | 1722(2) | 7500(5) | -315.8(18) | 22.1(6) |

| | | | | |
|---|---|---|---|---|
| C8 | 2113(2) | 7798(5) | 755.0(17) | 21.4(6) |
| C9 | 597(2) | 8536(5) | -908.7(17) | 23.1(6) |

**Table 3 Anisotropic Displacement Parameters ($Å^2 \times 10^3$) for elrx04. The Anisotropic displacement factor exponent takes the form: $-2\pi^2[h^2a^{*2}U_{11}+2hka^*b^*U_{12}+\ldots]$.**

| Atom | $U_{11}$ | $U_{22}$ | $U_{33}$ | $U_{23}$ | $U_{13}$ | $U_{12}$ |
|---|---|---|---|---|---|---|
| Cl1 | 17.2(4) | 32.8(4) | 29.6(4) | 10.2(3) | 7.0(3) | 5.3(3) |
| O1 | 14.8(8) | 32.2(12) | 23.6(9) | -9.3(8) | 3.7(7) | -1.5(7) |
| N1 | 20(1) | 21.4(12) | 18.8(10) | -2.0(9) | 5.3(8) | -4.3(9) |
| N2 | 22.4(11) | 22.8(12) | 18.9(10) | 2.4(9) | 2.8(8) | -4.3(9) |
| N5 | 15.9(10) | 26.7(13) | 18.3(10) | 3.9(9) | 4.6(8) | -2.1(9) |
| N4 | 14.5(10) | 25.2(13) | 16.4(10) | -2.6(9) | 1.4(8) | 2.6(9) |
| C | 16.6(11) | 26.3(15) | 12.7(11) | -2.4(10) | -0.4(9) | -3.2(11) |
| C1 | 16.3(11) | 21.7(15) | 12.1(10) | -1.1(10) | 1.1(9) | -2.2(10) |
| C2 | 19.3(12) | 24.0(15) | 18.1(12) | -0.7(11) | 4.8(9) | 1.8(11) |
| C3 | 16.2(11) | 25.0(15) | 13.4(11) | 0.8(10) | 0.4(9) | -1.3(10) |
| C4 | 16.3(12) | 22.9(15) | 18.3(11) | 0.7(10) | 4.7(9) | -1.9(10) |
| C5 | 24.1(13) | 22.0(15) | 19.7(12) | 0.3(10) | 5.1(10) | -6.1(10) |
| C6 | 13.6(11) | 24.5(15) | 16.9(11) | -0.2(10) | 3.3(9) | 0.8(10) |
| C7 | 18.8(13) | 26.0(15) | 19.9(12) | 1.0(11) | 3.6(10) | 1.2(11) |
| C8 | 19.2(12) | 22.2(14) | 20.2(12) | 1.5(10) | 2.5(10) | 2.4(10) |

| | | | | | |
|---|---|---|---|---|---|
| C9 | 21.1(12) | 25.5(15) | 18.8(12) | -0.3(11) | 0.7(10) | 3.4(11) |

**Table 4 Bond Lengths for elrx04.**

| Atom | Atom | Length/Å | Atom | Atom | Length/Å |
|---|---|---|---|---|---|
| Cl1 | C3 | 1.723(3) | N4 | C4 | 1.360(3) |
| O1 | C6 | 1.416(3) | N4 | C8 | 1.468(3) |
| N1 | C3 | 1.324(3) | C | C1 | 1.392(4) |
| N1 | C5 | 1.347(3) | C1 | C3 | 1.387(3) |
| N2 | C | 1.332(3) | C2 | C6 | 1.545(3) |
| N2 | C5 | 1.333(3) | C2 | C7 | 1.542(4) |
| N5 | C1 | 1.391(3) | C6 | C9 | 1.526(4) |
| N5 | C4 | 1.324(3) | C7 | C8 | 1.518(3) |
| N4 | C | 1.374(3) | C7 | C9 | 1.555(3) |

**Table 5 Bond Angles for elrx04.**

| Atom | Atom | Atom | Angle/° | Atom | Atom | Atom | Angle/° |
|---|---|---|---|---|---|---|---|
| C3 | N1 | C5 | 117.4(2) | N1 | C3 | Cl1 | 117.10(17) |
| C | N2 | C5 | 111.9(2) | N1 | C3 | C1 | 121.2(2) |
| C4 | N5 | C1 | 103.2(2) | C1 | C3 | Cl1 | 121.66(19) |
| C | N4 | C8 | 125.9(2) | N5 | C4 | N4 | 114.2(2) |

| | | | | | | | |
|---|---|---|---|---|---|---|---|
| C4 | N4 | C | 106.2(2) | N2 | C5 | N1 | 127.9(2) |
| C4 | N4 | C8 | 127.7(2) | O1 | C6 | C2 | 118.9(2) |
| N2 | C | N4 | 127.8(2) | O1 | C6 | C9 | 115.3(2) |
| N2 | C | C1 | 126.6(2) | C9 | C6 | C2 | 88.91(18) |
| N4 | C | C1 | 105.6(2) | C2 | C7 | C9 | 87.98(19) |
| N5 | C1 | C | 110.7(2) | C8 | C7 | C2 | 118.0(2) |
| C3 | C1 | N5 | 134.3(2) | C8 | C7 | C9 | 119.1(2) |
| C3 | C1 | C | 115.0(2) | N4 | C8 | C7 | 109.9(2) |
| C7 | C2 | C6 | 86.8(2) | C6 | C9 | C7 | 86.94(19) |

**Table 6 Torsion Angles for elrx04.**

| A | B | C | D | Angle/° | A | B | C | D | Angle/° |
|---|---|---|---|---|---|---|---|---|---|
| O1 | C6 | C9 | C7 | 144.6(2) | C4 | N5 | C1 | C3 | -179.6(3) |
| N2 | C | C1 | N5 | -179.7(2) | C4 | N4 | C | N2 | 179.7(2) |
| N2 | C | C1 | C3 | -0.1(4) | C4 | N4 | C | C1 | -0.3(2) |
| N5 | C1 | C3 | Cl1 | -2.9(4) | C4 | N4 | C8 | C7 | -107.2(3) |
| N5 | C1 | C3 | N1 | 178.7(3) | C5 | N1 | C3 | Cl1 | -177.43(18) |
| N4 | C | C1 | N5 | 0.3(3) | C5 | N1 | C3 | C1 | 1.1(3) |
| N4 | C | C1 | C3 | 179.9(2) | C5 | N2 | C | N4 | -179.3(2) |
| C | N2 | C5 | N1 | -0.4(4) | C5 | N2 | C | C1 | 0.7(4) |
| C | N4 | C4 | N5 | 0.3(3) | C6 | C2 | C7 | C8 | 144.9(2) |

| | | | | | |
|---|---|---|---|---|---|
| C | N4 C8 C7 | 68.5(3) | C6 C2 C7 C9 | 22.67(18) | |
| C | C1 C3 Cl1 | 177.62(18) | C7 C2 C6 O1 | -141.7(2) | |
| C | C1 C3 N1 | -0.8(3) | C7 C2 C6 C9 | -23.11(18) | |
| C1 | N5 C4 N4 | -0.1(3) | C8 N4 C | N2 | 3.3(4) |
| C2 | C6 C9 C7 | 22.90(18) | C8 N4 C | C1 | -176.7(2) |
| C2 | C7 C8 N4 | 62.3(3) | C8 N4 C4 N5 | | 176.6(2) |
| C2 | C7 C9 C6 | -22.96(18) | C8 C7 C9 C6 | | -144.2(2) |
| C3 | N1 C5 N2 | -0.4(4) | C9 C7 C8 N4 | | 166.8(2) |
| C4 | N5 C1 C | -0.1(3) | | | |

**Table 7 Hydrogen Atom Coordinates (Å×10$^4$) and Isotropic Displacement Parameters (Å$^2$×10$^3$) for elrx04.**

| **Atom** | ***x*** | ***y*** | ***z*** | **U(eq)** |
|---|---|---|---|---|
| H1 | -671.39 | 4605.62 | -2265.01 | 36 |
| H2A | 908.69 | 4375.63 | -324.38 | 25 |
| H2B | 1781.76 | 4260.77 | -901.74 | 25 |
| H4 | 2415.16 | 3912.18 | 1851.25 | 23 |
| H5 | 5839.6 | 8640.67 | 397.03 | 27 |
| H6 | 768.81 | 6736.25 | -2059.37 | 22 |
| H7 | 2304.78 | 7959.96 | -579.14 | 27 |
| H8A | 2346.44 | 9334.3 | 911.69 | 26 |

| | | | | |
|---|---|---|---|---|
| H8B | 1510.2 | 7481.65 | 1005.45 | 26 |
| H9A | 60.01 | 8655.26 | -568.7 | 28 |
| H9B | 662.94 | 9933.61 | -1219.72 | 28 |

**Crystal structure determination of *N*-9 alcohol 62**

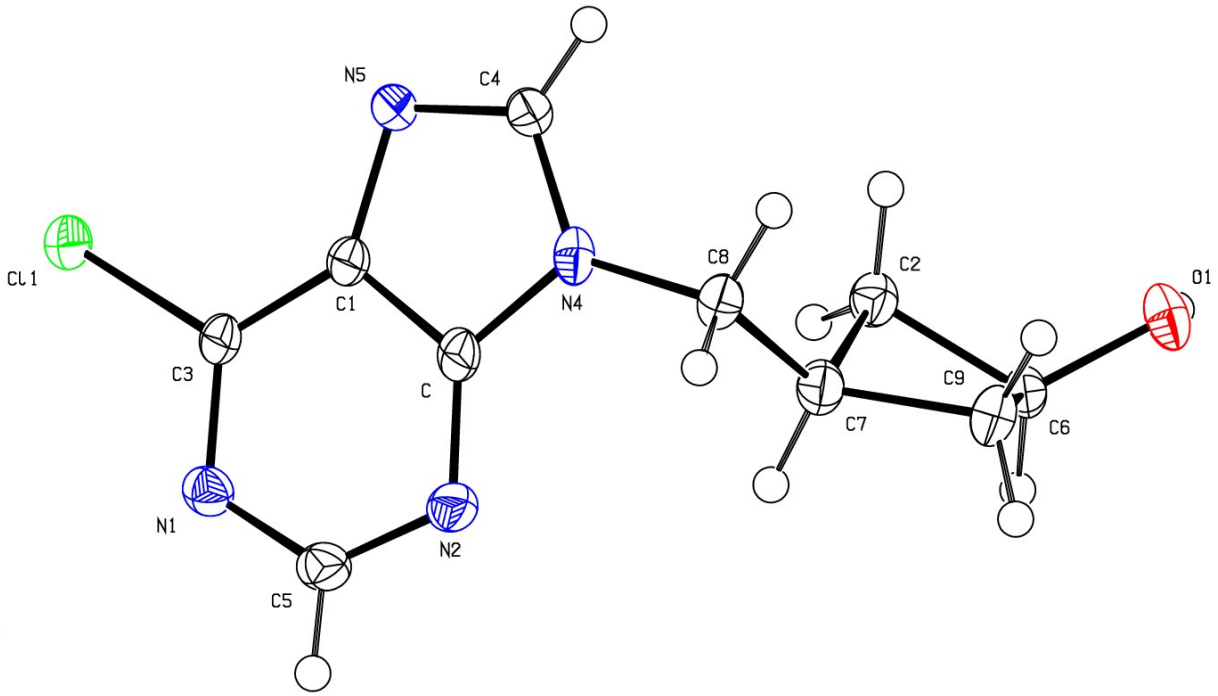


**Crystal Data** for $C_{10}H_{12}ClN_4O$ (*M* =239.69 g/mol): monoclinic, space group $P2_1/n$ (no. 14), *a* = 12.7276(8) Å, *b* = 5.9725(4) Å, *c* = 14.8190(10) Å, *β* = 108.250(3)°, *V* = 1069.81(12) Å$^3$, *Z* = 4, *T* = 273.15 K, μ(CuKα) = 3.045 mm$^{-1}$, *Dcalc* = 1.488 g/cm$^3$, 7082 reflections measured (8.012° ≤ 2Θ ≤ 129.852°), 1736 unique ($R_{int}$ = 0.0448, $R_{sigma}$ = 0.0269) which were used in all calculations. The final $R_1$ was 0.0390 (I > 2σ(I)) and $wR_2$ was 0.1226 (all data).

**X-ray Structure data for *N*-7 alcohol 64**

**Table 1 Crystal data and structure refinement for 64**

| | |
|---|---|
| Identification code | n17088 |
| Empirical formula | $C_{10}H_{13}N_4OCl$ |
| Formula weight | 240.69 |
| Temperature/K | 293(2) |
| Crystal system | triclinic |
| Space group | P-1 |
| a/Å | 6.1023(5) |
| b/Å | 8.5936(6) |
| c/Å | 10.9942(8) |
| α/° | 68.952(7) |
| β/° | 83.796(6) |
| γ/° | 87.198(6) |
| Volume/Å$^3$ | 534.89(7) |
| Z | 2 |
| $\rho_{calc}$g/cm$^3$ | 1.494 |
| μ/mm$^{-1}$ | 3.045 |
| F(000) | 252.0 |
| Crystal size/mm$^3$ | ? × ? × ? |
| Radiation | CuKα (λ = 1.54184) |
| 2Θ range for data collection/° | 8.658 to 130.148 |

| | |
|---|---|
| Index ranges | $-7 \leq h \leq 5, -10 \leq k \leq 10, -12 \leq l \leq 12$ |
| Reflections collected | 9083 |
| Independent reflections | 1785 [$R_{int} = 0.0297$, $R_{sigma} = 0.0161$] |
| Data/restraints/parameters | 1785/0/146 |
| Goodness-of-fit on $F^2$ | 1.084 |
| Final R indexes [I>=2σ (I)] | $R_1 = 0.0515$, $wR_2 = 0.1349$ |
| Final R indexes [all data] | $R_1 = 0.0566$, $wR_2 = 0.1437$ |
| Largest diff. peak/hole / e $Å^{-3}$ | 1.08/-0.45 |

**Table 2 Fractional Atomic Coordinates ($\times 10^4$) and Equivalent Isotropic Displacement Parameters ($Å^2 \times 10^3$) for n17088. $U_{eq}$ is defined as 1/3 of of the trace of the orthogonalised $U_{IJ}$ tensor.**

| Atom | *x* | *y* | *z* | U(eq) |
|---|---|---|---|---|
| Cl0A | 1683.7(11) | 9180.6(9) | 4062.4(7) | 25.7(3) |
| O1AA | 1574(4) | 7578(3) | 11236(2) | 27.8(5) |
| N0AA | 4842(4) | 7161(3) | 6459(2) | 18.9(5) |
| N1 | 7920(4) | 6240(3) | 3861(2) | 20.1(5) |
| C0AA | 5141(4) | 7253(3) | 5168(3) | 17.2(6) |
| C3AA | 7123(5) | 6387(3) | 4989(3) | 18.0(6) |
| N2 | 4816(4) | 7849(3) | 2899(2) | 20.7(5) |
| C5AA | 6671(5) | 7013(4) | 2865(3) | 21.2(6) |

| | | | | |
|---|---|---|---|---|
| C6AA | 4060(5) | 7988(3) | 4073(3) | 18.0(6) |
| C7AA | 6670(5) | 6188(4) | 7144(3) | 21.4(6) |
| C2AA | 2169(5) | 8451(4) | 9901(3) | 26.6(7) |
| N | 8030(4) | 5773(3) | 6130(2) | 21.0(5) |
| C | 627(5) | 8206(4) | 8984(3) | 27.5(7) |
| C1 | 4092(6) | 7874(5) | 9159(3) | 34.9(8) |
| C2 | 2724(6) | 7174(5) | 7213(3) | 34.2(8) |
| C3 | 2643(6) | 8270(5) | 8002(3) | 35.3(8) |

**Table 3 Anisotropic Displacement Parameters ($Å^2 \times 10^3$) for n17088. The Anisotropic displacement factor exponent takes the form: $-2\pi^2[h^2a^{*2}U_{11}+2hka^*b^*U_{12}+\ldots]$.**

| Atom | $U_{11}$ | $U_{22}$ | $U_{33}$ | $U_{23}$ | $U_{13}$ | $U_{12}$ |
|---|---|---|---|---|---|---|
| Cl0A | 21.5(4) | 32.4(4) | 23.7(4) | -11.0(3) | -4.8(3) | 9.8(3) |
| O1AA | 27.1(12) | 40.8(13) | 16.8(10) | -11.6(9) | -3.9(9) | 1.7(9) |
| N0AA | 16.9(12) | 25.9(12) | 15.9(12) | -10.4(10) | -2.1(9) | 6.2(9) |
| N1 | 18.9(12) | 25.9(13) | 16.9(12) | -10(1) | 1.4(9) | 0.3(10) |
| C0AA | 16.9(14) | 19.1(13) | 17.1(14) | -8.8(11) | 0.0(11) | -1.5(11) |
| C3AA | 16.5(14) | 19.1(13) | 19.1(14) | -8.3(11) | 0.3(11) | -0.5(11) |
| N2 | 21.4(13) | 25.7(13) | 16.1(12) | -8.8(10) | -0.8(9) | -1.2(10) |
| C5AA | 22.8(15) | 27.3(15) | 15.6(14) | -11.0(12) | 2.0(11) | -1.6(12) |
| C6AA | 16.3(14) | 19.9(13) | 18.2(14) | -7.7(11) | -0.6(11) | 1.8(11) |

| | | | | | | |
|---|---|---|---|---|---|---|
| C7AA | 20.5(15) | 29.4(15) | 17.5(14) | -12.3(12) | -3.2(11) | 5.6(12) |
| C2AA | 28.0(17) | 35.4(17) | 17.5(14) | -10.8(13) | -0.7(12) | -2.3(13) |
| N | 17.3(12) | 29.7(13) | 17.8(12) | -11.3(10) | -3.3(9) | 9.5(10) |
| C | 24.8(16) | 39.4(18) | 21.4(15) | -15.1(13) | -5.9(13) | 11.7(13) |
| C1 | 26.0(17) | 53(2) | 33.5(18) | -25.5(16) | -1.7(14) | -1.5(15) |
| C2 | 24.9(17) | 55(2) | 27.0(17) | -20.4(16) | -2.0(13) | 5.9(15) |
| C3 | 33.7(19) | 46(2) | 28.9(17) | -18.2(15) | -0.4(14) | 3.7(15) |

**Table 4 Bond Lengths for n17088.**

| Atom | Atom | Length/Å | Atom | Atom | Length/Å |
|---|---|---|---|---|---|
| Cl0A | C6AA | 1.732(3) | C3AA | N | 1.343(4) |
| O1AA | C2AA | 1.404(4) | N2 | C5AA | 1.315(4) |
| N0AA | C0AA | 1.385(4) | N2 | C6AA | 1.367(4) |
| N0AA | C7AA | 1.465(4) | C7AA | N | 1.454(4) |
| N0AA | C2 | 1.460(4) | C2AA | C | 1.524(4) |
| N1 | C3AA | 1.330(4) | C2AA | C1 | 1.521(5) |
| N1 | C5AA | 1.352(4) | C | C3 | 1.536(4) |
| C0AA | C3AA | 1.421(4) | C1 | C3 | 1.556(5) |
| C0AA | C6AA | 1.367(4) | C2 | C3 | 1.489(5) |

**Table 5 Bond Angles for n17088.**

| Atom | Atom | Atom | Angle/° | Atom | Atom | Atom | Angle/° |
|---|---|---|---|---|---|---|---|
| C0AA | N0AA | C7AA | 108.4(2) | C0AA | C6AA | N2 | 121.7(3) |
| C0AA | N0AA | C2 | 125.8(2) | N2 | C6AA | Cl0A | 115.5(2) |
| C2 | N0AA | C7AA | 118.7(2) | N | C7AA | N0AA | 103.7(2) |
| C3AA | N1 | C5AA | 113.7(2) | O1AA | C2AA | C | 114.6(3) |
| N0AA | C0AA | C3AA | 108.5(2) | O1AA | C2AA | C1 | 121.3(3) |
| C6AA | C0AA | N0AA | 136.0(3) | C1 | C2AA | C | 89.3(2) |
| C6AA | C0AA | C3AA | 115.5(3) | C3AA | N | C7AA | 110.5(2) |
| N1 | C3AA | C0AA | 124.4(3) | C2AA | C | C3 | 88.6(2) |
| N1 | C3AA | N | 126.7(3) | C2AA | C1 | C3 | 87.9(2) |
| N | C3AA | C0AA | 108.9(2) | N0AA | C2 | C3 | 114.2(3) |
| C5AA | N2 | C6AA | 116.7(2) | C | C3 | C1 | 87.6(2) |
| N2 | C5AA | N1 | 127.9(3) | C2 | C3 | C | 119.2(3) |
| C0AA | C6AA | Cl0A | 122.8(2) | C2 | C3 | C1 | 120.7(3) |

**Table 6 Hydrogen Atom Coordinates (Å×10$^4$) and Isotropic Displacement Parameters (Å$^2$×10$^3$) for n17088.**

| Atom | *x* | *y* | *z* | U(eq) |
|---|---|---|---|---|
| H1AA | 2499.38 | 7731.42 | 11668.99 | 42 |

| | | | | |
|---|---|---|---|---|
| H5AA | 7185.51 | 6943.75 | 2058.28 | 25 |
| H7AA | 7486.05 | 6843 | 7496.32 | 26 |
| H7AB | 6139.08 | 5188.86 | 7851.59 | 26 |
| H2AA | 2302.58 | 9642.31 | 9740.36 | 32 |
| H | 9244.39 | 5211.53 | 6245.02 | 25 |
| HA | -415.02 | 9116.8 | 8670.46 | 33 |
| HB | -112.03 | 7139.64 | 9326.99 | 33 |
| H1A | 4466.17 | 6702.11 | 9557.31 | 42 |
| H1B | 5389.89 | 8563.69 | 8956.8 | 42 |
| H2A | 2385.86 | 6044.01 | 7796.55 | 41 |
| H2B | 1588.25 | 7537.02 | 6613.75 | 41 |
| H3 | 2883.52 | 9426.92 | 7412.69 | 42 |

**Crystal structure determination of 64**

**Crystal Data** for $C_{10}H_{13}N_4OCl$ ($M$ =240.69 g/mol): triclinic, space group P-1 (no. 2), $a$ = 6.1023(5) Å, $b$ = 8.5936(6) Å, $c$ = 10.9942(8) Å, $\alpha$ = 68.952(7)°, $\beta$ = 83.796(6)°, $\gamma$ = 87.198(6)°, $V$ = 534.89(7) Å$^3$, $Z$ = 2, $T$ = 293(2) K, μ(CuKα) = 3.045 mm$^{-1}$, $Dcalc$ = 1.494 g/cm$^3$, 9083 reflections measured (8.658° ≤ 2Θ ≤ 130.148°), 1785 unique ($R_{int}$ = 0.0297, $R_{sigma}$ = 0.0161) which were used in all calculations. The final $R_1$ was 0.0515 (I > 2σ(I)) and $wR_2$ was 0.1437 (all data).

**Crystal structure determination of N-7 alcohol 64**

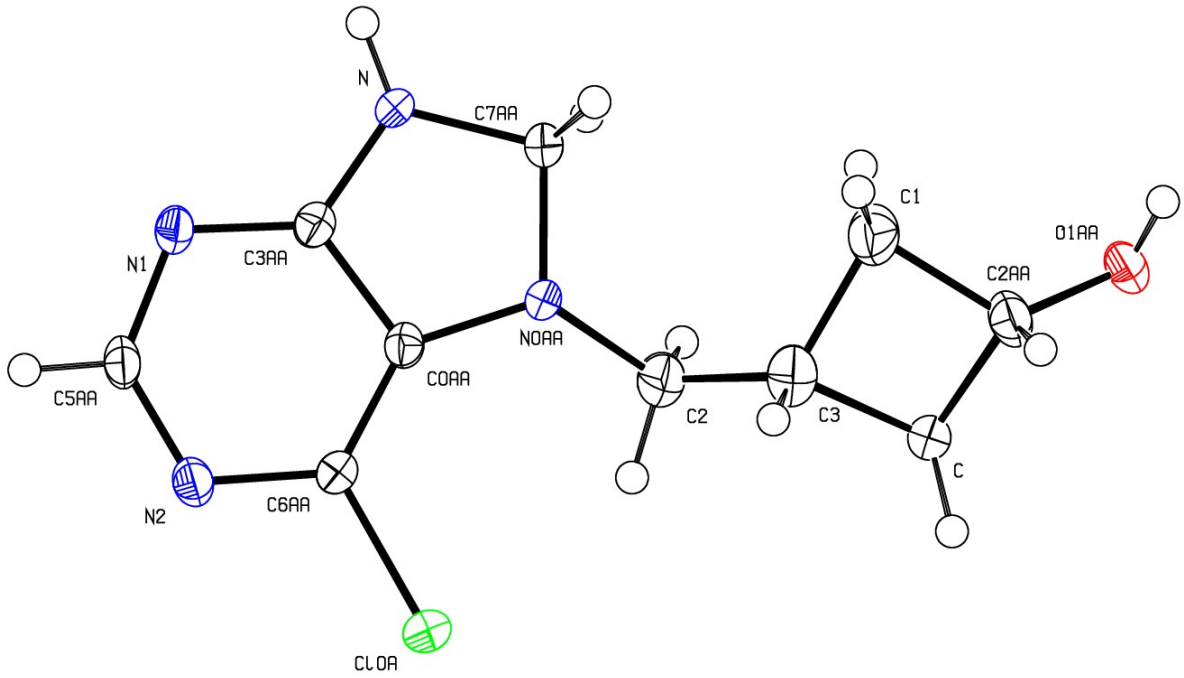


***[1]H NMR, [13]C-NMR, MS and IR-spectra***

[1]H NMR spectrum of alcohol **50** (300 MHz, $CDCl_3$)

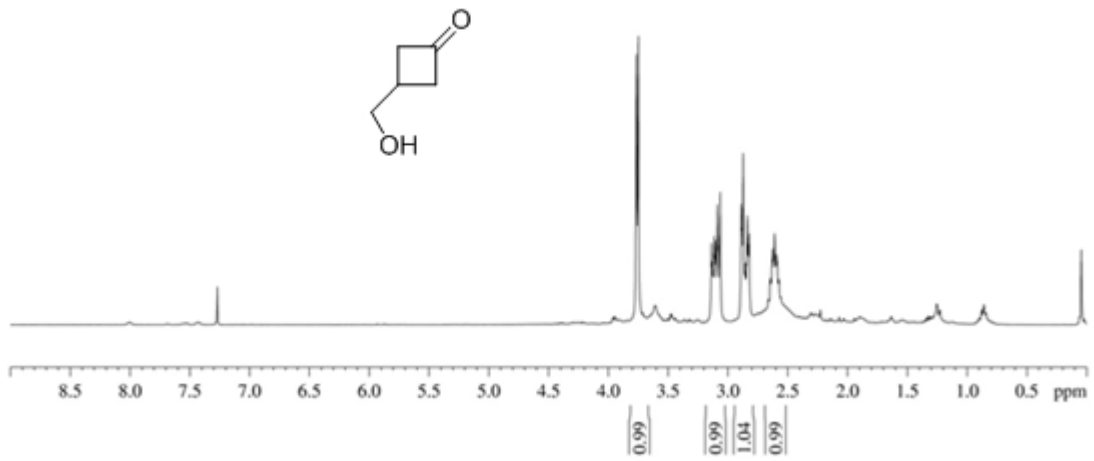

$^1$H NMR spectrum of crude triflate **57** (400 MHz, $CDCl_3$)

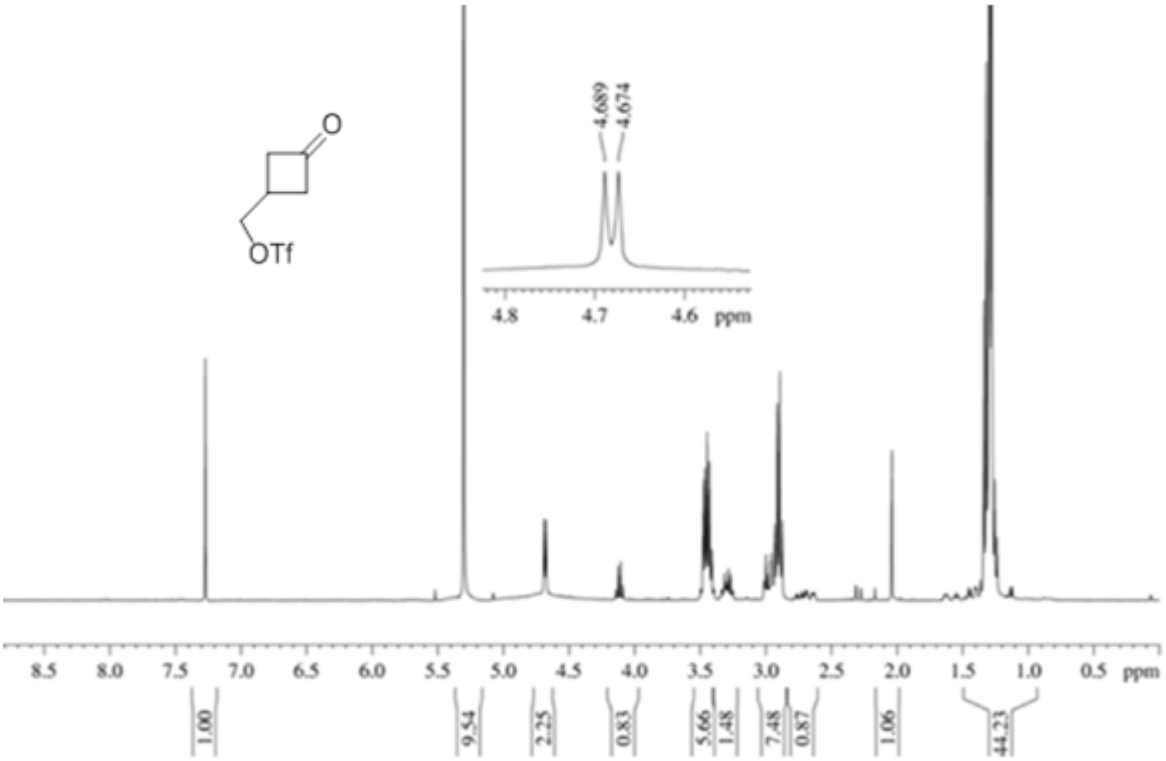


$^1$H NMR spectrum of *N*-9 coupled ketone **60** (700 MHz, $CDCl_3$)

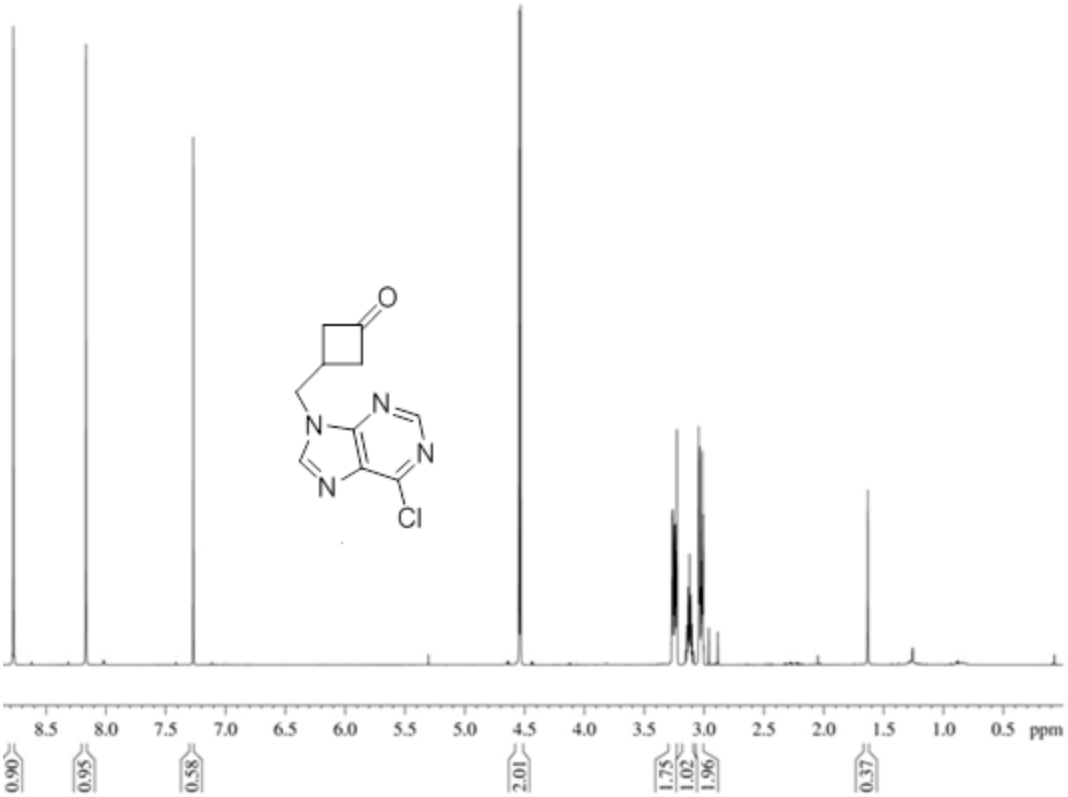

$^{13}$C-NMR spectrum of *N*-9 coupled ketone **60** (700 MHz, $CDCl_3$)

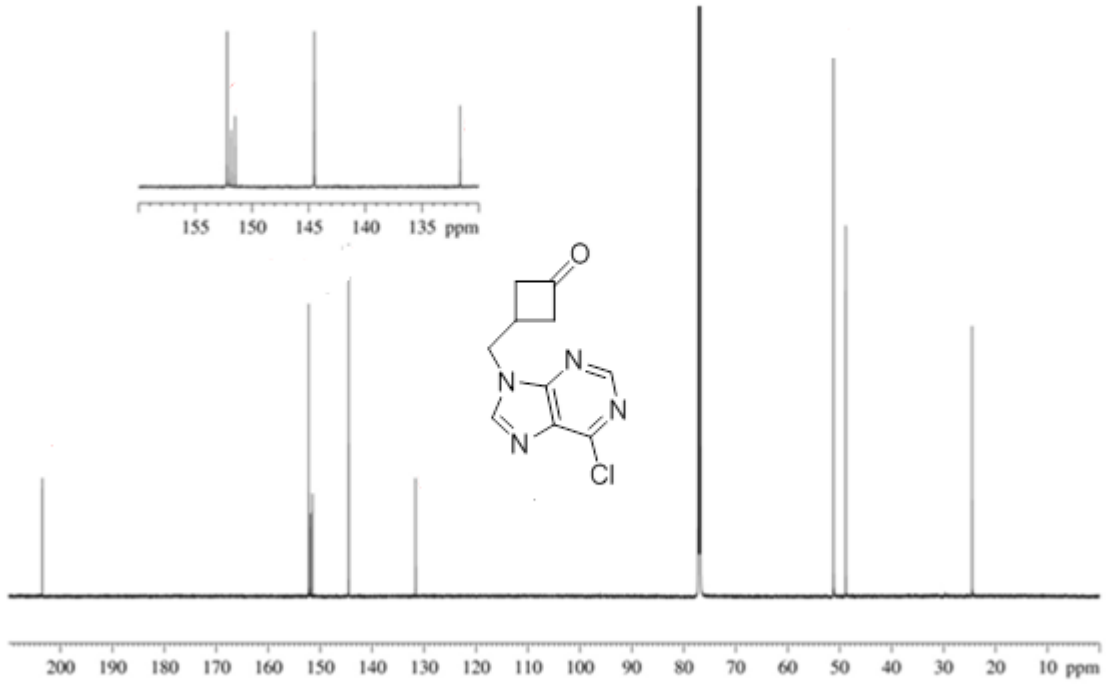

$^{1}$H-$^{13}$C HSQC of *N*-9 coupled ketone **60** (700 MHz, $CDCl_3$)

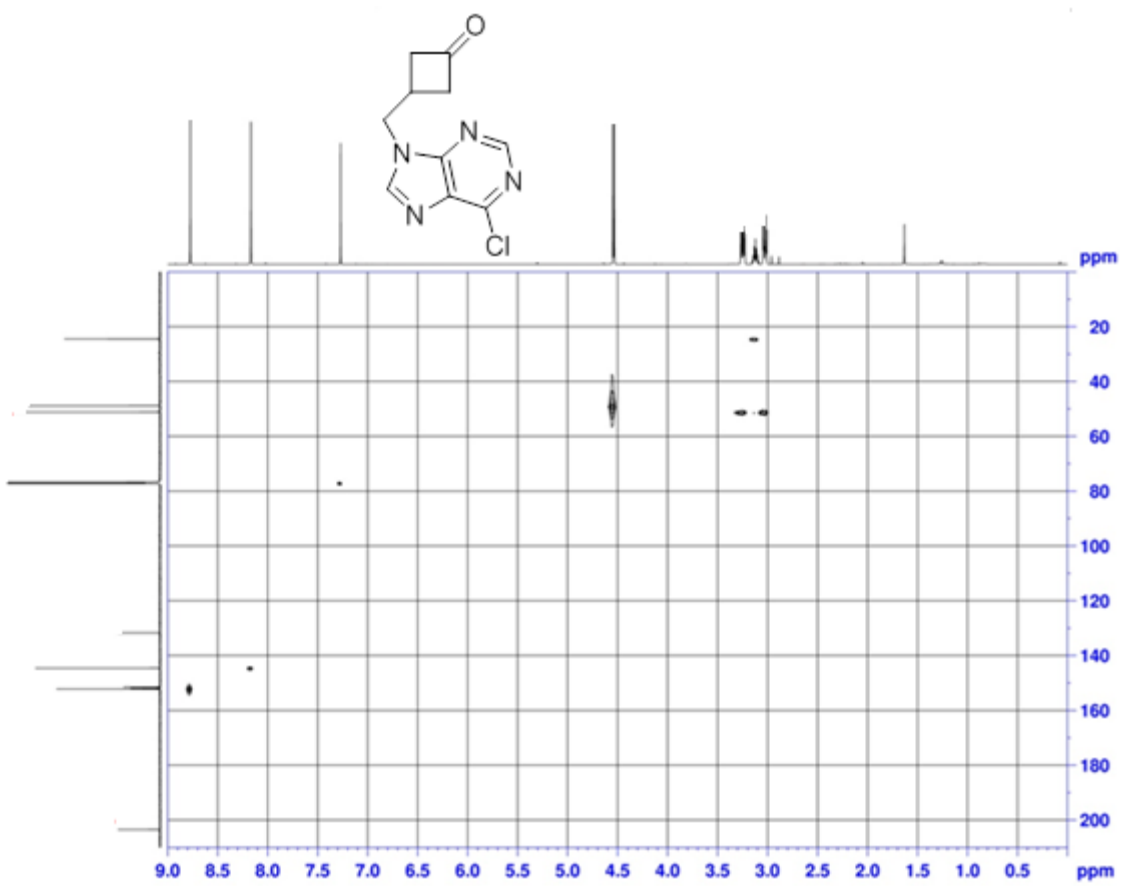

$^{1}$H-$^{13}$C HMBC of *N*-9 coupled ketone **60** (700 MHz, $CDCl_3$)

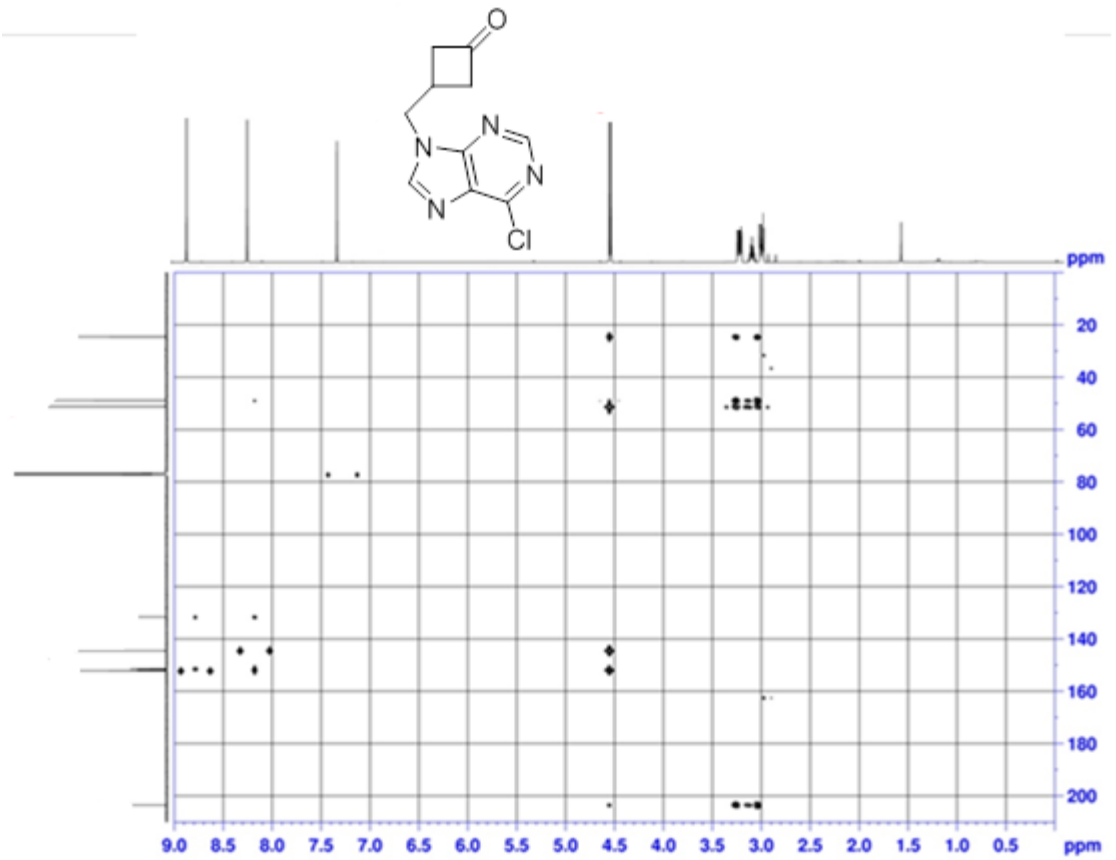

$^{1}$H-$^{15}$N HMBC of *N*-9 coupled ketone **60** (700 MHz, $CDCl_3$)

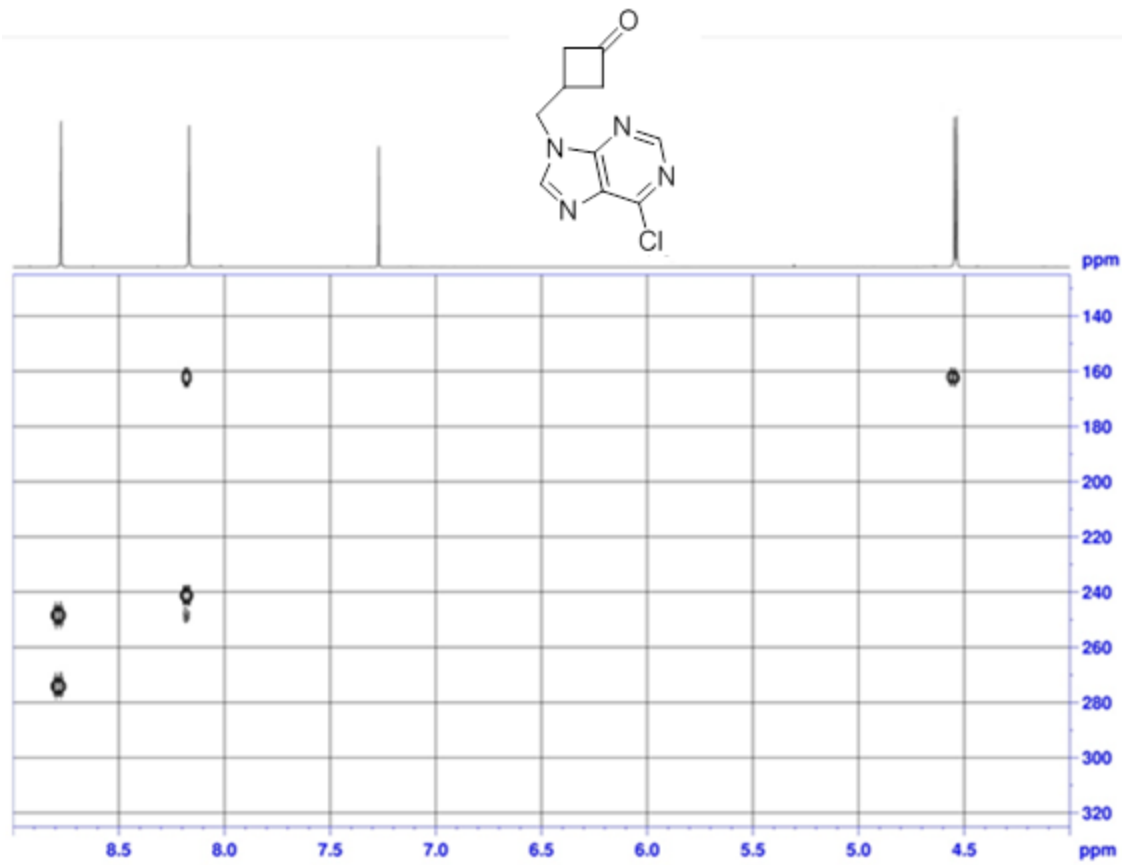

IR spectrum of *N*-9 coupled ketone **60**

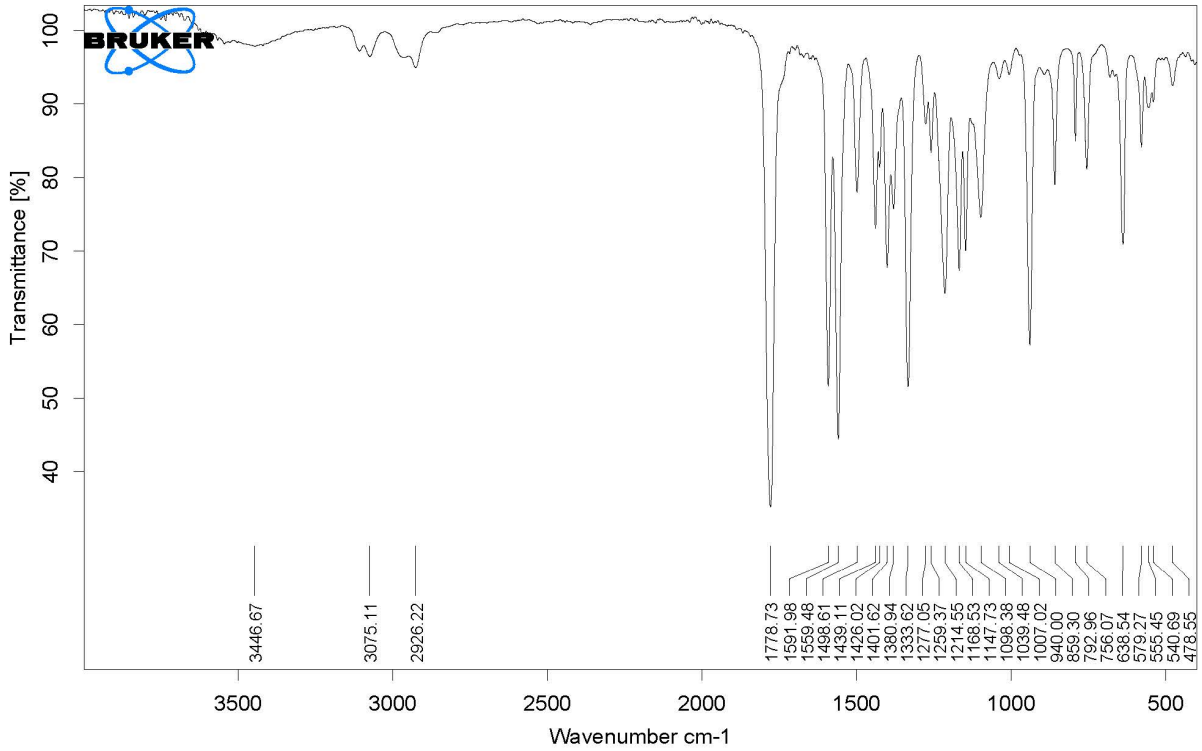

HRMS Spectrum of crude *N*-9 coupled ketone **60** ($C_{10}H_{10}ON_4Cl^+$)

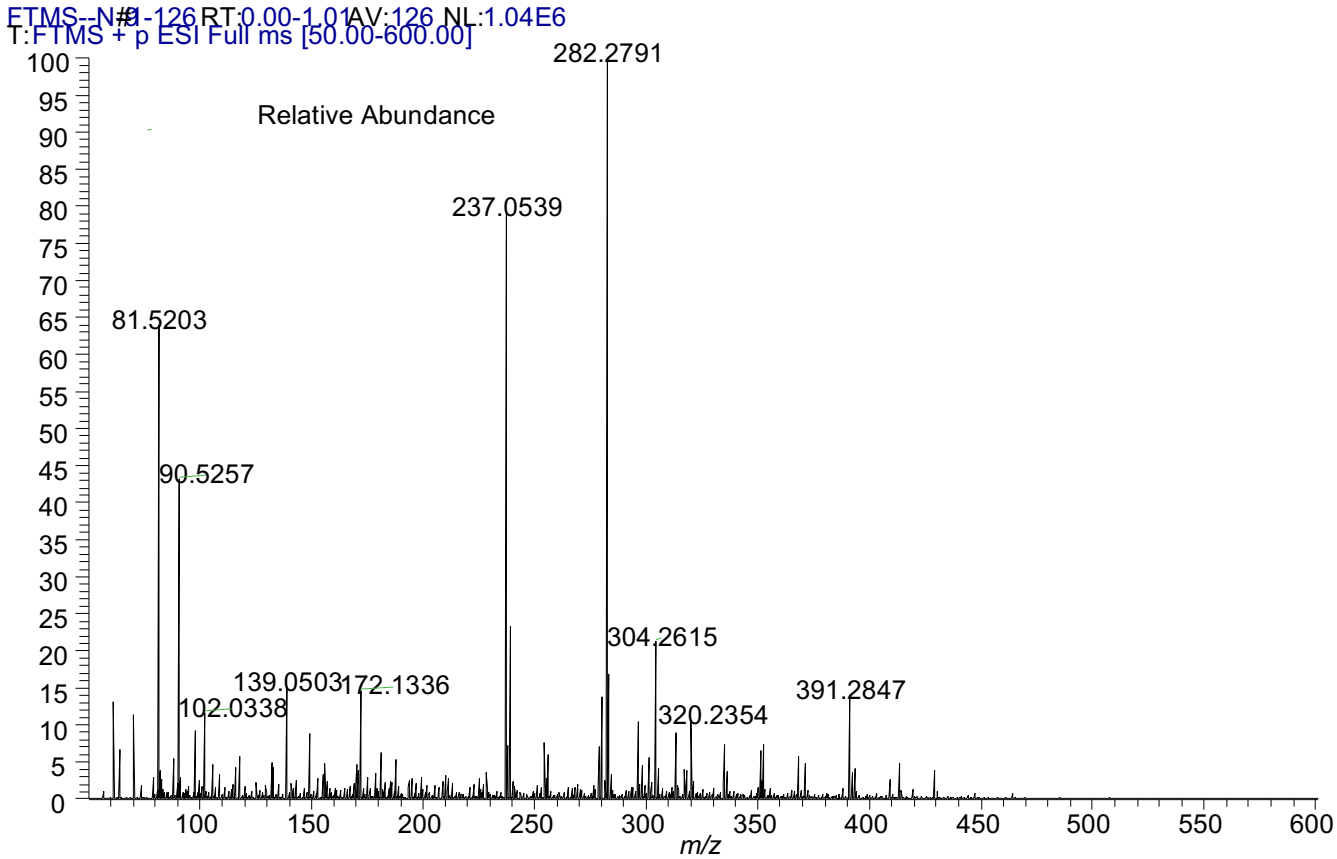


Target (**61** with $^{35}Cl$) - 237.0539 Observed- 237.0539 Ppm Error < 1

Target (**61** with $^{37}Cl$) - 239.0510 Observed- 239.0513 Ppm Error - 1.25

MSMS of *N*-9 coupled ketone **60** for peak m/z 237

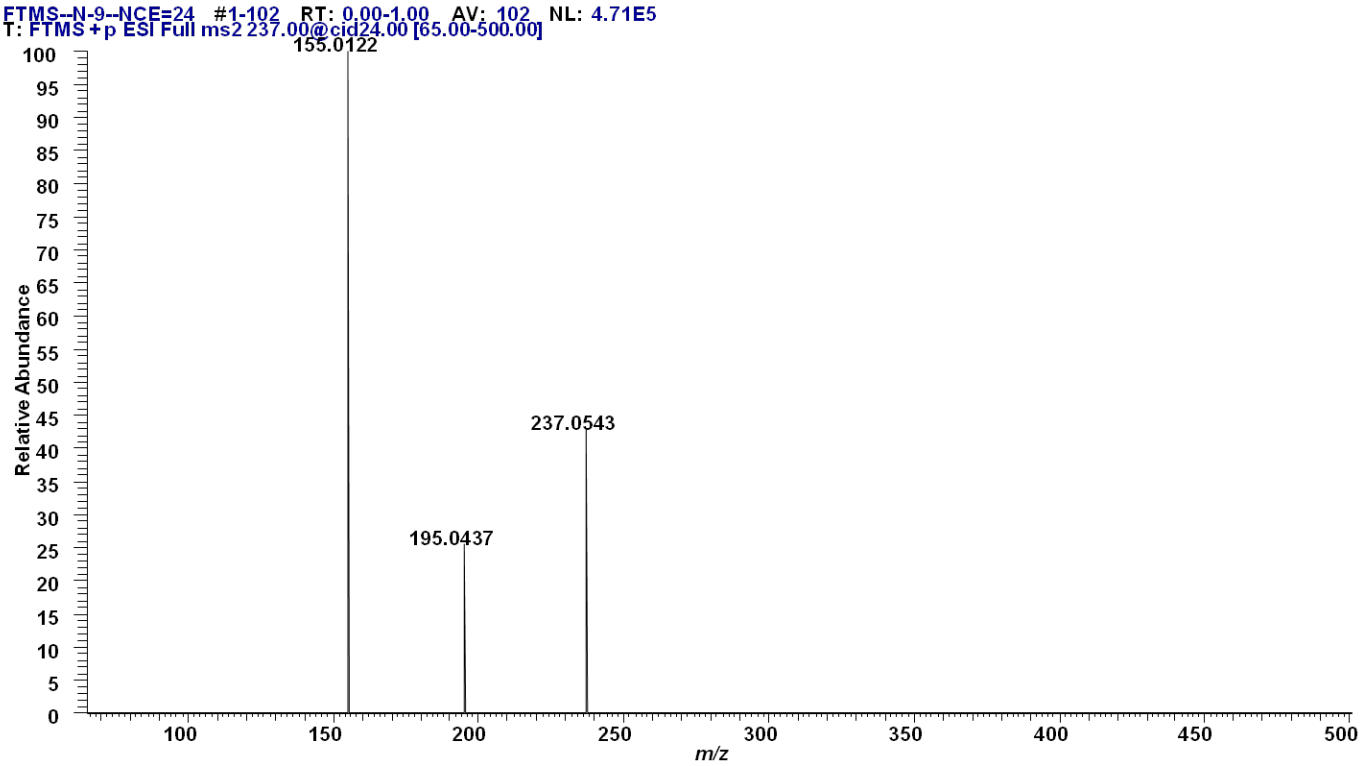


$^{1}$H NMR spectrum of *N*-7 coupled ketone **61** (400 MHz, $CDCl_3$)

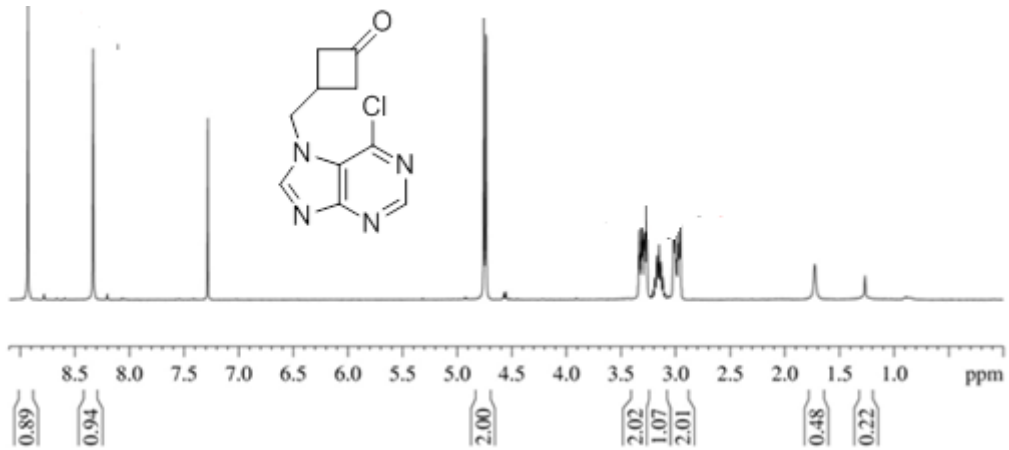

$^{13}$C- NMR spectrum of *N*-7 coupled ketone **61** (400 MHz, $CDCl_3$)

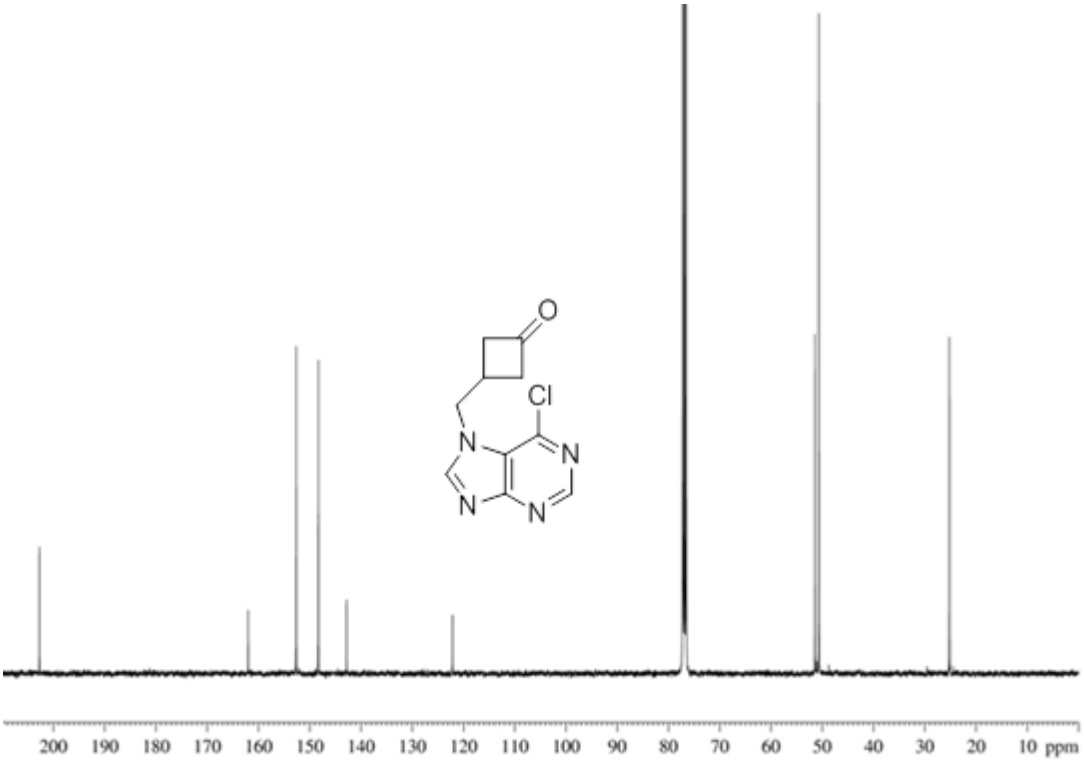

$^{1}$H-$^{1}$H COSY of *N*-7 coupled ketone **61** (400 MHz, $CDCl_3$)

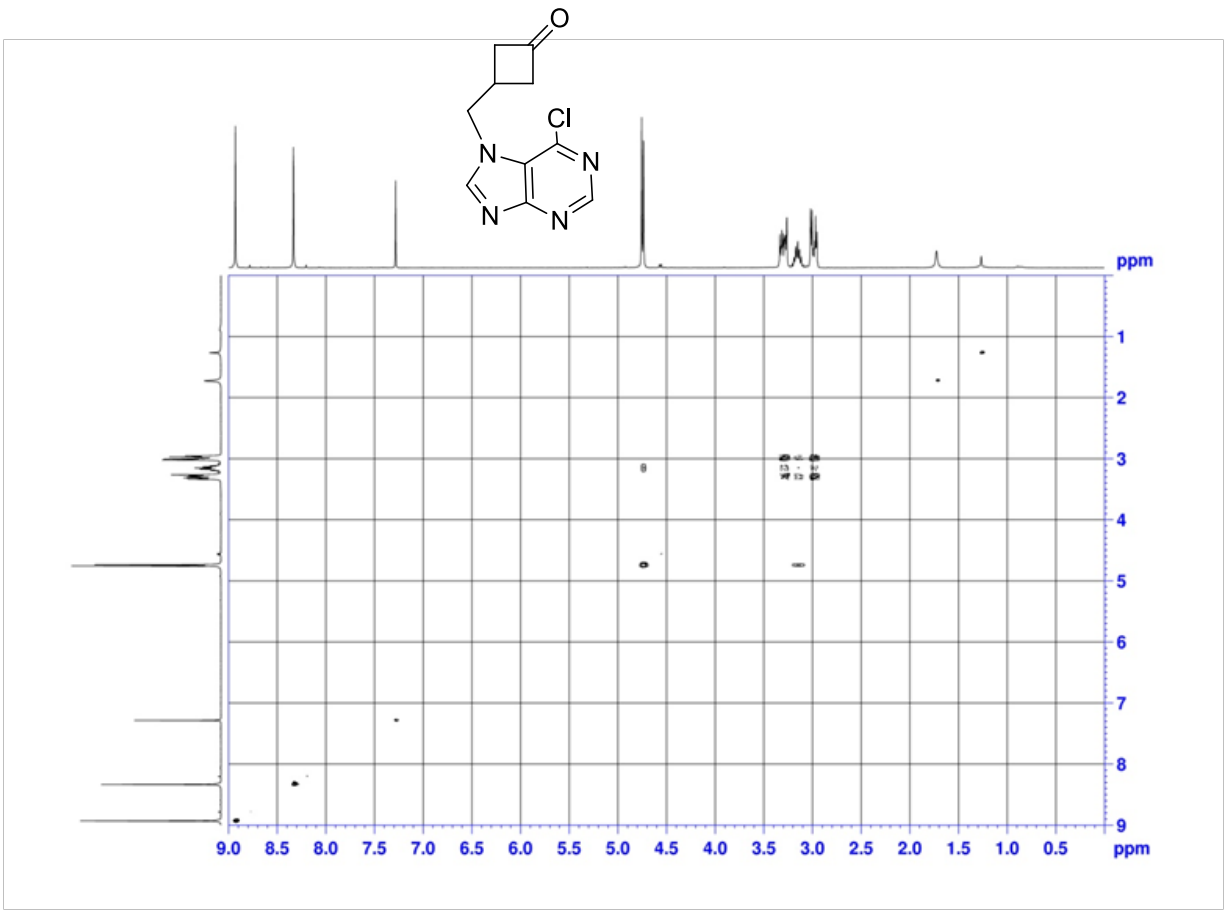

$^{1}$H-$^{13}$C HSQC of *N*-7 coupled ketone **61** (400 MHz, $CDCl_3$)

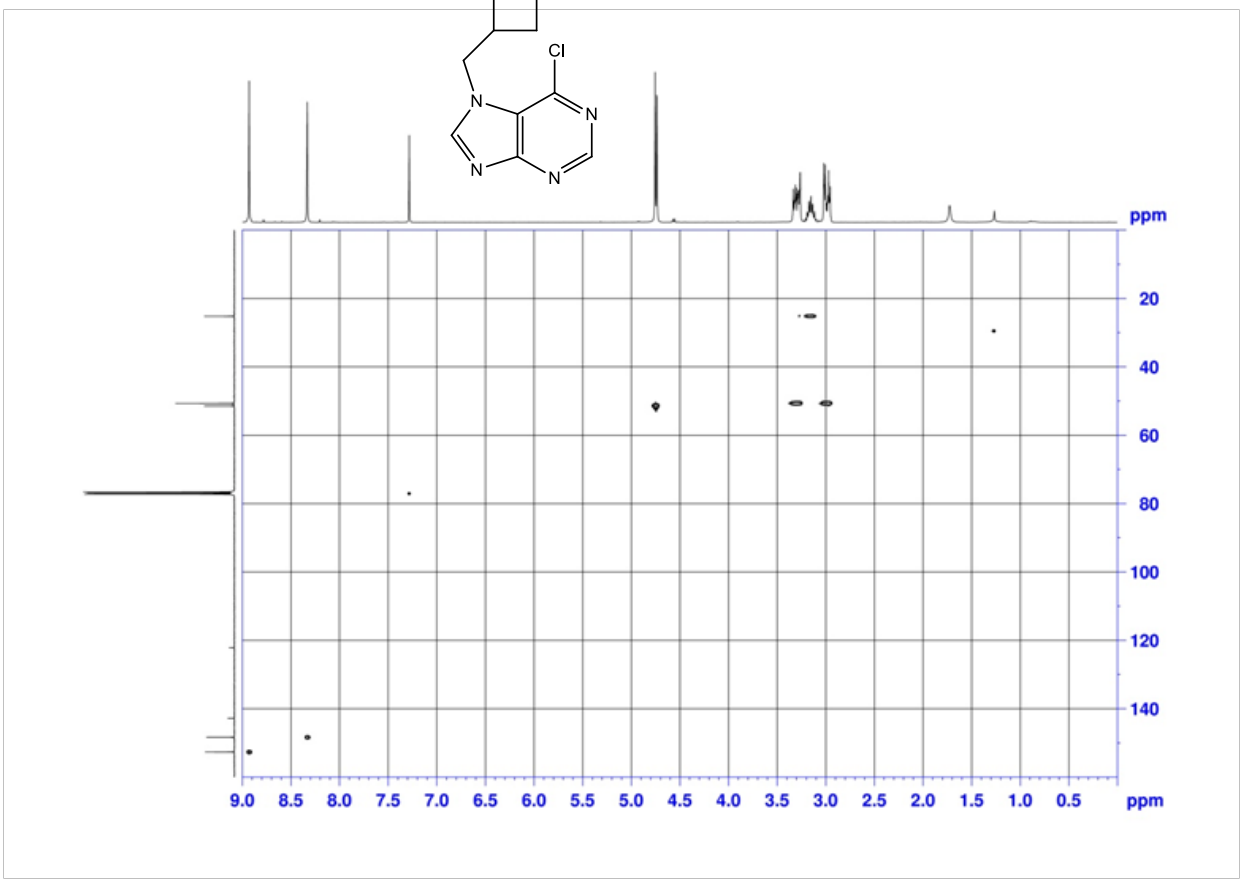

IR spectrum of *N*-7 coupled ketone **61**

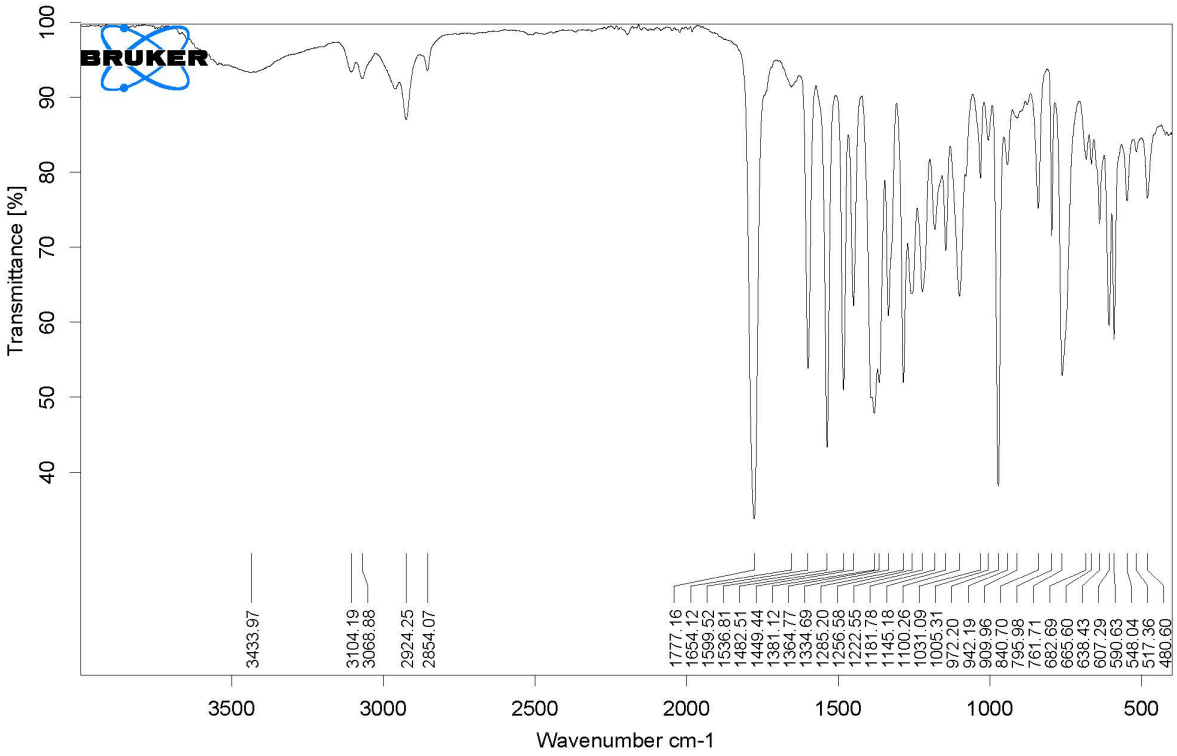

HRMS Spectrum of crude *N*-7 coupled ketone **61** ($C_{10}H_{10}ON_4Cl^+$)

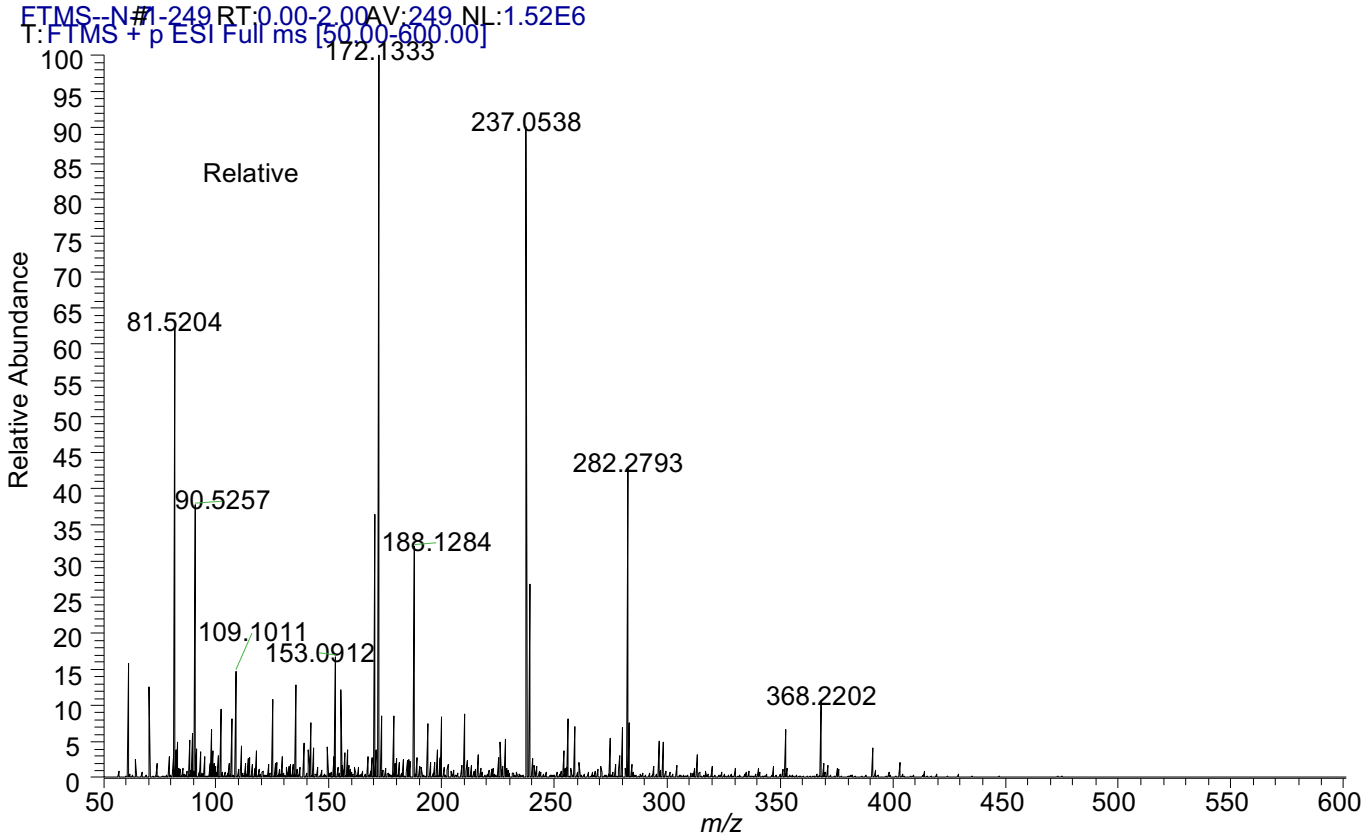


Target (**61** with $^{35}Cl$) - 237.0538 Observed- 237.0538 Ppm Error < 1

Target (**61** with $^{37}Cl$) - 239.0510 Observed- 239.0512 Ppm Error < 1

MSMS Spectrum of *N*-7 ketone **61** ($C_{10}H_{10}ON_4Cl^+$)

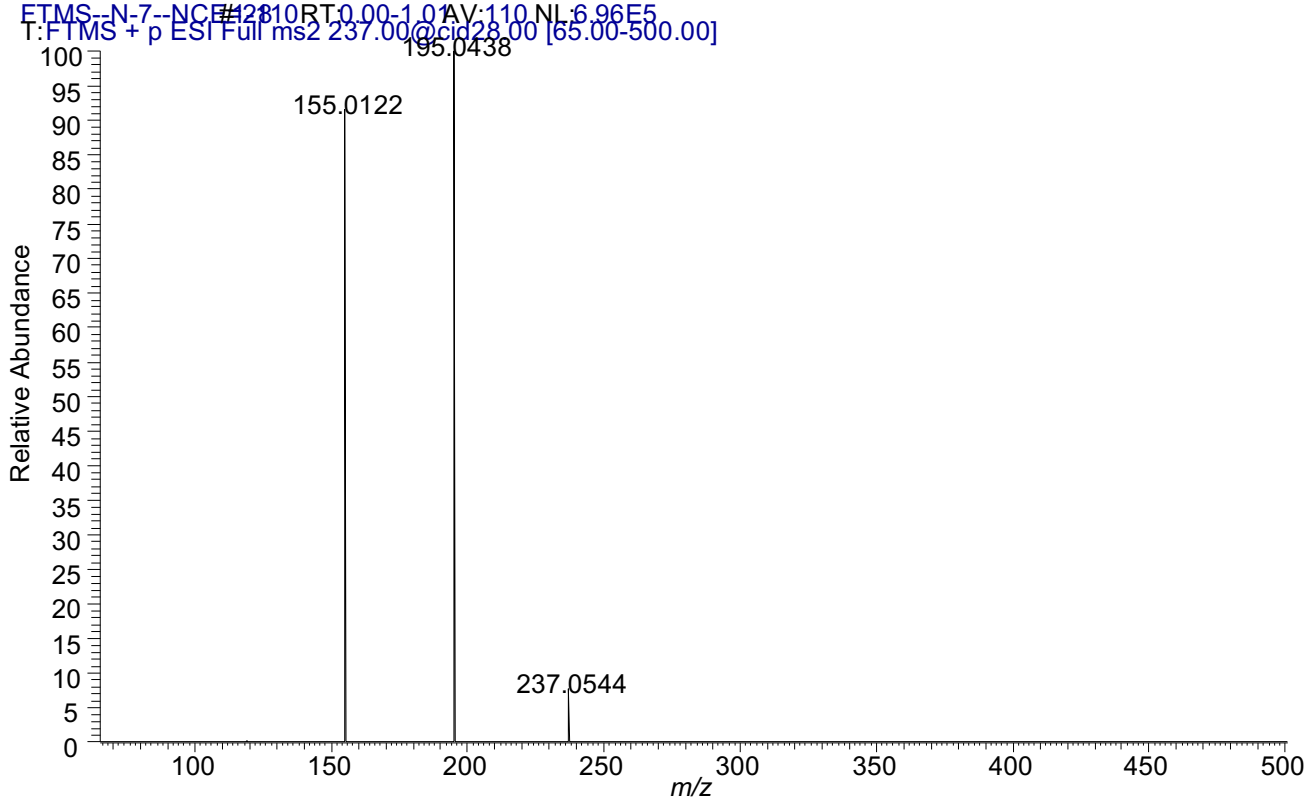

$^{1}$H NMR spectrum of *N*-9 alcohol **62** (400 MHz, $CDCl_3$)

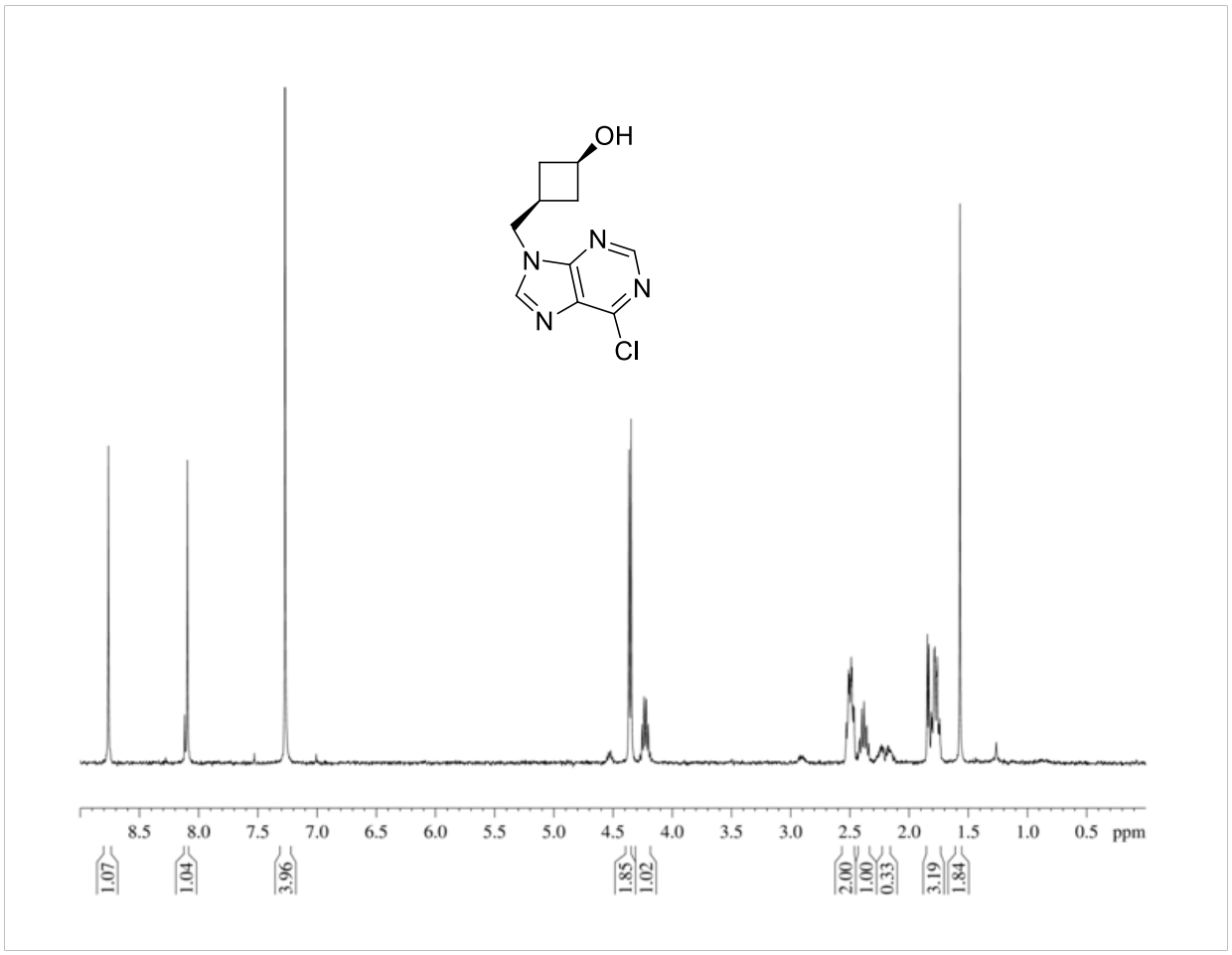

IR spectrum of *N*-9 alcohol **62**

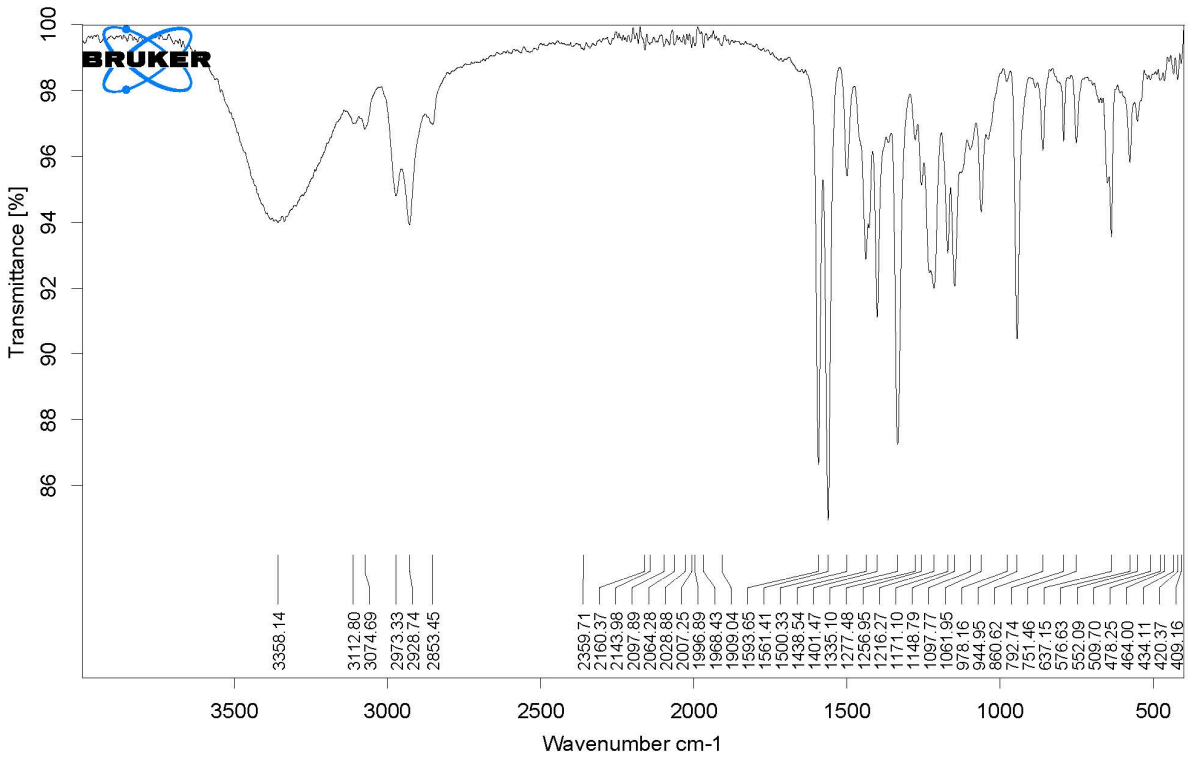

UV Spectrum of *N*-9 alcohol **62** in methanol

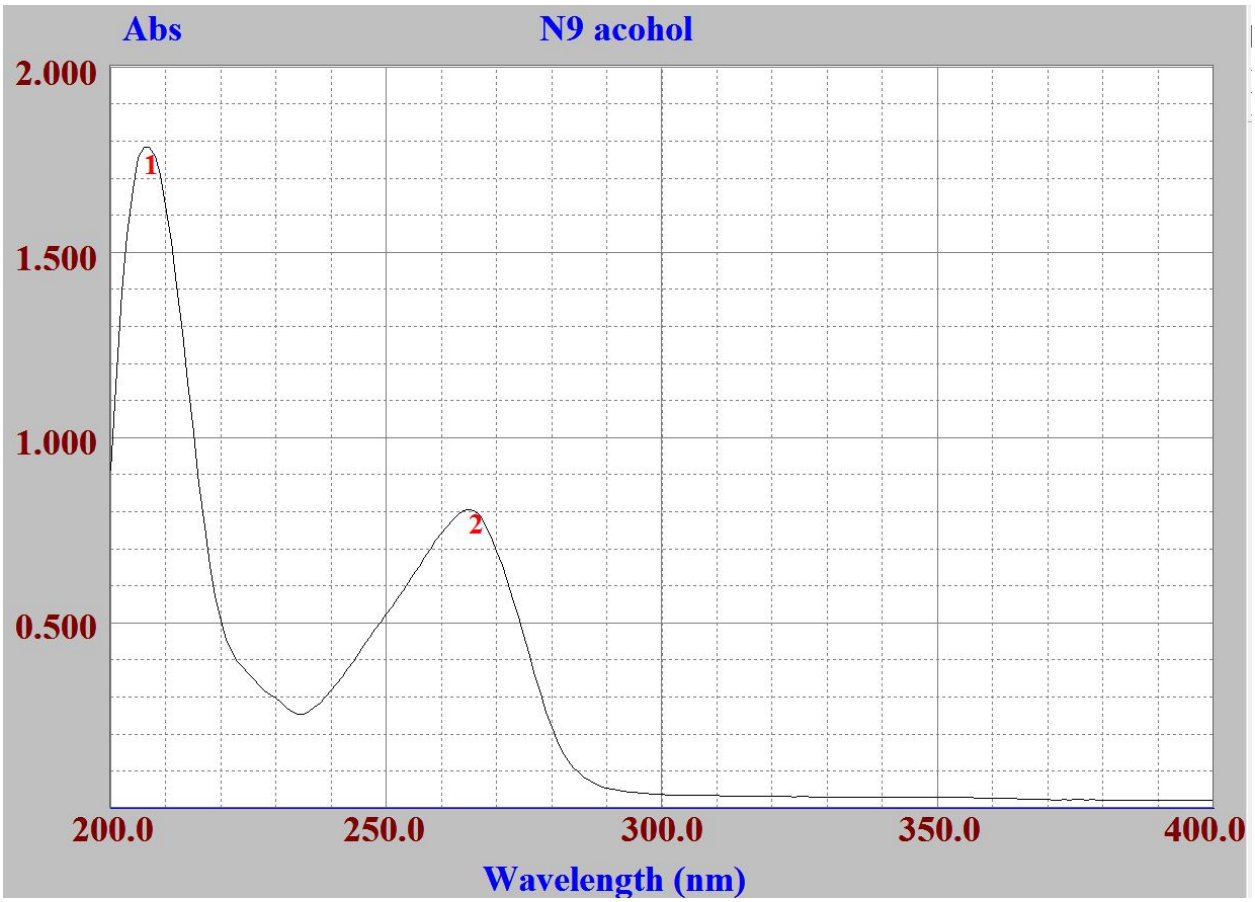


$\lambda = 206$ nm, $\varepsilon = 10676\ M^{-1}cm^{-1}$

HRMS Spectrum of crude *N*-9 alcohol **62** ($C_{10}H_{12}ON_4Cl^+$)

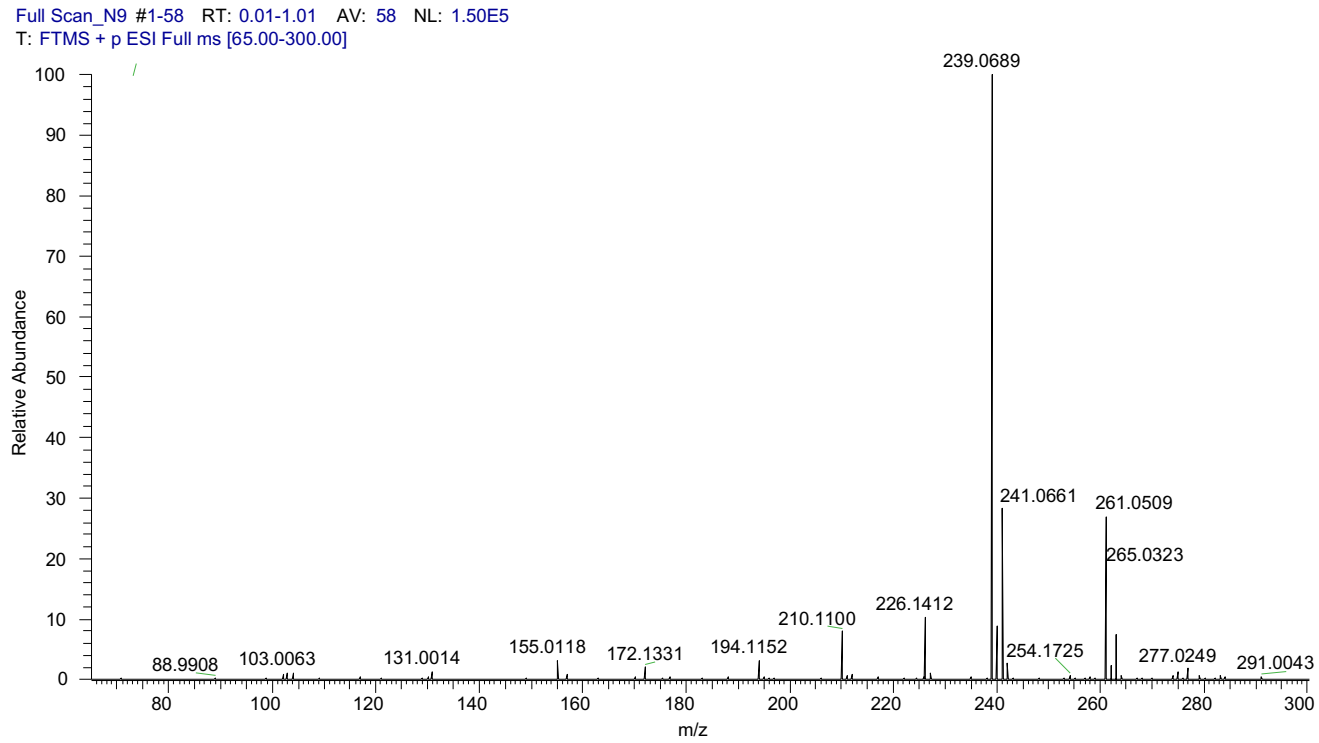


Target (**62** with $^{35}Cl$) - 239.0694 Observed- 239.0689 Ppm Error- 2.09

Target (**62** with $^{37}Cl$) - 241.0665 Observed- 241.0661 Ppm Error- 1.66

MSMS of *N*-9 alcohol **62** for peak 239m/z

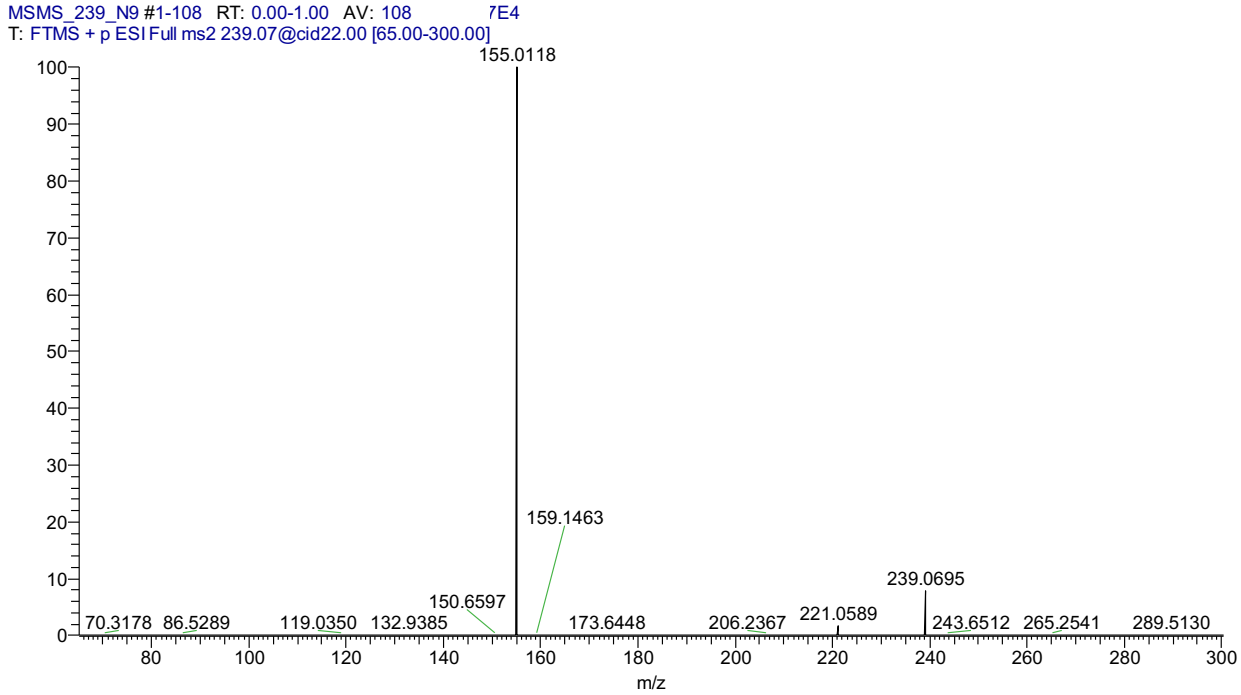


MSMS of *N*-9 alcohol **62** for peak 241m/z

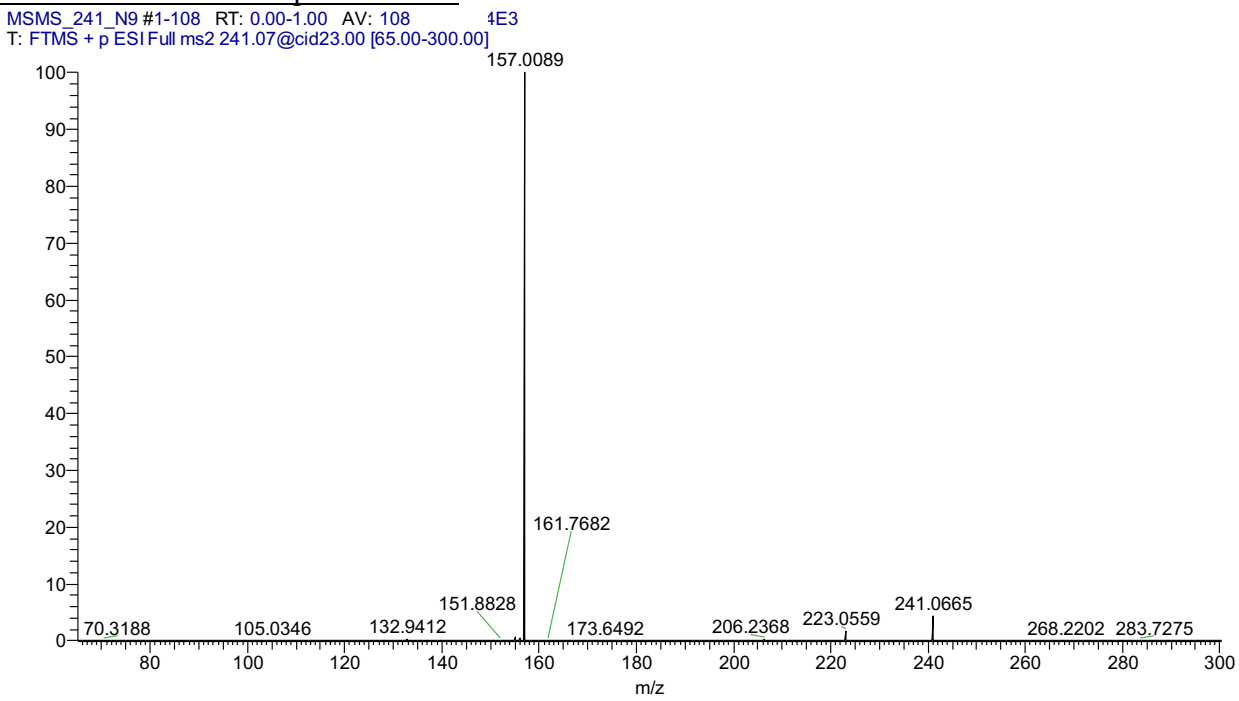

$^{1}$H NMR spectrum of *N*-7 alcohol **63** (400 MHz, $CDCl_3$)

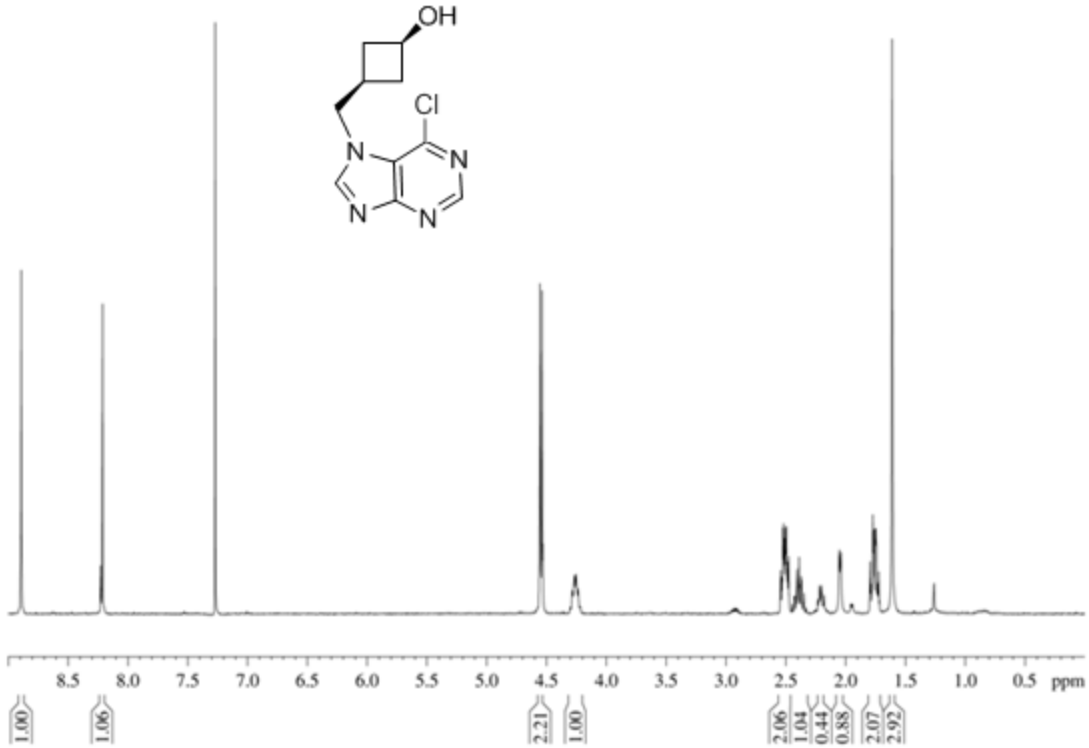

$^{13}$C- NMR spectrum of *N*-7 alcohol **63** (400 MHz, $CDCl_3$)

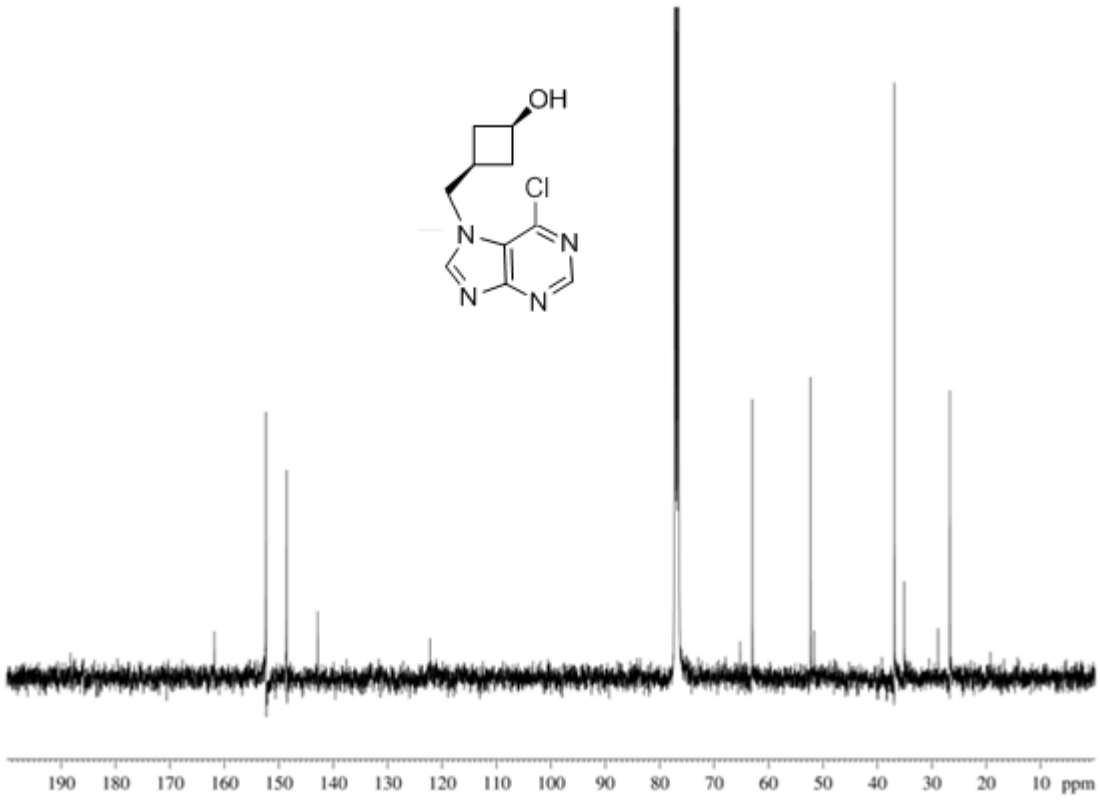

IR spectrum of *N*-7 alcohol **63**

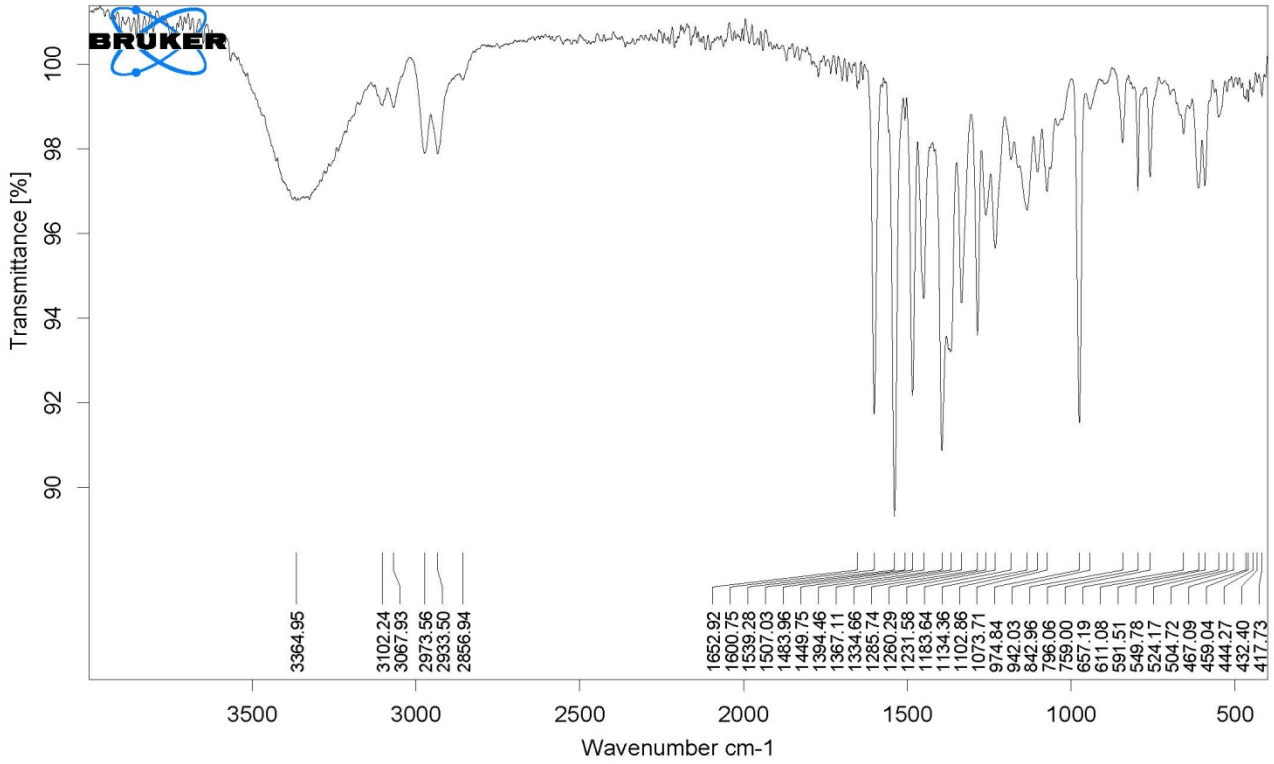

UV Spectrum of *N*-7 alcohol **63** in methanol

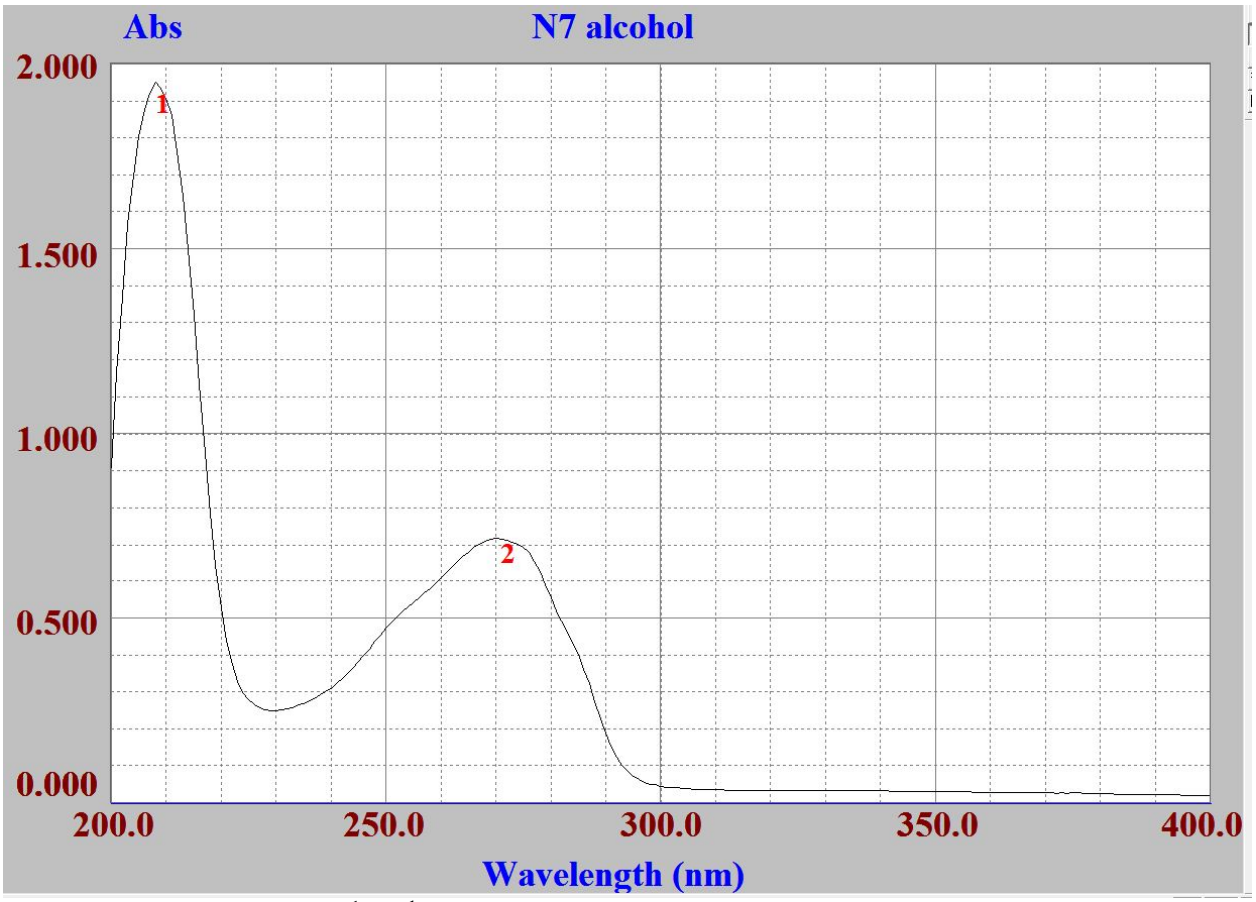


$\lambda = 208$ nm, $\varepsilon = 19487\ M^{-1}cm^{-1}$

HRMS Spectrum of crude *N*-7 alcohol **63** ($C_{10}H_{12}ON_4Cl^+$)

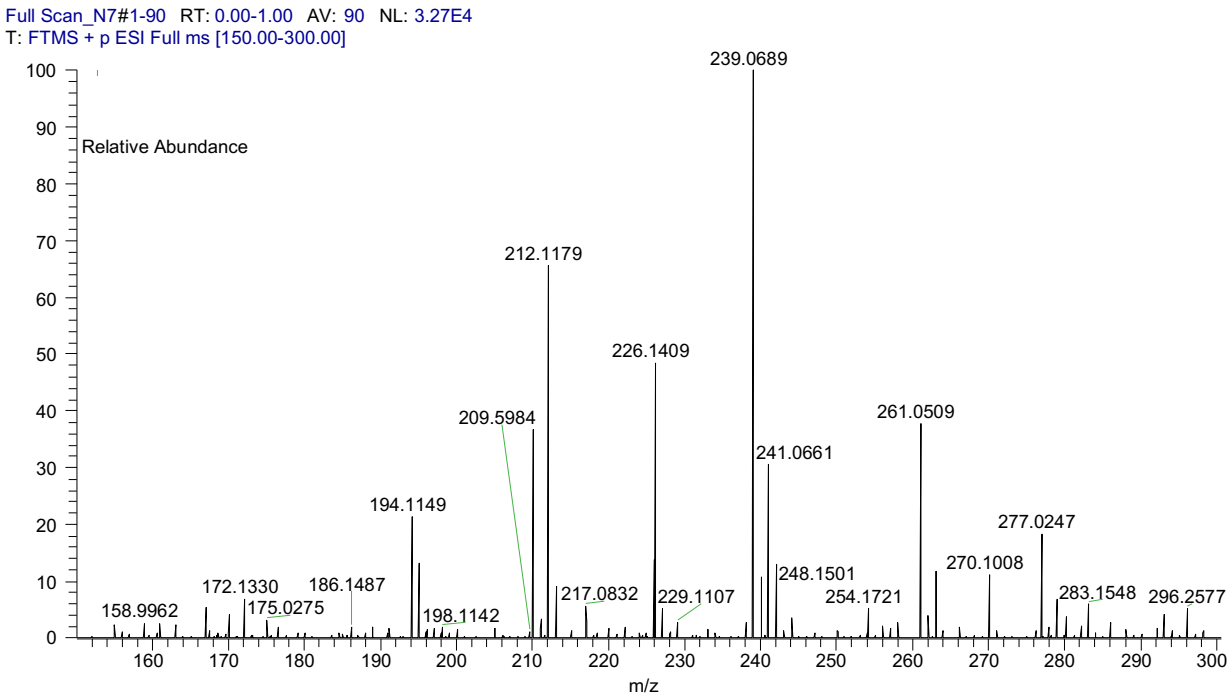


Target (**63** with $^{35}Cl$) - 239.0694 Observed- 239.0689 Ppm Error- 2.09
Target (**63** with $^{37}Cl$) - 241.0665 Observed- 241.0661 Ppm Error- 1.66

MSMS Spectrum of crude *N*-7 alcohol **63** for 239m/z peak

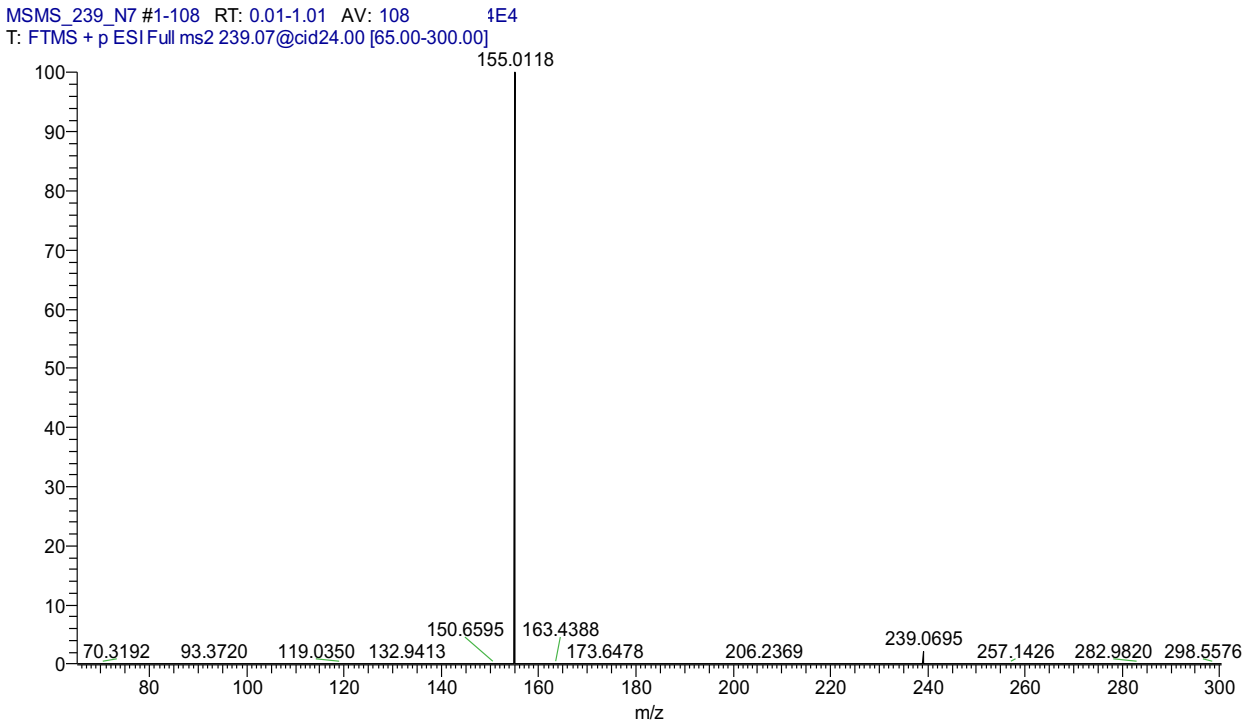

MSMS Spectrum of crude *N*-7 alcohol **63** for 241m/z peak

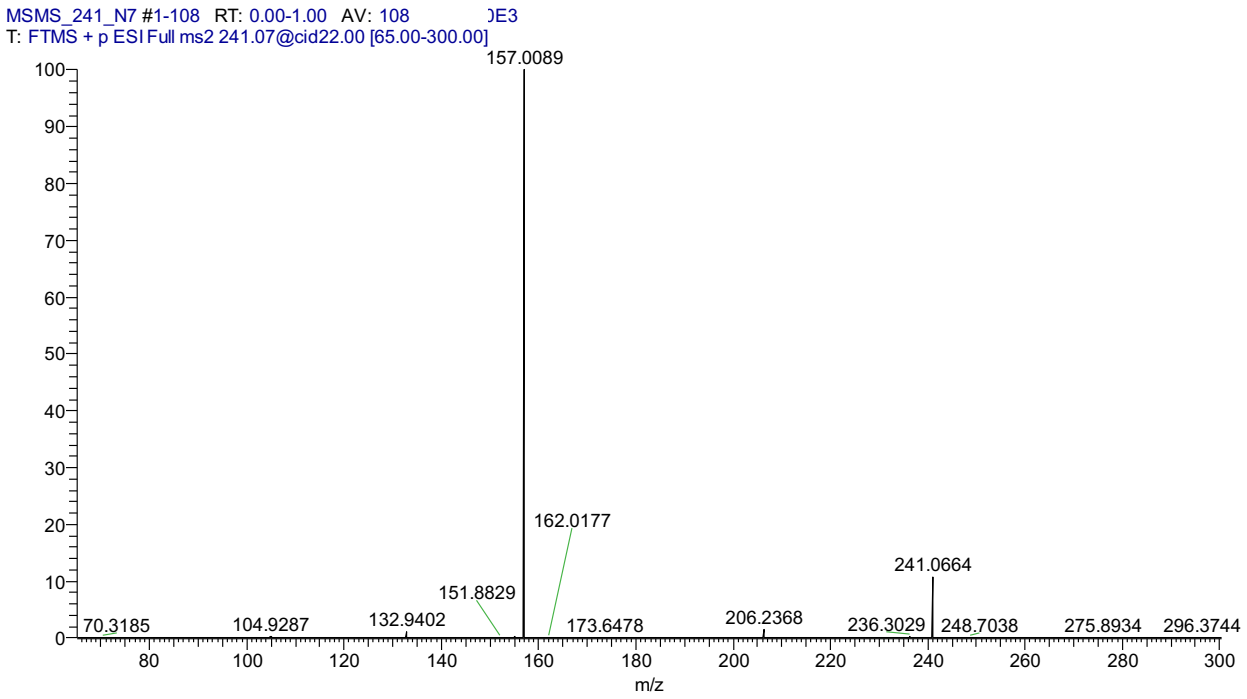

$^{1}$H NMR spectrum of product from photolysis of *N*-9 ketone **60** in MeOH (CDCl$_3$, 400 MHz)

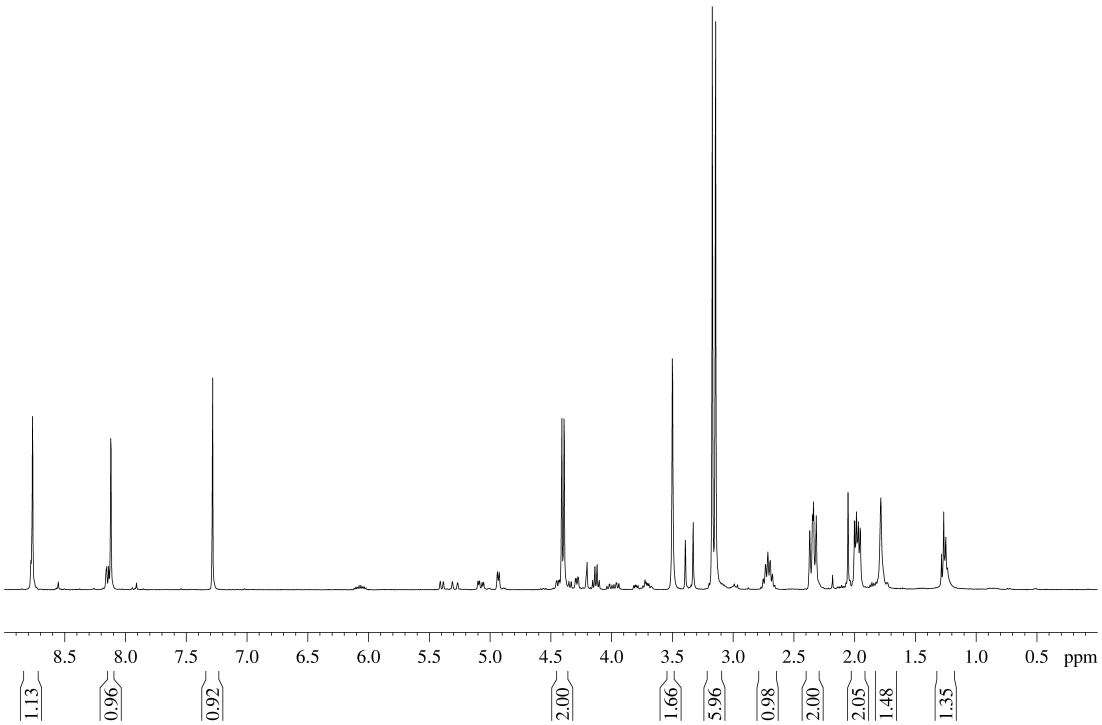

$^{1}$H NMR spectrum of product from photolysis of *N*-7 ketone **61** in MeOH (CDCl$_3$, 400 MHz)